

2015

## Characterization of Biofilm Formation, Chemotaxis, and the Genome of *Aliiroseovarius crassostreae*

Linda Kessner  
University of Rhode Island, kessner.linda@gmail.com

Follow this and additional works at: <https://digitalcommons.uri.edu/theses>

Terms of Use

All rights reserved under copyright.

---

### Recommended Citation

Kessner, Linda, "Characterization of Biofilm Formation, Chemotaxis, and the Genome of *Aliiroseovarius crassostreae*" (2015). *Open Access Master's Theses*. Paper 782.  
<https://digitalcommons.uri.edu/theses/782>

This Thesis is brought to you by the University of Rhode Island. It has been accepted for inclusion in Open Access Master's Theses by an authorized administrator of DigitalCommons@URI. For more information, please contact [digitalcommons-group@uri.edu](mailto:digitalcommons-group@uri.edu). For permission to reuse copyrighted content, contact the author directly.

CHARACTERIZATION OF BIOFILM FORMATION, CHEMOTAXIS, AND THE  
GENOME OF *ALIROSEOVARIUS CRASSOSTREAE*

BY

LINDA KESSNER

A THESIS SUBMITTED IN PARTIAL FULFILLMENT OF THE

REQUIREMENTS FOR THE DEGREE OF

MASTER OF SCIENCE

IN

CELL AND MOLECULAR BIOLOGY

UNIVERSITY OF RHODE ISLAND

2015

MASTER OF SCIENCE THESIS

OF

LINDA KESSNER

APPROVED:

Thesis Committee:

Major Professor      David R. Nelson

Jodi L. Camberg

Marta Gomez-Chiarri

Nasser H. Zawia

DEAN OF THE GRADUATE SCHOOL

UNIVERSITY OF RHODE ISLAND

2015

## ABSTRACT

*Aliiroseovarius crassostreae*, the causative agent of *Roseovarius* Oyster Disease, is a marine  $\alpha$ -Proteobacterium and a member of the *Roseobacter* clade. *Roseovarius* Oyster Disease, formerly known as Juvenile Oyster Disease, has been the reason for high mortality rates in hatchery-raised eastern oysters (*Crassostrea virginica*) since the late 1980s. Juvenile oysters less than 25 mm in shell length are more heavily impacted by the disease than large adult oysters. Because mortality rates can exceed 90%, the disease is responsible for large economic losses to the New England aquaculture industry. The probiotic organism, *Phaeobacter gallaeciensis* is a marine  $\alpha$ -Proteobacterium and like *A. crassostreae* a member of the *Roseobacter* clade. Oyster larvae that are pretreated with *P. gallaeciensis* show significantly reduced mortality rates in challenge experiments with *A. crassostreae*. The goal of this study was to elucidate the physiological responses of *A. crassostreae* and *P. gallaeciensis* to oyster pallial fluid and identify putative virulence factors via genome analysis of the pathogen. *A. crassostreae* and *P. gallaeciensis* grew rapidly in oyster pallial fluid. When growth medium was supplemented with oyster pallial fluid biofilm formation by *A. crassostreae* was significantly increased. Both organisms were chemoattracted to pallial fluid and a molecule >10 kDa seems to be responsible for this positive chemotactic response. These results suggest that oyster pallial fluid is likely to contribute to the initial colonization of *A. crassostreae* in the oyster in three ways – by promoting positive chemotaxis, growth, and biofilm formation. Genome analysis of *A. crassostreae* revealed multiple putative virulence genes including cytolysins, RTX toxin and related  $\text{Ca}^{2+}$ -binding proteins, and a serralyisin peptidase. In

addition, the genome encodes pilus/fimbriae biogenesis machinery and other proteins that appear to facilitate surface attachment.

## ACKNOWLEDGEMENTS

I would like to express my sincerest gratitude to my advisor Dr. Nelson. His support, immense knowledge, encouragement, and advice throughout my research in his lab were invaluable. His guidance and professional advice are always accompanied by a personal interest in his student's well-being.

I would like to thank Dr. Gomez-Chiarri, Dr. Rowley, and Dr. Camberg for their continuous interest, support, and advice throughout my time at URI. I would also like to thank Dr. Jenkins for her encouraging words and support.

Thank you to all of the current and former Nelson lab members that I had the privilege to work with: Dr. Wenjing Zhao, Ted Spinard, Jason LaPorte, and Chris Schuttert. Thank you all for creating an amazing lab environment to work in. I would especially like to thank Dr. Wenjing Zhao who helped me to get set-up in the lab when I initially joined and introduced me to many lab techniques. Thank you to Ted Spinard for his time and tremendous help and guidance with genome assemblies. I would also like to thank Nicholas Labrakis for all his work in the lab.

I would especially like to thank Perry Raso from the Matunuck Oyster Bar. His generous donations of healthy and fresh oysters made this research possible.

Thank you to all the other former and current members of the Probiotics group that I have had the pleasure to work or share research ideas and results with: Dr. Christine Dao, Meagan Hamblin, Hilary Ranson, and a special thanks to Dr. Sae Bom Sohn for her help with oyster larvae experiments.

Thank you to Robert Deering for his help with analyzing oyster pallial fluid for free amino acids. I would also like to thank Jiadong Sun for his help with the carbohydrate analysis of pallial fluid. The availability of these data sets was invaluable to much of my research.

I would also like to thank Paul Johnson and Janet Atoyan at the URI Genomics and Sequencing Center for their tremendous help with sequencing.

I would like to thank the entire faculty as well as all the graduate students of the Cell and Molecular Biology department. It was an honor to get to know every one of you, to learn from you, and to work with you over these last couple of years.

## **DEDICATION**

I dedicate this thesis to my parents Luise and Ulli Keßner. Thank you for always believing in me and encouraging me to further my education and professional career. I am unendingly grateful for your support and continuous confidence in me.

I would also like to dedicate this thesis to Jason LaPorte. Thank you for being my rock and continuously supporting me. I am incredibly grateful that we share a passion for microbiology and that I was able to undertake this journey through graduate school together with you.



## PREFACE

The following thesis has been prepared in Manuscript format according to the guidelines of the Graduate School of the University of Rhode Island. This thesis contains a literature review and two manuscripts.

The first manuscript “Physiological Effect of Oyster Pallial Fluid on *Aliiroseovarius crassostreae* and *Phaeobacter gallaeciensis S4*” has not been published.

A short version of the second manuscript “Draft genome sequence of *Aliiroseovarius crassostreae* CV919-312<sup>T</sup>Sm, causative agent of *Roseovarius* Oyster Disease (formerly Juvenile Oyster Disease)” will be submitted to Genome Announcements.

## TABLE OF CONTENTS

<b><u>CONTENT</u></b>	<b><u>PAGE</u></b>
Abstract.....	ii
Acknowledgements.....	iv
Dedication.....	vi
Preface.....	vii
Table of Contents.....	viii
List of Figures.....	ix
List of Tables.....	x
Literature Review.....	1
Manuscript I.....	23
Manuscript II.....	63
Appendix.....	113

## LIST OF FIGURES

<b><u>FIGURE</u></b>	<b><u>PAGE</u></b>
<i>Literature Review</i>	
Figure 1. Electron micrograph images illustrating the cell morphology of <i>A. crassostreae</i> CV919-312 <sup>T</sup> .....	6
Figure 2. Conchiolin deposits in oysters affected by ROD.....	9
Figure 3. SEM images of inner shell surface of oysters affected by ROD	11
Figure 4. Effect of pre-incubation with <i>P. gallaeciensis</i> on oyster larvae survival when challenged with <i>A. crassostreae</i> .....	15
<i>Manuscript I</i>	
Figure 1. Growth of <i>A. crassostreae</i> in YP30 and oyster pallial fluid.....	38
Figure 2. Growth of <i>P. gallaeciensis</i> in YP30 and oyster pallial fluid.....	40
Figure 3. <i>A. crassostreae</i> growth on agar plates supplemented with 5% fish blood after 2 d incubation.....	41
Figure 4. Chemotaxis assay results of <i>A. crassostreae</i> .....	44
Figure 5. Chemotaxis assay results of <i>P. gallaeciensis</i> .....	45
Figure 6. Biofilm formation of <i>A. crassostreae</i> with various amounts of pallial fluid.....	48
Figure 7. <i>A. crassostreae</i> cells grown under static conditions in oyster pallial fluid and under shaking conditions in YP30.....	49
Figure 8. Planktonic cell density of <i>A. crassostreae</i> during biofilm formation with various amounts of pallial fluid added.....	50

Figure 9. Effects of oyster pallial fluid on biofilm formation by <i>A. crassostreae</i> in glass, polypropylene, and polystyrene tubes.....	51
Figure 10. Effects of oyster pallial fluid on biofilm formation by <i>P. gallaeciensis</i> in glass, polypropylene, and polystyrene tubes.....	53

*Manuscript II*

Figure 1. Hypothetical model of Tad/Flp secretion.....	71
Figure 2. <i>Tad/flp</i> gene cluster on contig 6.....	74
Figure 3. <i>Tad/flp</i> gene cluster on contig 19.....	78
Figure 4. Genes encoding TadE-like protein and TadG.....	80
Figure 5. Assembly and schematic operation of a T1SS.....	85
Figure 6. Putative RTX toxin gene with cytolysin activating protein.....	87
Figure 7. IMG/ER annotation of T1SS and adhesin biogenesis cluster.....	94
Figure 8. Core structure of a typical T4ASS.....	96
Figure 9. T4ASS gene cluster on contig 7.....	97
Figure 10. Partial T4BSS gene cluster on contig 8.....	101
Figure 11. Putative core complex assembly and localization of T4BSS proteins in <i>L. pneumophila</i> .....	102

## LIST OF TABLES

<b><u>TABLE</u></b>	<b><u>PAGE</u></b>
<i>Literature Review</i>	
Table 1. Biofilm formation of bacterial probiont and pathogens in glass tubes under static conditions.....	17
<i>Manuscript I</i>	
Table 1. Constituent concentrations of oyster pallial fluid.....	35
Table 2. HPLC data of free amino acids present in oyster pallial fluid....	36
Table 3. Generation times of <i>A. crassostreae</i> in YP30 and pallial fluid...	39
Table 4. Generation times of <i>P. gallaeciensis</i> in YP30 and pallial fluid...	40
Table 5. Extracellular protease activity of <i>A. crassostreae</i> .....	43
<i>Manuscript II</i>	
Table 1. Contig numbers and associated GenBank accession numbers.....	69
Table 2. BLASTX results of two <i>tadE</i> -like genes on contig 19.....	78
Table 3. ORFs annotated as or containing conserved regions associated with RTX toxins and related Ca <sup>2+</sup> -binding proteins.....	83
Table 4. Putative cytolysin activating acyltransferases .....	87
Table 5. Putative hemolysins .....	91
Table 6. Annotations of genes involved in secretion of putative adhesin...	94

## **Literature Review**

## Introduction

*Roseovarius* Oyster Disease (ROD), formerly known as Juvenile Oyster Disease (JOD), was first reported in the late 1980s and has since been the cause of high mortality rates in hatchery raised eastern oysters (1-4). High mortality rates result in significant economic loss for the shellfish industry (3). Oysters are one of the most important aquaculture products in the U.S. and worldwide. The United States consumes almost 60% of the world's total supply of oysters (5). Approximately 66% of the U.S. aquaculture production value lies in bivalve mollusks like oysters, clams, and mussels (6).

In 2005, *Aliiroseovarius crassostreae*, formerly known as *Roseovarius crassostreae*, was reported to be the causative agent of ROD (7). *A. crassostreae* is an aerobic, Gram-negative  $\alpha$ -Proteobacterium and a member of the *Roseobacter* clade (7). *Phaeobacter gallaeciensis* is a marine organism that has been isolated from the inner shell surface of a healthy oyster (8). Like *A. crassostreae*, *P. gallaeciensis* is an  $\alpha$ -Proteobacterium and a member of the *Roseobacter* clade. *P. gallaeciensis* is a probiotic organism that has been shown to increase survival of oyster larvae when challenged with *A. crassostreae* or *Vibrio coralliilyticus* (8). The probiotic mechanisms of *P. gallaeciensis* include the ability to form biofilms, the production of tropodithietic acid (TDA), and quorum quenching with N-acyl-homoserine lactones (9).

## Main Body

### *Roseobacter* clade overview

*Roseobacter* clade members share  $\geq 89\%$  identity of their 16S rRNA gene sequence and are heterotrophic organisms (10-12). Members of the *Roseobacter* clade represent a large part of the marine microbiota and many of its species live in symbiotic relationships with marine phytoplankton, invertebrates, as well as vertebrates (11). This clade is found exclusively in marine or hypersaline environments (11, 12). Depending on location, more than 20% of the coastal bacterioplankton communities in the upper mixed ocean waters may consist of the *Roseobacter* clade alone (11, 12). In addition to forming symbiotic relationships with other marine organisms, members of the *Roseobacter* clade inhabit diverse niches in ocean waters including coastal and polar regions, sea ice, hydrothermal vents, macroalgae, and sediments (13). Most often however, members of this clade are found to be attached to organic particles or near phytoplankton or macroalgae blooms (14). Some of these microorganisms are capable of chemotaxis which provides an advantage to locate nutrients or hosts in heterogeneous and nutrient poor ocean waters (14, 15).

While a great metabolic diversity can be observed in the *Roseobacter* clade, certain physiological traits appear to be characteristic for the clade. These traits include aerobic anoxygenic phototrophy (11, 13), carbon monoxide oxidation (11, 13), aromatic compound degradation (11), sulfur metabolism (11), production of secondary metabolites(11), and quorum sensing (13). Many *Roseobacters* have the ability to utilize two key pathways for the degradation of the sulfur based compound



dimethylsulfoniopropionate (DMSP) (9, 11, 16). Marine algae and coastal vascular plants produce this compound as an osmolyte, which is an important sulfur source in the oceans and plays a significant role in marine biogeochemical processes (11, 16, 17). One of the two pathways, the so called cleavage pathway, plays a role in the release of the volatile gas dimethylsulfide (DMS) while the other pathway is involved in demethylation to 3-(methylmercapto) propionic acid (MMPA), which can then be converted into methanethiol (MeSH) and incorporated into the sulfur containing amino acid methionine (16, 18). *P. gallaeciensis* is known to have this ability to degrade DMSP (9). However, no studies have yet been performed on the ability of *A. crassostreae* to degrade DMSP.

*Roseobacter* clade members are the most dominant primary surface colonizing group of bacteria and it is common for them to form rosettes (8, 11, 19). The ability of *Roseobacters* to form pili is most likely an important feature for these characteristics (14). Slightom et al. (14) selected 28 members of the clade to perform a comparative genome analysis and found that all of the 28 members contain gene clusters that encode the machinery for *flp* (fimbrial low-molecular-weight protein) pili formation. This widespread colonization island has been implicated with biofilm formation, colonization of surfaces, and pathogenesis in various genera (20). The presence of *flp*-pili has been confirmed in *Phaeobacter gallaeciensis* strain 2.10 and strain BS107 (14). Components of the type 4 secretion system can also be found in many *Roseobacter* clade genomes (14).

### *Aliioseovarius crassostreae* CV919-312<sup>T</sup>

Previously isolated from *Crassostrea virginica* tissue during the 1997 epizootics at the Damariscotta River in Maine, *A. crassostreae* measures approximately 0.25 x 1.0 µm and is motile via one or two polar flagella (4, 7). Cells are rod to ovoid in shape (7). The organism can also possess a polar tuft of fimbriae that appear to facilitate the attachment of the organism to the inner shell surface of oysters (Figure 1) (7, 21, 22). Colonies take approximately two days to grow ~1 mm in diameter at 27°C and are grey in color. According to Boettcher et al. (2005), *A. crassostreae* grows optimally at temperatures ranging from 34 to 37°C and prefers pH levels between 6.5 and 8.0. Optimal growth has been observed at salinities between 1‰ and 1.5‰ (7). These observations suggest the adaptation of this organism to shallow coastal waters (7).

*A. crassostreae* is an aerobic, non-fermentative organism, produces a weak catalase reaction and is oxidase positive (7). The organism's whole cell fatty acid content is predominantly made up of C<sub>18:1ω7c</sub> (7). In addition, Boettcher et al. (2005) showed that *A. crassostreae* is capable of utilizing glycerol and β-hydroxybuturate and has the ability to perform denitrification by reducing nitrate to nitrite and further reducing nitrite to nitrogen gas (7). Esterase, esterase lipase, acid and alkaline phosphatase, leucine and valine acylamidase, as well as lipase activity have been observed (7).

*Aliioseovarius crassostreae* CV919-312<sup>T</sup> (*Roseovarius crassostreae* at the time) was first described in 1999 in association with oysters affected by *Roseovarius*

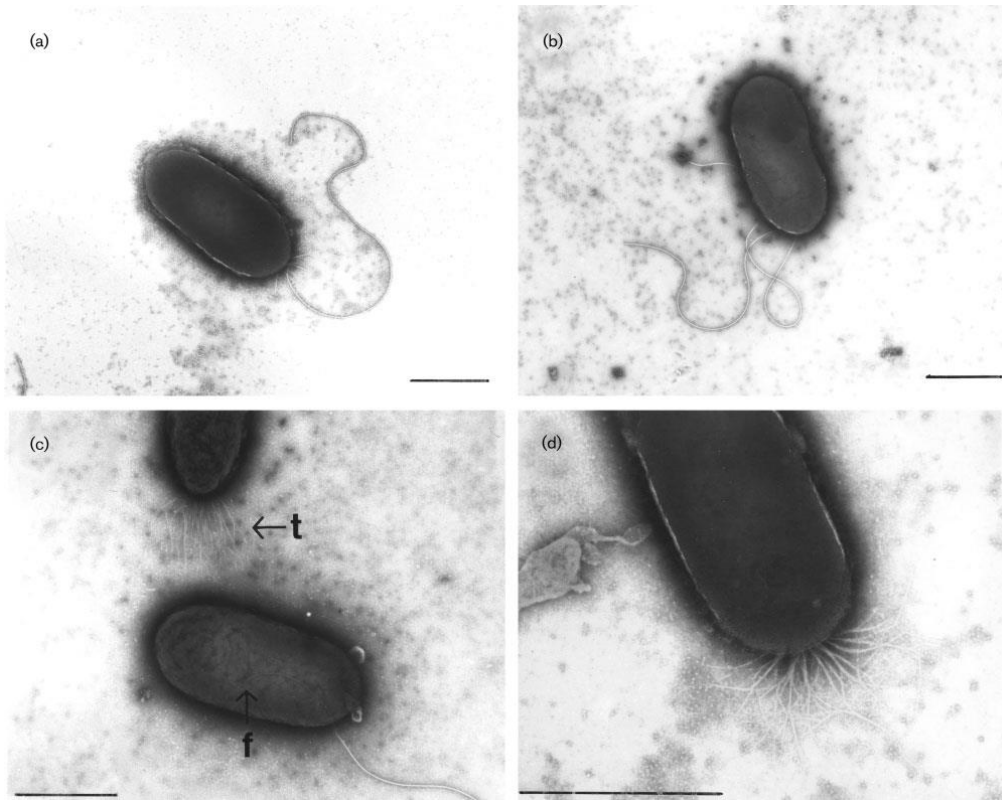


**Figure 1.** Electron micrographs of *A. crassostreae* CV919-312. *A. crassostreae* is a short ovoid rod with one (a) or two (b) flagella. A polar tuft of fimbriae (indicated by ‘t’) and a lateral flagellum can be observed (point of insertion indicated by ‘f’). Bars represent 1  $\mu\text{m}$  (7). Figure from Boettcher et al. (2005) (7).

Oyster Disease, and in 2005 the organism was identified to be the sole cause of the disease (7). Based on 16S rRNA phylogenetic analysis the organism was re-classified as *Aliiroseovarius crassostreae* in 2015 (23). *A. crassostreae* still appears to be the only pathogenic organism in the *Roseobacter* clade (21).

*A. crassostreae* is responsible for ROD outbreaks along the entire U.S. northeast coast, from New York to Maine (1, 24, 25). Isolates collected in Maine, Massachusetts, and New York showed  $\geq 99.8\%$  identity of the 16S rRNA genomic sequence (26).

Prior to this research, only the internal transcribed spacer (ITS) region and 16S rRNA gene sequences of *A. crassostreae* were publically available. Virulence factors responsible for *Roseovarius* Oyster Disease have yet to be uncovered.

### ***Roseovarius* Oyster Disease**

Mass mortalities caused by *Roseovarius* Oyster were first reported in the late 1980s. The disease has since been prevalent in hatchery raised juvenile oysters in the Northeast United States (1, 24, 25). However, this disease may not be isolated to only the United States as signs and symptoms identical to *Roseovarius* Oyster Disease have previously been reported in France (27, 28). Because ROD does not become apparent until water temperatures reach at least 20°C, outbreaks occur annually and only in the summer months (3, 29). Mortality rates in excess of 90% have previously been reported (3, 29). Mortality rate seems to be related to animal size and age since small juvenile oysters <25mm in shell length are more heavily impacted by the disease than

fully grown adults (3, 24, 29). Typical symptoms of ROD can be observed as excessive cupping of the left valve, uneven valve margins, lesions and retraction of the mantle, emaciated tissue, as well as conchiolin deposits (proteinaceous insoluble organic matrix (4, 30)) on the inner shell surface and overall retarded growth of juvenile oysters (1, 3, 21, 26, 29, 31, 32). Conchiolin deposits can range from mild to severe depending on size of the animal and severity of infection (Figure 2) (26). Myoepithelial and muscle degradation was observed in some affected oysters resulting in detachment of soft tissues from the shell (3). In addition, dense coccoid bodies can be observed in the epithelial tissue of affected oysters (3, 24, 33). Hemocyte infiltration of affected epithelial tissue has also been observed (1, 3, 24). This hemocyte infiltration is an indicator of microbial infections, as phagocytosis by hemocytes is one of the major immune responses of oysters to bacterial invasion (34-37). Signs of the disease are often not apparent until one week prior to mortality (24, 26, 31).

Conchiolin deposits may not be evident in very young oysters that are less than 10 mm in shell length (26). It has been proposed that very young oysters may not have the metabolic resources for rapid conchiolin formation (26). However, large adult oysters have been observed to grow large conchiolin depositions without any evidence of growth cessation or tissue damage (26) (Figure 2). Conchiolin formation may serve as a barrier to the invading microorganism. This barrier can isolate the organism and thus prevent it from reaching the soft tissue (3, 21, 24, 38).

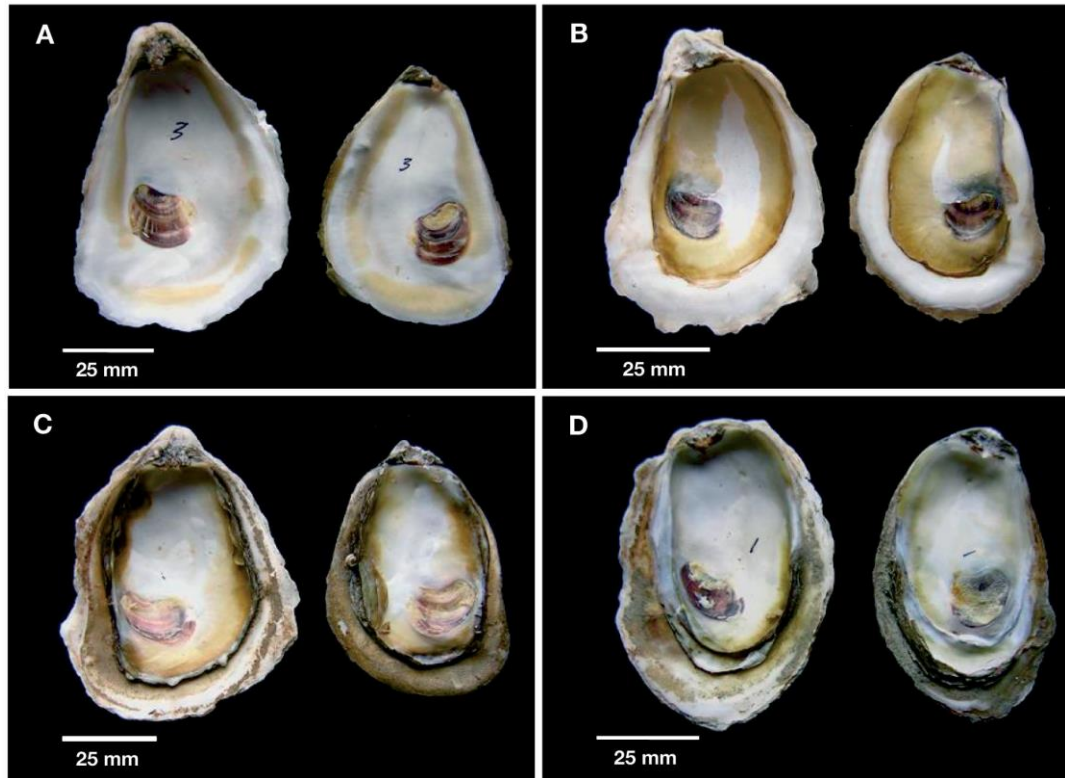


**Figure 2.** Conchiolin deposits on the inner shell surfaces of oysters affected by ROD. Conchiolin deposits may range from mild discolorations (A) to heavier deposits (B) and even multiple layers (C). Adult animals that suffer chronically from the disease may form successive ridges of conchiolin (D) (26). Figure from Maloy et al. (2007) (26).

## **Pathogen-Host interactions**

*A. crassostreae*-shaped organisms can be observed via *A. crassostreae*-specific immunofluorescent labeling within conchiolin deposits and on the mantle surface of juvenile oysters challenged with *A. crassostreae* (22, 28). *A. crassostreae* cells attached to and embedded in conchiolin deposits can also be visualized in infected animals by electron microscopy (21, 22, 28). SEM images show that *A. crassostreae* attaches to the oyster's inner shell surface by its polar end (21, 22) (Figure 3). In affected oysters that showed visible signs of ROD, the organism can be recovered from the inner shell in 89% and 95% of the left and right valves, respectively (21). However, in affected animals, *A. crassostreae* was isolated by culture from only 21% of pallial fluid samples and 47% of tissue surface samples (21). Of animals that tested positive for *A. crassostreae* by culture, ~ 66% of total CFUs cultured from the inner shell surface were identified as *A. crassostreae*, whereas 13.1% and 9% of total CFUs were identified as *A. crassostreae* in tissue surface samples and pallial fluid, respectively (21). These observations suggest that *A. crassostreae* prefers to colonize the oyster's inner shell surface over oyster tissues. Pallial fluid (fluid in pallial cavity) and extrapallial fluid (fluid in mantle cavity) are always in contact with the inner shell surface of oysters and conchiolin deposits form at the pallial line (edge of mantle) on the shell surface (1, 3, 7, 21, 29). Thus, pallial fluid may facilitate or even induce colonization of *A. crassostreae* to the shell surface.

Since oysters obtain food sources and nutrients directly from seawater, it is suspected that an exchange of oyster pallial and extrapallial fluid and ocean water occurs when oysters are feeding. The filter-feeding behavior of oysters may result in

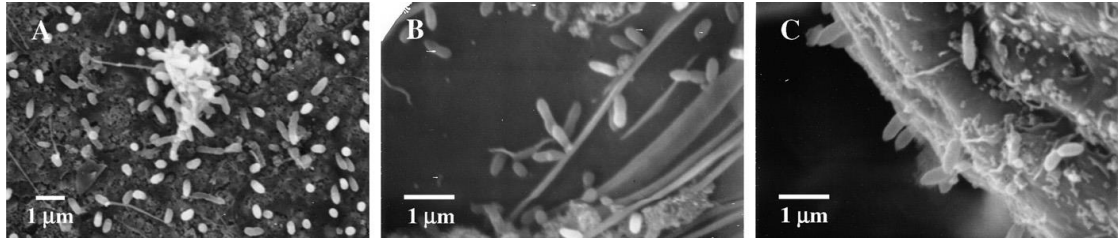


**Figure 3.** Scanning electron microscopy images of the inner shell and conchiolin deposits of oysters affected by ROD. (A) Attachment of colonizing bacteria to shell of ROD-affected oyster. (7200X). (B) Cells attached to conchiolin (12,000X) (C) side view of cells attached to conchiolin deposits (12,000X) (21). Figure from Boardman et al. (2008) (21).



the accumulation of bacteria from ocean waters inside the oyster (36, 39). Besides the shell, pallial fluid is one of the first parts of the oyster that marine organisms come in contact with when encountering the host. Pallial fluid may offer a nutrient source for *A. crassostreae* as well as *P. gallaeciensis* in the generally nutrient poor ocean water. As a result, pallial and extrapallial fluid may play an important role in disease onset and progression.

Previous research shows that virulence as well as growth of certain marine pathogens can be induced when the organism is exposed to mucus or mucus-like substances that can be found in the natural host. For example, growth rates of *Perkinsus marinus*, the causative agent of ‘dermo’ disease in oysters, were significantly increased when growth medium was supplemented with oyster mucus (40). Cultures of this organism that were supplemented with oyster pallial mucus appeared to be significantly more virulent in challenge experiments (40). Exposure to oyster pallial mucus was found to significantly increase the expression of putative virulence genes in *P. marinus* (41). Furthermore, previous research shows that the fish pathogen *V. anguillarum* grows rapidly in Nine Salt Solution supplemented with salmon gastrointestinal mucus (42-44). In addition, expression of the extracellular metalloprotease EmpA, a virulence factor of *V. anguillarum*, is induced by salmon intestinal mucus (42). Studies suggest that the alimentary tract containing the mucus is the site of amplification for *V. anguillarum* (43). Just as fish intestinal mucus is an excellent growth medium for *V. anguillarum* and induces expression of virulence factors, pallial fluid may represent a similar growth medium for *A. crassostreae* and *P. gallaeciensis* and might induce expression of virulence genes in the pathogen.

Metalloproteases and/or cytolysins are virulence factors that are secreted by many marine pathogens. The genomes of the two marine pathogens *V. anguillarum* and *V. coralliilyticus* encode multiple metalloprotease genes and both organisms produce hemolysins as virulence factors (42, 45, 46). *Vibrio cholerae*, *Vibrio vulnificus*, and *Pseudomonas aeruginosa* are known to secrete proteases as virulence factors (47-49). *P. marinus* secretes a serine-protease that is involved in virulence of ‘dermo’ in oysters (41, 50). Studies by Gomez-Leon et al. (2008) show that oyster hemocyte viability decreased when hemocytes were co-incubated with *A. crassostreae* (28). A similarly low viability of oyster hemocytes can be observed when hemocytes are treated only with extracellular products of the pathogen (28). These results infer that *A. crassostreae* produces an extracellular protein that kills the oyster hemocytes. Pore-forming cytolysins have been described in many Gram-negative bacteria (51) and might be the cause for this significant drop in hemocyte viability. Oyster pallial fluid may mimic the host environment and induce expression of these potential virulence factors. The expression of virulence genes can also be controlled by the stringent response. For example, virulence processes of *Pseudomonas aeruginosa* are tightly regulated by the organism’s ability to enter the stringent response because synthesis of virulence factors was impaired in a *relA* and *spoT* double mutant (52). Thus, a starvation induced stringent response may elicit the upregulation of virulence factors as can be observed in other organisms (53).

Substances that are naturally secreted by a host can also promote positive chemotaxis of pathogens. Bordas et al. (54) have shown that *V. anguillarum* demonstrates a strong chemotactic response towards gilt-head sea bream mucus. In

addition, chemotaxis is required for virulence and host colonization of the soilborne plant pathogen *Ralstonia solanacearum* (55). Since oyster pallial fluid is one of the first parts of the oyster that microorganisms encounter, it may stimulate a chemotaxis response in *A. crassostreae* and *P. gallaeciensis*.

#### ***Phaeobacter gallaeciensis* S4**

*P. gallaeciensis* S4 has been isolated from the inner shell surface of a healthy oyster (8). *P. gallaeciensis* is a short Gram-negative rod that can elongate and form rosettes in stationary phase (8). The organism is a strict aerobe and heterotrophic. It has one or two polar flagella and is an excellent biofilm former (9). *P. gallaeciensis* grows optimally at temperatures between 18 to 30 °C and prefers salinities of either 2 or 3%. *P. gallaeciensis* is a probiotic organism that has been shown to protect oyster larvae from bacterial pathogens (8). Oyster larvae that are pretreated with *P. gallaeciensis* show significantly increased survival rates when challenged with *A. crassostreae* CV919-312<sup>T</sup> or *Vibrio coralliilyticus* RE22 (8). While oyster larvae that were challenged with *A. crassostreae* or *V. coralliilyticus* resulted in only 14-31% survival, survival rates of oyster larvae that were first pretreated for 24 hr with S4 were significantly increased (Figure 4). Furthermore, *P. gallaeciensis* can protect cod and turbot larvae infected with *Vibrio anguillarum*, the causative agent of vibriosis (56, 57). This antagonistic effect of *Phaeobacter* against bacterial pathogens has been confirmed by surface attached *Phaeobacter* cells that are capable of killing *Vibrio anguillarum* in *in vitro* assays (58). These probiotic properties can be attributed to the organism's ability to produce secondary metabolites like the broad spectrum antibiotic

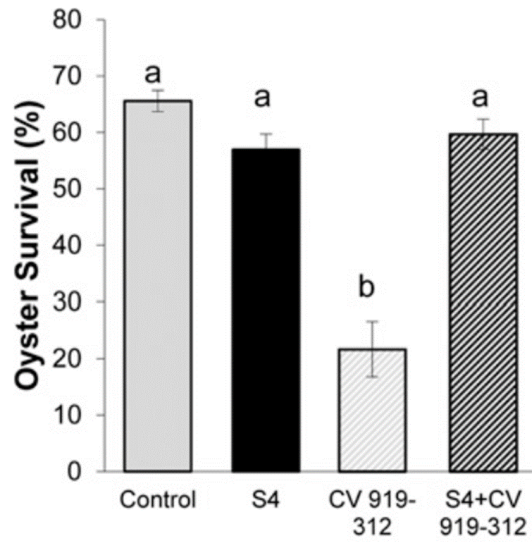


**Figure 4.** Effect of pre-incubation on survival of oyster larvae with *P. gallaeciensis* S4 ( $10^4$  CFU/ml) for 24 h before challenge with *A. crassostreae* CV919-312<sup>T</sup> ( $10^5$  CFU/ml). Different letters indicate statistical significance between treatments (8).

Figure from Karim et al. (2013) (8).

tropodithietic acid (TDA) as well as N-acyl homoserine lactones (AHLs), but also the organism's superior ability to form biofilms (9). The ability to form a thick biofilm is an essential part of the probiotic mechanism of *P. gallaeciensis*, not just by competing for adhesion sites and nutrients, but also to by preventing contact of pathogenic organisms with the host (9). Previous studies show that *P. gallaeciensis* S4 forms thick biofilms on glass surfaces under static culture conditions (9). In comparison, *A. crassostreae* forms much weaker biofilms with only 13.4% the amount of biofilm formed by *P. gallaeciensis* S4 (9) (Table 1). Similar results have been obtained for two other aquaculture pathogens, *V. coralliilyticus*, a pathogen of oyster larvae, and *V. anguillarum*, a fish pathogen (9). Additionally, previous studies have shown that TDA production by *P. gallaeciensis* plays a key role in the organism's probiotic activity because a TDA null mutant did not protect cod larvae challenged with *Vibrio anguillarum* as well as wild type did (56). Furthermore, the TDA null mutant did not reduce cell densities of *V. anguillarum* while wild type *Phaeobacter* significantly reduced or completely killed *V. anguillarum* in culture based systems (58).

In addition to biofilm formation and TDA production, AHLs have been shown to contribute to the probiotic effect of *P. gallaeciensis* against *V. coralliilyticus* by reducing transcription of *vtpB* and *vtpR*, two genes involved in protease activity of the pathogen (9). These AHLs are thought to disrupt the quorum-sensing pathway in *V. coralliilyticus* that is responsible for activating transcription of genes involved in protease activity (9).

**Table 1.** Biofilm formation under static conditions after 60 h incubation. Biofilm was quantified with crystal violet method. Crystal violet that was attached to cells forming a biofilm on glass tubes was measured at OD<sub>580</sub> (9). Figure from Zhao (2014) (9).

	<b>OD580</b>
<i>P. gallaeciensis</i> S4Sm	3.89±0.06
<i>R. crassostreae</i> CV919Sm	0.52±0.08 <sup>b</sup>
<i>V. anguillarum</i> NB10Sm	0.58±0.02 <sup>b</sup>
<i>V. coralliilyticus</i> RE22Sm	0.54±0.02 <sup>b</sup>

## Goals of this study

The overall goal of this study was to elucidate the physiological responses of *A. crassostreae* and *P. gallaeciensis* when exposed to oyster pallial fluid. In order to obtain nutrients it is suspected that an exchange of oyster pallial fluid and ocean water occurs when oyster are open (34, 59). When encountering the host, both organisms come in contact with the oyster shell and pallial fluid. Thus, pallial fluid may play an important role in colonization of oysters with *P. gallaeciensis* or *A. crassostreae*. Furthermore, pallial fluid may affect ROD onset and progression by *A. crassostreae*.

The first aim of this investigation was to determine the effects of pallial fluid on growth of *A. crassostreae* and *P. gallaeciensis* and establish a chemotactic response pattern of these organisms to oyster pallial fluid. *A. crassostreae* and *P. gallaeciensis* were both grown in pallial fluid and growth rates were compared to the traditional growth medium. Chemotaxis assays were performed to study chemotactic responses.

The second aim of this study was to investigate the effects of pallial fluid on biofilm formation of *A. crassostreae*. Biofilm assays with *A. crassostreae* and *P. gallaeciensis* were performed on various materials with and without supplementing the growth medium with pallial fluid.

The third aim was to obtain the genomic sequence of *A. crassostreae* CV919-312<sup>T</sup> and analyze it for potential virulence factors. The genome of *A. crassostreae* CV919-312<sup>T</sup> was sequenced and subsequently annotated by various software programs to identify potential virulence factors.

## REFERENCES

1. **Maloy AP, Ford SE, Karney RC, Boettcher KJ.** 2007. *Roseovarius crassostreae*, the etiological agent of Juvenile Oyster Disease (now to be known as *Roseovarius* Oyster Disease) in *Crassostrea virginica*. *Aquaculture* **269**:71-83.
2. **Davis CV, Barber BJ.** 1999. Growth and survival of selected lines of eastern oysters, *Crassostrea virginica* (Gmelin 1791) affected by juvenile oyster disease. *Aquaculture* **178**:253-271.
3. **Bricelj VM, Ford ES, Borrero FJ, Perkins FO, Rivara G, Hillman RE, Elston RA, Chang J.** 1992. Unexplained mortalities of hatchery-reared, juvenile oysters, *Crassostrea virginica* (Gmelin). *J Shellfish Res* **11**:331-347.
4. **Boettcher KJ, Barber BJ, Singer JT.** 1999. Use of antibacterial agents to elucidate the etiology of juvenile oyster disease (JOD) in *Crassostrea virginica* and numerical dominance of an  $\alpha$ -Proteobacterium in JOD-affected animals. *Appl Environ Microbiol* **65**:2534-2539.
5. **Anonymous.** 2014. Species Fact Sheets. Food and Agriculture Organization of the United Nations Fisheries and Aquaculture Department,
6. **Anonymous.** Aquaculture in the United States. [http://www.nmfs.noaa.gov/aquaculture/aquaculture\\_in\\_us.html](http://www.nmfs.noaa.gov/aquaculture/aquaculture_in_us.html). Accessed 8-11-15.
7. **Boettcher KJ, Geaghan KK, Maloy AP, Barber BJ.** 2005. *Roseovarius crassostreae* sp. nov., a member of the *Roseobacter* clade and the apparent cause of juvenile oyster disease (JOD) in cultured Eastern oysters. *Int J Syst Evol Microbiol* **55**:1531-1537.
8. **Karim M, Zhao W, Rowley D, Nelson D, Gomez-Chiarri M.** 2013. Probiotic Strains for Shellfish Aquaculture: Protection of Eastern Oyster, *Crassostrea virginica*, Larvae and Juveniles Against Bacterial Challenge. *J Shellfish Res* **32**:401-408.
9. **Zhao W.** 2014. Characterization of the Probiotic Mechanism of *Phaeobacter gallaeciensis* S4 Against Bacterial Pathogens University of Rhode Island.
10. **Luo H, Moran MA.** 2014. Evolutionary ecology of the marine *Roseobacter* clade. *Microbiol Mol Biol Rev* **78**:573-587.
11. **Buchan A, González JM, Moran MA.** 2005. Overview of the marine *Roseobacter* lineage. *Appl Environ Microbiol* **71**:5665-5677.
12. **Brinkhoff T, Giebel H-A, Simon M.** 2008. Diversity, ecology, and genomics of the *Roseobacter* clade: a short overview. *Arch Microbiol* **189**:531-539.
13. **Wagner-Dobler I, Biebl H.** 2006. Environmental biology of the marine *Roseobacter* lineage. *Annu Rev Microbiol* **60**:255-280.
14. **Slightom RN, Buchan A.** 2009. Surface colonization by marine *Roseobacters*: integrating genotype and phenotype. *Appl Environ Microbiol* **75**:6027-6037.
15. **Stocker R, Seymour JR, Samadani A, Hunt DE, Polz MF.** 2008. Rapid chemotactic response enables marine bacteria to exploit ephemeral microscale nutrient patches. *Proc Natl Acad Sci U S A* **105**:4209-4214.



16. **Moran MA, González JM, Kiene RP.** 2003. Linking a bacterial taxon to sulfur cycling in the sea: studies of the marine *Roseobacter* group. *Geomicrobiol J* **20**:375-388.
17. **Kiene RP, Linn LJ, Bruton JA.** 2000. New and important roles for DMSP in marine microbial communities. *J Sea Res* **43**:209-224.
18. **Dickschat JS, Zell C, Brock NL.** 2010. Pathways and substrate specificity of DMSP catabolism in marine bacteria of the *Roseobacter* clade. *ChemBioChem* **11**:417-425.
19. **Dang H, Li T, Chen M, Huang G.** 2008. Cross-ocean distribution of *Rhodobacterales* bacteria as primary surface colonizers in temperate coastal marine waters. *Appl Environ Microbiol* **74**:52-60.
20. **Tomich M, Planet PJ, Figurski DH.** 2007. The *tad* locus: postcards from the widespread colonization island. *Nat Rev Microbiol* **5**:363-375.
21. **Boardman CL, Maloy AP, Boettcher KJ.** 2008. Localization of the bacterial agent of juvenile oyster disease *Roseovarius crassostreae* within affected eastern oysters *Crassostrea virginica*. *J Invertebr Pathol* **97**:150-158.
22. **Boardman C.** 2005. Host-pathogen interactions between Eastern oysters (*Crassostrea virginica*) and the bacterial agent of juvenile oyster disease (*Roseovarius crassostreae*) The University of Maine.
23. **Park S, Park JM, Kang CH, Yoon JH.** 2015. *Aliiroseovarius pelagivivens* gen. nov., sp. nov., isolated from seawater, and reclassification of three species of the genus *Roseovarius* as *Aliiroseovarius crassostreae* comb. nov., *Aliiroseovarius halocynthiae* comb. nov. and *Aliiroseovarius sediminilitoris* comb. nov. *Int J Syst Evol Microbiol* **65**:2646-2652.
24. **Ford SE, Borrero FJ.** 2001. Epizootiology and pathology of juvenile oyster disease in the Eastern oyster, *Crassostrea virginica*. *J Invertebr Pathol* **78**:141-154.
25. **Barber BJ, Carnegie RB, Davis CV, Mook W.** 1996. Effect of Timing of Seed Deployment on Growth and Mortality of Oysters, *Crassostrea virginica*, Affected by Juvenile Oyster Disease (JOD). *J World Aquacult Soc* **27**:443-448.
26. **Maloy AP, Barber BJ, Boettcher KJ.** 2007. Use of the 16S-23S rDNA internal transcribed spacer of *Roseovarius crassostreae* for epizootiological studies of juvenile oyster disease (JOD). *Dis Aquat Org* **76**:151.
27. **Renault T, Chollet B, Cochenec N, Gerard A.** 2002. Shell disease in eastern oysters, *Crassostrea virginica*, reared in France. *J Invertebr Pathol* **79**:1-6.
28. **Gomez-Leon J, Villamil L, Salger SA, Sallum R, Remacha-Trivino A, Leavitt DF, Gomez-Chiarri M.** 2008. Survival of eastern oysters *Crassostrea virginica* from three lines following experimental challenge with bacterial pathogens. *J Shellfish Res* **32**:401-408.
29. **Davis CV, Barber BJ.** 1994. Size-dependent mortality in hatchery-reared populations of oysters, *Crassostrea virginica*, Gmelin 1791, affected by Juvenile Oyster Disease. *J Shellfish Res* **13**:137-142.

30. **Kennedy V, Newell R, Eble A.** 1996. The Eastern Oyster - *Crassostrea virginica*. Maryland Sea Grant College, University of Maryland System, College Park.
31. **Sunila I.** *Roseovarius* Oyster Disease. <http://www.ct.gov/doag/lib/doag/aquaculture/rod.pdf>. Accessed 3-12-15.
32. **Boettcher KJ, Barber BJ, Singer JT.** 2000. Additional Evidence that Juvenile Oyster Disease Is Caused by a Member of the Roseobacter Group and Colonization of Nonaffected Animals by *Stappia stellulata*-Like Strains. *Appl Environ Microbiol* **66**:3924-3930.
33. **Lewis EJ, Farley CA, Small EB, Baya AM.** 1996. A synopsis of juvenile oyster disease (JOD) experimental studies in *Crassostrea virginica*. *Aquat Living Resour* **9**:169-178.
34. **Allam B, Paillard C.** 1998. Defense factors in clam extrapallial fluids. *Dis Aquat Org* **33**:123-128.
35. **Song L, Wang L, Qiu L, Zhang H.** 2010. Bivalve Immunity, p 44-65. *In* Söderhäll K (ed), *Invertebrate Immunity*, vol 708. Springer US.
36. **Canesi L, Gallo G, Gavioli M, Pruzzo C.** 2002. Bacteria-hemocyte interactions and phagocytosis in marine bivalves. *Microsc Res Tech* **57**:469-476.
37. **Roch P.** 1999. Defense mechanisms and disease prevention in farmed marine invertebrates. *Aquaculture* **172**:125-145.
38. **Elston RA, Frelier P, Cheney D.** 1999. Extrapallial abscesses associated with chronic bacterial infections in the intensively cultured juvenile Pacific oyster *Crassostrea giga*. *Dis Aquat Org* **37**:115-120.
39. **Allam B, Carden WE, Ward JE, Ralph G, Winnicki S, Pales Espinosa E.** 2013. Early host-pathogen interactions in marine bivalves: Evidence that the alveolate parasite *Perkinsus marinus* infects through the oyster mantle during rejection of pseudofeces. *J Invertebr Pathol* **113**:26-34.
40. **Espinosa EP, Winnicki S, Allam B.** 2013. Early host-pathogen interactions in a marine bivalve: *Crassostrea virginica* pallial mucus modulates *Perkinsus marinus* growth and virulence. *Dis Aquat Org* **104**:237-247.
41. **Pales Espinosa E, Corre E, Allam B.** 2014. Pallial mucus of the oyster *Crassostrea virginica* regulates the expression of putative virulence genes of its pathogen *Perkinsus marinus*. *Int J Parasitol* **44**:305-317.
42. **Denkin SM, Nelson DR.** 1999. Induction of protease activity in *Vibrio anguillarum* by gastrointestinal mucus. *Appl Environ Microbiol* **65**:3555-3560.
43. **Olsson JC, Westerdahl A, Conway PL, Kjelleberg S.** 1992. Intestinal colonization potential of turbot (*Scophthalmus maximus*)-and dab (*Limanda limanda*)-associated bacteria with inhibitory effects against *Vibrio anguillarum*. *Appl Environ Microbiol* **58**:551-556.
44. **Garcia T, Otto K, Kjelleberg S, Nelson D.** 1997. Growth of *Vibrio anguillarum* in Salmon Intestinal Mucus. *Appl Environ Microbiol* **63**:1034-1039.
45. **Rock JL, Nelson DR.** 2006. Identification and characterization of a hemolysin gene cluster in *Vibrio anguillarum*. *Infect Immun* **74**:2777-2786.

46. **Spinard EK, L; Gomez-Chiarri, M; Rowley, D; Nelson, D.** 2015. Draft genome of the marine pathogen *Vibrio coralliilyticus* RE22 Genome Announc **3**.
47. **Booth B, Boesman-Finkelstein M, Finkelstein R.** 1983. *Vibrio cholerae* soluble hemagglutinin/protease is a metalloenzyme. Infect Immun **42**:639-644.
48. **Kothary MH, Kreger AS.** 1987. Purification and characterization of an elastolytic protease of *Vibrio vulnificus*. J Gen Microbiol **133**:1783-1791.
49. **Nicas TI, Iglewski BH.** 1985. The contribution of exoproducts to virulence of *Pseudomonas aeruginosa*. Can J Microbiol **31**:387-392.
50. **Peyre JFL, Schafhauser DY, Rizkalla EH, Faisal M.** 1995. Production of Serine Proteases by the Oyster Pathogen *Perkinsus marinus* (*Apicomplexa*) *In Vitro*. J Eukaryot Microbiol **42**:544-551.
51. **Welch RA.** 1991. Pore-forming cytolysins of gram-negative bacteria. Mol Microbiol **5**:521-528.
52. **Vogt SL, Green C, Stevens KM, Day B, Erickson DL, Woods DE, Storey DG.** 2011. The stringent response is essential for *Pseudomonas aeruginosa* virulence in the rat lung agar bead and *Drosophila melanogaster* feeding models of infection. Infect Immun **79**:4094-4104.
53. **Chatterji D, Ojha AK.** 2001. Revisiting the stringent response, ppGpp and starvation signaling. Curr Opin Microbiol **4**:160-165.
54. **Bordas MA, Balebona MC, Rodriguez-Maroto JM, Borrego JJ, Moriñigo MA.** 1998. Chemotaxis of Pathogenic *Vibrio* Strains towards Mucus Surfaces of Gilt-Head Sea Bream (*Sparus aurata* L.). Appl Environ Microbiol **64**:1573-1575.
55. **Yao J, Allen C.** 2006. Chemotaxis is required for virulence and competitive fitness of the bacterial wilt pathogen *Ralstonia solanacearum*. J Bacteriol **188**:3697-3708.
56. **D'Alvise PW, Lillebo S, Prol-Garcia MJ, Wergeland HI, Nielsen KF, Bergh O, Gram L.** 2012. *Phaeobacter gallaeciensis* reduces *Vibrio anguillarum* in cultures of microalgae and rotifers, and prevents vibriosis in cod larvae. PLoS One **7**:e43996.
57. **Planas M, Pérez-Lorenzo M, Hjelm M, Gram L, Uglenes Fiksdal I, Bergh Ø, Pintado J.** 2006. Probiotic effect in vivo of *Roseobacter* strain 27-4 against *Vibrio* (*Listonella*) *anguillarum* infections in turbot (*Scophthalmus maximus* L.) larvae. Aquaculture **255**:323-333.
58. **D'Alvise PW, Melchiorson J, Porsby CH, Nielsen KF, Gram L.** 2010. Inactivation of *Vibrio anguillarum* by attached and planktonic *Roseobacter* cells. Appl Environ Microbiol **76**:2366-2370.
59. **Pomeroy LR, Haskin HH.** 1954. The Uptake and Utilization of Phosphate Ions from Sea Water by the American Oyster, *Crassostrea virginica* (Gmel.). Biol Bull **107**:123-129.

## Manuscript I

**Publication status:** Unpublished; formatted according to guidelines of Applied and Environmental Microbiology (ASM).

**Title:** Physiological effects of oyster pallial fluid on *Aliiroseovarius crassostreae* CV919-312<sup>T</sup> and *Phaeobacter gallaeciensis* S4

**Authors:** Linda Kessner<sup>1</sup>, Marta Gomez-Chiarri<sup>2</sup>, David Rowley<sup>3</sup>, David Nelson<sup>1</sup>

Author affiliation: <sup>1</sup>Department of Cell and Molecular Biology, <sup>2</sup>Department of Fisheries, Animal and Veterinary Sciences, <sup>3</sup>Department of Biomedical and Pharmaceutical Sciences, University of Rhode Island, Kingston, RI 02881, USA

**Key Words:** *Roseovarius* oyster disease, oyster larvae, oyster juveniles, oyster pallial fluid

## ABSTRACT

*Roseovarius* Oyster Disease (formerly Juvenile Oyster Disease) has been the cause of high mortality rates in eastern oysters since the late 1980s. *Aliiroseovarius crassostreae*, previously known as *Roseovarius crassostreae*, is a Gram-negative  $\alpha$ -Proteobacterium and the causative agent of *Roseovarius* Oyster Disease. *Phaeobacter gallaeciensis* also is a Gram-negative  $\alpha$ -Proteobacterium and like *A. crassostreae* a member of the *Roseobacter* clade. *P. gallaeciensis* is a probiotic organism that has shown to significantly increase oyster larvae survival when challenged with *A. crassostreae*. Oyster pallial is always in contact with the mantle and inner shell surface of the oyster where the first signs of ROD are apparent. Additionally, *A. crassostreae* cells attach to the inner shell surfaces during the infectious process. In this study, we investigate the effects of oyster pallial fluid on physiological responses of *A. crassostreae* and *P. gallaeciensis*. Both organisms were able to grow in oyster pallial fluid, serving as a nutrient source. Pallial fluid was shown to be a chemoattractant for both organisms. A molecule >10 kDa seems to be responsible for the chemoattractive properties of oyster pallial fluid. These data suggest that oyster pallial fluid facilitates *A. crassostreae* or *P. gallaeciensis* colonization of oysters by attracting *A. crassostreae* cells towards the oyster and providing an excellent growth medium for the organism. Additionally, we show that biofilm formation of *A. crassostreae* on glass surfaces is increased when growth medium is supplemented with pallial fluid. Thus, pallial fluid enhances colonization of *A. crassostreae* by promoting biofilm formation, which may contribute to progression of the disease. However,

virulence mechanisms of *A. crassostreae* remain to be discovered as the organism does not seem to exhibit any extracellular hemolytic or proteolytic activities.

## INTRODUCTION

*Roseovarius* Oyster Disease (ROD) was first reported in the late 1980s and has since been the cause of high mortality rates for hatchery raised eastern oysters along the northeastern coast of the United States (1-3). ROD is a seasonal event with increasing rates during the summer months when water temperature rises to ~20°C (3-5). Typical signs of ROD include excessive cupping of the left valve, uneven valve margins, lesions and retraction of the mantle, emaciated tissue, as well as conchiolin deposits and overall retarded growth of juvenile oysters (1, 3, 4, 6-8). These clinical symptoms are often not apparent until one week prior to mortality (5, 6, 8).

In 2005, *Aliiroseovarius crassostreae*, *Roseovarius crassostreae* at the time, was identified as the causative agent of ROD (9). *A. crassostreae* is a marine Gram-negative  $\alpha$ -Proteobacterium and a member of the *Roseobacter* clade (9). The organism is motile via one or two flagella and has a polar tuft of fimbriae (9). *A. crassostreae* colonizes the inner shell surface of affected oysters where signs of the disease appear in form of conchiolin deposits (1, 3, 4, 7, 9). The oyster's mantle tissues and inner surfaces of the shell are in contact with pallial and extrapallial fluid. Since *A. crassostreae* primarily colonizes the inner shell surface of affected animals, pallial and extrapallial fluid may play a significant role in shell surface colonization of *A. crassostreae* (7). Furthermore, based on the primary clinical signs of ROD, Ford et al.

(5) suggested that the etiological agent responsible for the disease enters from the pallial cavity. Exact virulence mechanisms of this organism remain to be discovered.

Many marine pathogens secrete metalloproteases and/or hemolysins during pathogenesis (10-14). Gomez-Leon et al. (2008) (15) have shown that significantly lower survival rates of oyster hemocytes can be observed when hemocytes are challenged with *A. crassostreae*. Interestingly, similar mortality rates were observed when oyster hemocytes were treated with only extracellular proteins from the organism (15). These results suggest that *A. crassostreae* secretes a protein that kills the oyster hemocytes, the oyster's primary immune cells. This extracellular protein could be either a protease or a molecule with hemolytic or cytotoxic properties. Expression of these potential virulence factors might be induced by exposure to an environment that mimics the milieu found in the natural host, i.e. pallial fluid. Alternatively, a starvation induced stringent response has been shown to induce expression of virulence genes in other pathogenic bacteria (16). Thus, any possible extracellular cytolytic and proteolytic activity of *A. crassostreae* needs to be characterized under various environmental conditions.

*Phaeobacter gallaeciensis* is also a Gram-negative  $\alpha$ -Proteobacterium and member of the *Roseobacter* clade (17). *P. gallaeciensis* is a probiotic organism and can protect oyster larvae from pathogens. Oyster larvae that are pre-treated with *P. gallaeciensis* have significantly higher survival rates when challenged with *A. crassostreae* (18). *P. gallaeciensis* S4 was originally isolated from the inner shell surface of a healthy oyster (18). *Roseobacter* clade members, including *P. gallaeciensis*, are excellent colonizers of marine surfaces (19). *P. gallaeciensis* forms

a thick biofilm when grown under static culture conditions (18). Furthermore, Zhao et al. (2014) have shown that biofilm formation is an important characteristics for the probiotic activity of *P. gallaeciensis* (20).

Previous research shows that natural host secretions may serve as a nutrient source for marine pathogens (10, 21, 22). Pales Espinosa et al. (2013) showed that growth rates of oyster pathogen *Perkinsus marinus*, the causative agent of ‘dermo’ disease, were significantly increased when growth medium was supplemented with mantle mucus (21). Additionally, virulence of *P. marinus* significantly increased in challenge experiments when cultures were supplemented with oyster pallial mucus (21). As a result, pallial fluid may represent an excellent growth medium for *A. crassostreae* and *P. gallaeciensis* and might induce expression of virulence genes in the pathogen.

Oyster pallial fluid may not only affect virulence, but also initial colonization of oysters by *A. crassostreae*. Because oyster pallial fluid is one of the first parts of the oyster that *A. crassostreae* and *P. gallaeciensis* come in contact with, it may serve as a chemotactic agent. Chemotaxis towards the host or molecules secreted by the host has been demonstrated in various pathogenic bacteria (23, 24). As a result, oyster pallial fluid may elicit a chemoattractive response in *A. crassostreae* and *P. gallaeciensis*.

In this study, we determine whether oyster pallial fluid is a nutrient source and growth medium for *A. crassostreae* and *P. gallaeciensis* and if it can serve as a chemoattractant. *A. crassostreae* was tested for potential virulence factors like hemolysins as well as extracellular protease activity. Additionally, we assess the



effects of oyster pallial fluid on biofilm formation by *A. crassostreae* and *P. gallaeciensis*.

## MATERIALS AND METHODS

### Bacterial strains and growth conditions

*A. crassostreae* CV919-312<sup>T</sup> was originally isolated from a ROD-affected oyster during the 1997 epizootic in the Damariscotta River in Maine (25). *P. gallaeciensis* S4 was isolated from the inner shell surface of a healthy oyster (18). Spontaneous streptomycin resistant mutants of both organisms were used for all experiments described in this study. Both organisms were grown in Yeast-Peptide broth plus 3% sea salt (YP30) (5 g/L peptone, 1 g/L yeast extract, 30 g/L sea salt, Instant Ocean) in a shaking water bath (175 rpm) at 27°C. In addition, both organisms were grown in oyster pallial fluid (see below) in a shaking water bath (175 rpm) at 27°C. A single isolated colony was picked and grown overnight in YP30 supplemented with streptomycin (200 µg/ml). Stationary phase cultures were back-diluted 1:1000 into either 2 ml YP30 or 2 ml prepared pallial fluid plus streptomycin (200 µg/ml). Viable cell counts were taken by dilution series and spot plating 10 µl in triplicate on YP30 agar plates supplemented with streptomycin (200 µg/ml).

### Collection and analysis of oyster pallial fluid

Oysters raised in Potter Pond in South Kingstown, Rhode Island, were generously donated by Perry Raso from the Matunuck Oyster Bar. Oyster pallial fluid was prepared by a modified process that is based on the methods described by Pales Espinosa et al. (2009) (26). For this study, oyster pallial fluid was collected on

separate occasions. One batch was collected in the late fall (October 30, 2014) and will be referred to as oyster pallial fluid #1 (opf#1) throughout this study, while the second batch was collected in the spring (April 1, 2015) and will be referred to as opf #2.

The oysters were shucked and the pallial fluid and extrapallial fluid removed with a 16-gauge needle and syringe. While pallial fluid is located within the pallial cavity of oysters, extrapallial fluid can be found between the external epithelium of the mantle and the inner surface of the shell (27, 28). Pooled pallial and extrapallial fluid (here referred to as pallial fluid) was centrifuged twice at 10,500×g for 10 min to remove any sediments, shell debris, as well as some microorganisms. The supernatant was then passed through successively smaller filters (MF-Millipore™ membrane filters, mixed cellulose esters) with the final filter pore size of 0.22 µm. Pallial fluid was stored at -20°C until use. The Bradford assay was used to determine protein concentration of oyster pallial fluid as a representation of overall pallial fluid concentration. Pallial fluid was tested for carbohydrate content by the phenol-sulfuric acid assay as described by Masuko et al. (2005) (29) with the exception that 96-well plate was placed in a floating thin plastic tray and incubated for 30 min in a 90°C water bath. In addition, pallial fluid was analyzed by HPLC for free unbound amino acids and tested by Ion Chromatography for monosaccharides and oligosaccharides (< 7-mers). In order to separate pallial fluid contents by molecular weight, 0.5 ml of pallial fluid was centrifuged for 15 min in Amicon Ultra-0.5 centrifugal filter units (Millipore) according to manufacturer's recommendations. Centrifugal filter units with a Nominal Molecular Weight Limit of 10 kDa were used for this purpose.

### **Hemolytic activity of *A. crassostreae***

*A. crassostreae* was tested for hemolytic activity by toothpicking isolated colonies on various agar plates that were supplemented with 5% heparinized fish blood (rainbow trout). Agar plates supplemented with fish blood were inoculated within 1-2 h after being poured in order to ensure that red blood cells were intact at time of use. In order to test the effects of various environmental conditions on hemolytic activity agar plates containing 5% fish blood in YP30, YP30 supplemented with pallial fluid (0.5 mg/ml protein from pallial fluid, opf #1), nine salt solution (NSS) (30), and marine minimal media (3M) (31) were used to test *A. crassostreae* for patterns of hemolysis. Agar plates were incubated for 3 d at 27°C and every day plates were observed for hemolysis. Pictures were taken of agar plates that were backlit with fluorescent white light.

### **Extracellular protease activity**

Protease activity in *A. crassostreae* culture supernatant was determined by the azocasein protease activity assay as described by Denkin and Nelson (1999) (10). Stationary phase cultures grown in YP30 were washed twice with YP30 and then backdiluted (2-fold dilution) into fresh YP30 or opf #2. Briefly, culture supernatant was obtained by centrifuging (10 min at 12,000 × g) 1 ml of log or stationary phase *A. crassostreae* in YP30 or YP30 supplemented with pallial fluid (1.75 mg/ml protein from pallial fluid, opf #2). Pallial fluid was previously boiled for 10 min (100°C) to eliminate any inherent protease activity. *Vibrio coralliilyticus* RE22 culture was used as a positive control. Supernatant (100 µl) was incubated with 100 µl azocasein (6

mg/ml dissolved in Tris-HCl [50 mM pH 8.0] containing 0.04% NaN<sub>3</sub>) at 27°C for 30 min. The reaction was terminated by adding 400 µl trichloroacetic acid (10% [wt/vol]). The reaction was incubated for 2 min at room temperature and centrifuged at 12,000 × g for 8 min to remove unreacted azocasein. The resulting supernatant (500 µl) was suspended in 700 µl 525mM NaOH and the absorbance of azopeptides in supernatant was measured at OD<sub>442</sub> using the Versa-Max microplate spectrophotometer (Molecular Devices). Additionally, viable cell counts of cultures were determined at each time point by serial dilution and spot plating (10 µl in triplicate). Protease activity units were calculated using the following equation: protease activity units=[1,000 × (OD<sub>442</sub>)/CFU] × (10<sup>9</sup>). Blank controls were prepared for each sample by boiling culture supernatant for 10 min at 100°C. Trichloroacetic acid was added immediately after combining azocasein and blank control supernatant.

### **Chemotaxis assay**

Chemotaxis was determined by using a modification of the method described by Adler (32). Stationary phase *A. crassostreae* or *P. gallaeciensis* cells were diluted into artificial sea water (30 g L<sup>-1</sup> of ocean salt, Instant Ocean) (1000-fold dilution). This cell suspension (10 ml) (~2×10<sup>6</sup> CFU/ml) was placed in a sterile petri dish. Through a small hole in the lid of the petri dish, the cells were exposed to a microcapillary tube containing 10 µl of pallial fluid that had been diluted to a protein concentration of 3 mg/ml (opf #1 and 2). As a control, a microcapillary tube filled with 10 µl of artificial seawater was placed in the petri dish cell suspension 180° opposite of the experimental microcapillary tube. After a 30 min incubation, the

pipettes were removed from the bacterial cell suspension and serially diluted with 3% artificial seawater and spot plated (10  $\mu$ l) in triplicate on YP30 agar plates containing 200  $\mu$ g/ml streptomycin. Plates were incubated for 2 d and the colonies counted to determine the number of cells that were present in each microcapillary tube. Data was expressed in colony forming units per microcapillary tube. In addition, individual amino acids (L-serine, L-alanine, glycine, L-proline) suspended in artificial seawater or suspensions of multiple amino acids that were detected by HPLC in pallial fluid were tested for their chemoattractive properties at concentrations similar to levels measured in pallial fluid (1 mM for L-serine (Sigma-Aldrich), L-alanine (Sigma-Aldrich), glycine (Fisher Scientific), and L-proline (Sigma-Aldrich)). The remaining amino acids were suspended in artificial seawater at 0.1 mM concentrations and tested as a cocktail (aspartate (Sigma-Aldrich), valine (ICN Biomedicals), methionine (Sigma-Aldrich), lysine (Sigma-Aldrich), isoleucine (ICN Biomedicals), leucine (Sigma-Aldrich), phenylalanine (Sigma-Aldrich), histidine (Sigma-Aldrich)). Pallial fluid (opf #2) separated by molecular weight cut off centrifugal filter units (10kDa) was also tested by this assay. The retentate containing molecules  $\geq$ 10kDa was further diluted (7.5-fold) to obtain their approximate natural concentrations in pallial fluid. The flow through containing molecules <10kDa was tested undiluted.

### **Biofilm formation**

Biofilm formation was determined using a modified version of the crystal violet staining method described by Belas et al. (2009) (33). Bacterial cultures were grown to stationary phase as described above. YP30 (2 ml) was placed in 15 $\times$ 150 mm

borosilicate (Pyrex) glass tubes, polypropylene tubes (15ml, Celltreat), or polystyrene tubes (17×100 mm, USA-Scientific). The broth was then inoculated with a 2 µl stationary phase culture (1:1000 dilution) of either *A. crassostreae* or *P. gallaeciensis* and incubated at 27°C without shaking. The volume of YP30 broth was adjusted for treatment groups that were supplemented with oyster pallial fluid (opf #1, protein concentration of pallial fluid added: 0.05 mg/ml, 0.1 mg/ml, 0.2 mg/ml, 0.5 mg/ml, 1 mg/ml, or 2 mg/ml) in order to obtain a total volume of 2 ml, while controls were grown in YP30 broth only. In addition, *A. crassostreae* and *P. gallaeciensis* were grown in pallial fluid alone. After incubating the cultures for 24 h at 27°C, the liquid cultures were removed and the glass tubes were gently washed twice with artificial sea water to remove loosely attached cells. Cells attached to the glass tubes were stained by adding 2 ml of 0.2% crystal violet solution and incubated at room temperature for 20 min. The crystal violet solution was then carefully removed without disturbing the biofilm and the glass tubes were washed twice with artificial seawater. The biofilm-bound crystal violet was eluted with 95% ethanol for 30 min and the optical density (OD) of the eluted crystal violet was measured at 580 nm by spectrophotometry using a Versa-Max microplate reader (Molecular Devices). Treatment and control groups were compared by their corresponding OD<sub>580</sub> values.

Cell densities of planktonic *A. crassostreae* in each tube were determined from culture medium after the 24 h incubation step. Culture medium was gently withdrawn with a 2 ml serological pipette and placed into a sterile 2 ml microcentrifuge tube. This culture medium was then serially diluted with artificial seawater and spot plated

(10  $\mu$ l/spot) in triplicate on YP30 agar plates containing 200  $\mu$ g/ml streptomycin. After a 2 d incubation, colonies were counted and CFU/ml determined.

### **Statistical analysis**

Statistical data analysis between the individual treatment groups and the control was performed using the Student's T-test. Data with  $p < 0.05$  was considered to be statistically significant.

## **RESULTS**

### **Analysis of pallial fluid**

Bradford assay results show that the protein concentration of opf #1 was 4 mg/ml while opf #2 contained 3.5 mg/ml protein (Table 1).

Analysis of both batches of untreated pallial fluid by HPLC revealed the presence of 12 different amino acids in concentrations ranging from 4 to 2200  $\mu$ M. These are free amino acids that were detected in pallial fluid and not amino acids that resulted from the hydrolysis of proteins. The four most abundant amino acids were found to be serine, glycine, alanine, and proline (Table 2).

Phenol-sulfuric acid assay results revealed that opf #1 contained 1.1 mg/ml of carbohydrates and opf #2 contained 0.6 mg/ml of carbohydrates (Table 1). Ion Chromatography of opf #2 only detected 31.9  $\mu$ g/L glucose to be present; no other mono- or oligosaccharides were identified by this method. Ion chromatography was not performed with opf #1.

**Table 1.** Protein, carbohydrate, and glucose concentrations of two batches of pallial fluid. Protein concentration was determined by Bradford assay and carbohydrate concentration was determined by phenol-sulfuric acid assay. Glucose concentration was tested by ion chromatography for opf #2. Opf #1 was collected on October 30, 2014 and opf #2 was collected on April 1, 2015.

<b>Constituent of oyster pallial fluid</b>	<b>Opf #1</b>	<b>Opf #2</b>
<b>Protein concentration in mg/ml</b>	3.5	4.0
<b>Carbohydrate concentration in mg/ml</b>	1.1	0.6
<b>Glucose concentration in <math>\mu\text{g/L}</math></b>	—*	31.9

\*Glucose concentration of opf #1 was not tested.



**Table 2.** HPLC data of free amino acids present in both batches of oyster pallial fluid collected on two separate occasions. Concentrations are shown in  $\mu\text{M}$ .

<b>Amino Acid</b>	<b>Opf #1 (<math>\mu\text{M}</math>)</b>	<b>Opf #2 (<math>\mu\text{M}</math>)</b>
Serine	757	1562
Glycine	978	2160
Alanine	1139	1442
Proline	517	952
Aspartate	236	516
Valine	142	172
Methionine	64	56
Lysine	255	381
Isoleucine	433	74
Leucine	28	79
Phenylalanine	4	48
Histidine	unknown	unknown

### **Growth of *A. crassostreae* in oyster pallial fluid**

Our results show that oyster pallial fluid is a good growth medium for both organisms with growth rates that are comparable to growth in YP30 (Figure 1 and 2). When *A. crassostreae* was grown in YP30 the shortest generation time observed was ~71 min while the average generation time was ~79 min. The shortest generation time when grown in pallial fluid (opf #1) was ~66 min whereas the average generation time was determined to be 94 min (Table 3). Additionally, when grown in pallial fluid, *A. crassostreae* reached a density ~2-fold higher than in YP30 ( $3.88 \times 10^9$  in pallial fluid vs  $1.99 \times 10^9$  in YP30).

*A. crassostreae* grown in opf #2 grew as well as in opf #1. The fastest generation time in opf #2 was ~68 min and the average generation time was ~102 min (Table 3).

### **Growth of *P. gallaeciensis* in oyster pallial fluid**

Like *A. crassostreae*, *P. gallaeciensis* grew well in oyster pallial fluid (Figure 2). The shortest generation time in YP30 was determined to be 73 min while the shortest generation time in opf #1 was ~96 min (Table 4). The average generation time in YP30 was 120 min and 138 min in opf #1.

### **Hemolytic activity**

No hemolytic activity against fish erythrocytes by *A. crassostreae* was detected in any of the four conditions tested (Figure 3). Dark zones around inoculum represent colony growth after 2 d.

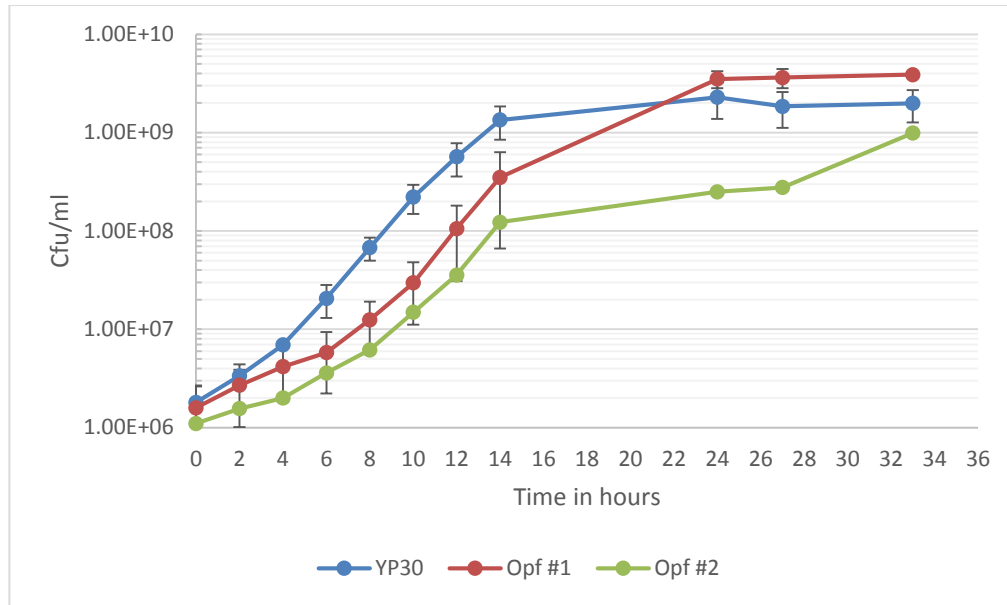


**Figure 1:** Growth of *A. crassostreae* in YP30, opf #1, and opf #2. Data for YP30 and opf #1 show the averages of three biological replicates. At each time point viable cell counts were obtained by dilution series and spot plating 10  $\mu$ l in triplicate. Data for opf #2 represents one trial only. Error bars equal one standard deviation.

**Table 3.** Generation times of *A. crassostreae* in YP30, pallial fluid collected on Oct-30-2014 (opf #1), and pallial fluid collected on Apr-1-2015 (opf #2). Data for YP30 and opf #1 is based on three biological replicates. Generation time for opf #2 represents one trial only.

	<b>YP30</b>	<b>Opf #1</b>	<b>Opf #2</b>
<b>shortest generation time in min<sup>1</sup></b>	70.6	65.9	67.7
<b>average generation time in min<sup>2</sup></b>	79.5	94.4	101.6

<sup>1</sup>Shortest generation time was determined between 6 h and 8 h timepoints for YP30, between 10 h and 12 h for opf #1, and between 12 h and 14 h for opf #2.

<sup>2</sup>Average generation times were determined between 4 h and 14 h timepoints in all three conditions.

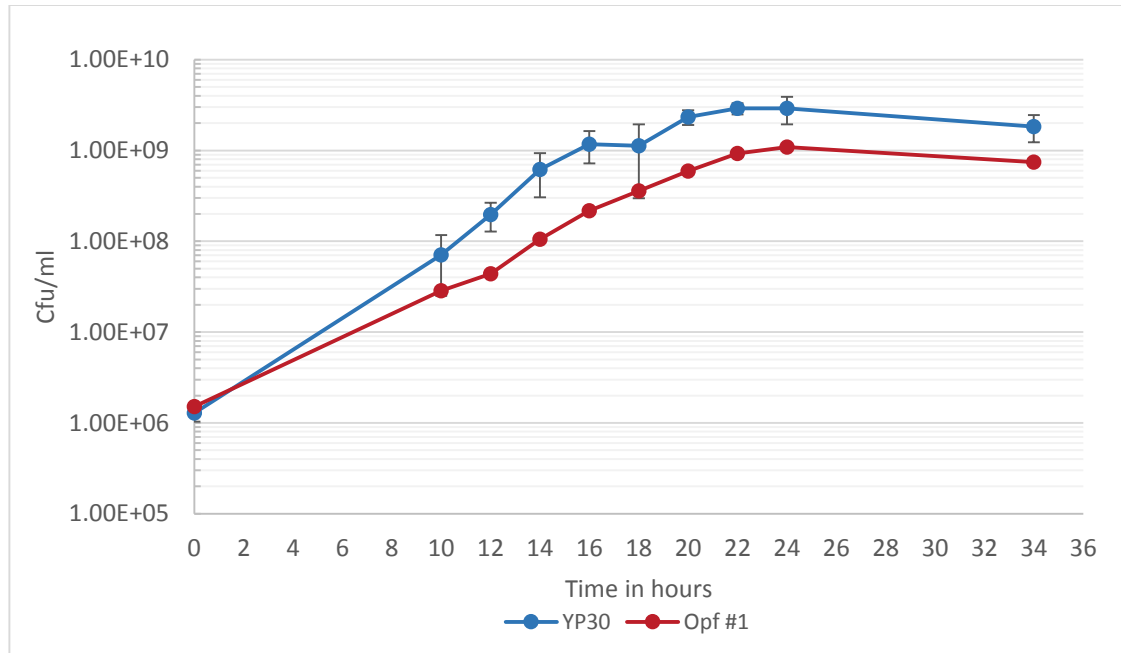


**Figure 2.** Growth of *P. gallaeciensis* in YP30 and opf #1. Data for YP30 and opf #1 show the average values of three biological replicates. At each time point viable cell counts were obtained by dilution series and spot plating 10  $\mu$ l in triplicate. Error bars for YP30 data equal one standard deviation.

**Table 4.** Generation times of *P. gallaeciensis* in YP30 and pallial fluid (opf #1). Data is based on three biological replicates.

	YP30	Opf #1
<b>shortest generation time in min<sup>1</sup></b>	73.0	95.9
<b>average generation time in min<sup>2</sup></b>	119.6	137.9

<sup>1</sup>Shortest generation times were determined between 12 h and 14 h timepoints for both YP30 and opf #1.

<sup>2</sup>Average generation times were determined between 10 h and 20 h timepoints.

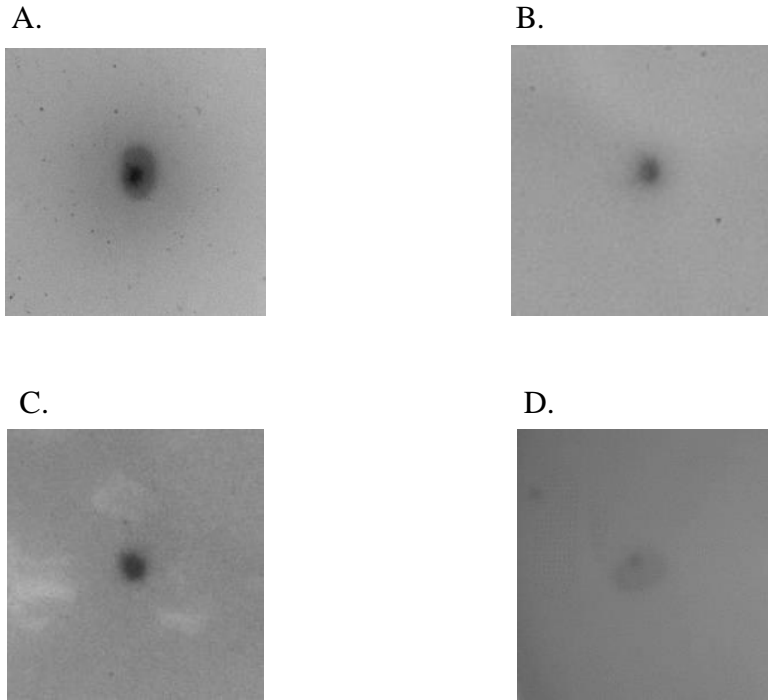


**Figure 3.** *A. crassostreae* growth on agar plates supplemented with 5 % fish blood after 2 d incubation. **A.** YP30 + 5% fish blood **B.** NSS agar + 5% fish blood **C.** 3M agar + 5% fish blood **D.** YP30 + 5% fish blood + pallial fluid (0.5mg/ml protein from pallial fluid). Darker zones around inoculum indicate growth by *A. crassostreae* and does not represent hemolysis.

### **Extracellular protease activity**

The highest amount of extracellular protease activity for the positive control organism *Vibrio coralliilyticus* was observed at 6 h with 100 protease activity units. While a low protease activity for *A. crassostreae* under both conditions was observed, these results are negligible and cannot be attributed to any significant extracellular protease activity (Table 5).

### **Chemotaxis of *A. crassostreae* and *P. gallaeciensis***

Chemotaxis assay results showed that pallial fluid (opf #2, diluted to 3.0 mg/ml protein) is a chemoattractant for both *A. crassostreae* and *P. gallaeciensis*. Microcapillary tubes filled with pallial fluid contained almost 8 times more *A. crassostreae* cells than tubes filled with artificial sea water ( $p=0.001$ ) (Figure 4) while microcapillary tubes filled with pallial fluid attracted almost 5 times more *P. gallaeciensis* cells than control tubes filled with artificial sea water ( $p=0.001$ ) (Figure 5). HPLC analysis of pallial fluid revealed that numerous free amino acids were present in pallial fluid. Early chemotaxis experiments performed by Mesibov and Adler (1972) (34) showed that *Escherichia coli* exhibited positive chemotaxis to multiple amino acids including alanine, serine, and glycine. Since these and other amino acids have been identified in pallial fluid, we tested all 12 amino acids detected in pallial fluid for their chemottractive properties using *A. crassostreae* and *P. gallaeciensis*. Neither *A. crassostreae* nor *P. gallaeciensis* showed any attraction towards the amino acids tested (Figures 4 and 5). An amino acid cocktail containing

**Table 5.** Extracellular protease activity units of *A. crassostreae* grown in YP30 and YP30 supplemented with opf #2 (1.75 mg/ml of protein from pallial fluid). Washed stationary phase cultures grown in YP30 were diluted into fresh YP30 or opf #2 (2-fold dilution) and incubated at 27°C under shaking conditions (175 rpm). Extracellular protease activity was determined at 0, 3, 6, and 24 h. *V. coralliilyticus* was used as a positive control.

Organism	Time in hours			
	0	3	6	24
<i>A. crassostreae</i> in YP30	0	0	1	3
<i>A. crassostreae</i> in YP30 + opf #2	6	4	1	4
<i>V. coralliilyticus</i> in YP30	4	81	100	73



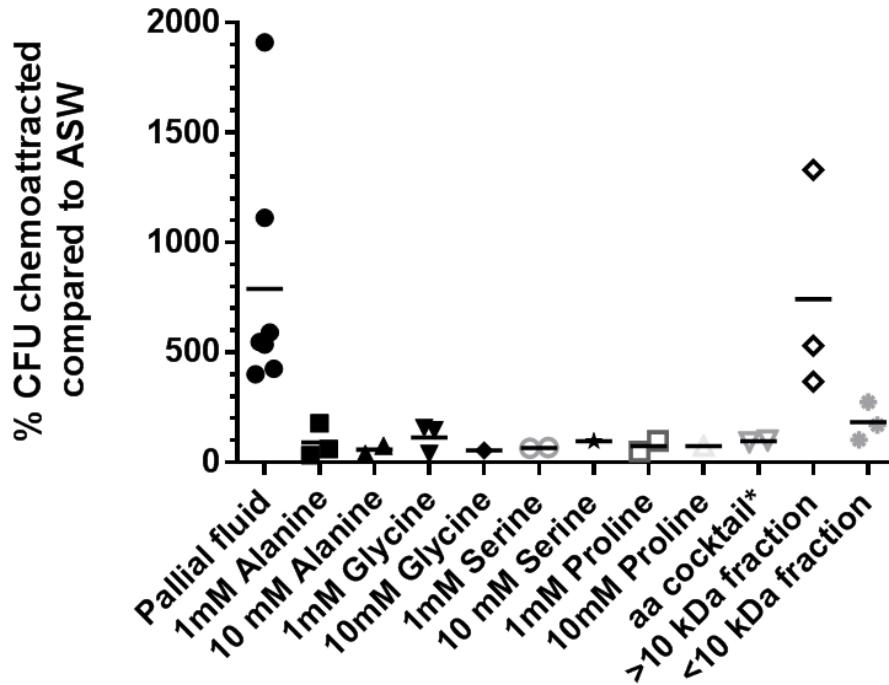


**Figure 4.** Chemotaxis assay results of *A. crassostreae*. Microcapillary tubes filled with 10  $\mu$ l artificial sea water, 10  $\mu$ l pallial fluid (standardized to 3 mg/ml protein), or the appropriate amino acid were placed in artificial sea water containing *A. crassostreae* at a cell density  $\sim 2 \times 10^6$  CFU/ml. After 30 min microcapillary tube contents were serially diluted and plated on YP30 agar + streptomycin.\*Amino acid cocktail contains 0.1mM aspartate, 0.1mM valine, 0.1mM methionine, 0.1mM lysine, 0.1mM isoleucine, 0.1mM leucine, 0.1mM phenylalanine, 0.1mM histidine.

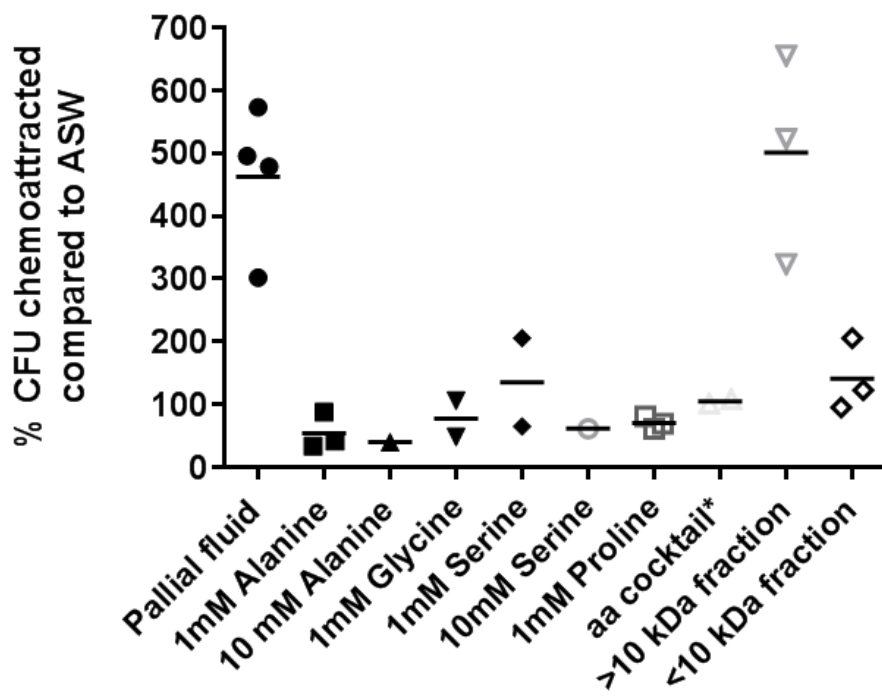


**Figure 5.** Chemotaxis assay results of *P. gallaeciensis*. Microcapillary tubes filled with 10  $\mu$ l artificial sea water, 10  $\mu$ l pallial fluid (standardized to 3 mg/ml protein), or the appropriate amino acid were placed in artificial sea water containing *P. gallaeciensis* at a cell density  $\sim 2 \times 10^6$  CFU/ml. After 30 min microcapillary tube contents were serially diluted and plated on YP30 agar + streptomycin.\*Amino acid cocktail contains 0.1mM aspartate, 0.1mM valine, 0.1mM methionine, 0.1mM lysine, 0.1mM isoleucine, 0.1mM leucine, 0.1mM phenylalanine, 0.1mM histidine.

0.1mM L-aspartate, 0.1mM L-valine, 0.1mM L-methionine, 0.1mM L- lysine, 0.1mM L-isoleucine, 0.1mM L-leucine, 0.1mM L-phenylalanine, and 0.1mM L-histidine suspended in artificial sea water did not serve as a chemoattractant when compared to artificial sea water alone (Figures 4 and 5).

After pallial fluid was separated by molecular weight using centrifugal filter units (10kDa), the diluted retentate containing molecules  $\geq 10$  kDa showed chemoattractive properties. *A. crassostreae* cells in the microcapillary tube with  $\geq 10$  kDa retentate were 8-times greater in number when compared to the control. *P. gallaeciensis* was also attracted to this fraction, showing 5-fold more cells in the microcapillary tube containing the  $\geq 10$  kDa retentate than the artificial sea water tube. The fraction containing molecules  $< 10$  kDa did not reveal any significant chemoattractive properties (Figures 4 and 5).

### **Biofilm formation of *A. crassostreae* and *P. gallaeciensis***

Biofilm assay results revealed that the addition of pallial fluid significantly increased biofilm formation of *A. crassostreae*. Without the addition of pallial fluid *A. crassostreae* produced no or very little biofilm (Figure 6). Increased amounts of pallial fluid and thus protein from pallial fluid resulted in increasing amounts of biofilm formed by the organism until a saturation point was reached at 0.5 mg/ml of protein added from pallial fluid (Figure 6). This increased amount of biofilm from cultures that were supplemented with 0.5 mg/ml protein from pallial fluid was statistically significant when compared to biofilm formation of cultures grown in YP30 only ( $p=0.0004$ ). Amounts  $> 0.5$  mg/ml of pallial fluid seemed to increase variation in

amount of biofilm formed. Pallial fluid alone (4 mg/ml in Figure 6) showed a large standard deviation ( $p=0.04$ ) indicating an increase in variability. Additionally, *A. crassostreae* cells grown statically in pallial fluid alone seem to form rosette-like morphologies when viewed under the microscope (Figure 7).

With exception of *A. crassostreae* grown in pallial fluid alone, planktonic cell densities ranged from  $7.5 \times 10^8$  to  $9.7 \times 10^8$  CFU/ml. Planktonic *A. crassostreae* concentration during biofilm formation in glass tubes in pallial fluid alone was  $4.3 \times 10^8$  CFU/ml (Figure 8).

The previously determined optimal addition of 0.5 mg/ml protein from pallial fluid for increased biofilm formation was used to test and compare biofilm formation of both *A. crassostreae* and *P. gallaeciensis* in polypropylene, polystyrene, and glass tubes. Again, a significant increase in biofilm formation was observed for *A. crassostreae* grown in glass tubes ( $p=0.0027$ ) (Figure 9). However, no significant increase in biofilm was observed in polypropylene, nor polystyrene tubes when compared to glass tubes. Additionally, no significant difference in biofilm formation in polypropylene and polystyrene tubes was detected when growth medium was supplemented with pallial fluid versus un-supplemented YP30 (Figure 9).

*P. gallaeciensis* did not form an increased amount of biofilm when the growth medium was supplemented with pallial fluid (Figure 10). The amount of biofilm produced by *P. gallaeciensis* was not affected by the addition of pallial fluid. However, biofilm formation is enhanced when the organism is grown in polypropylene ( $p=0.035$ ) or polystyrene ( $p=0.039$ ) tubes compared to biofilm formation in glass tubes (Figure 10).

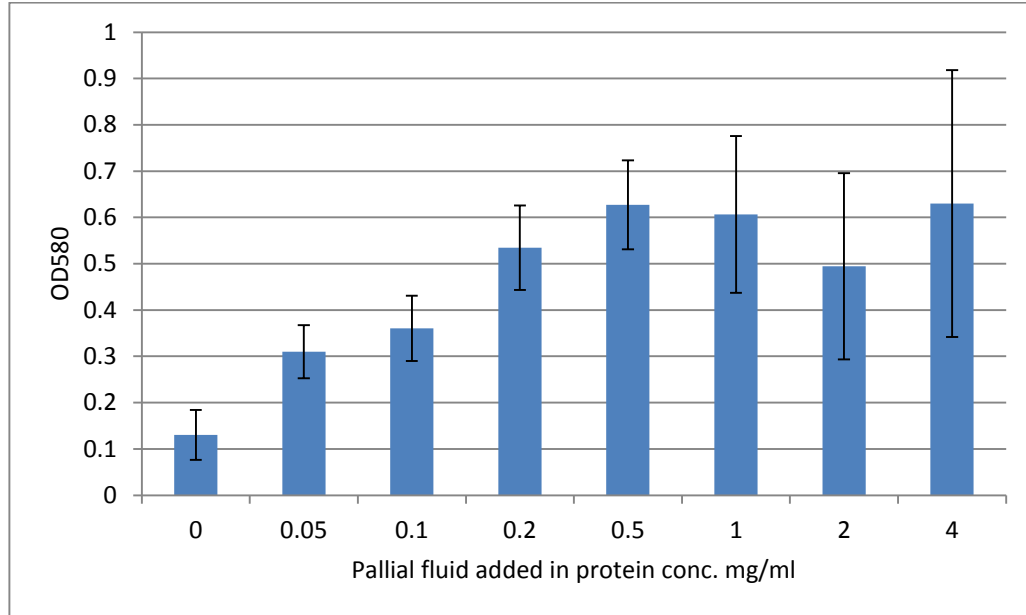
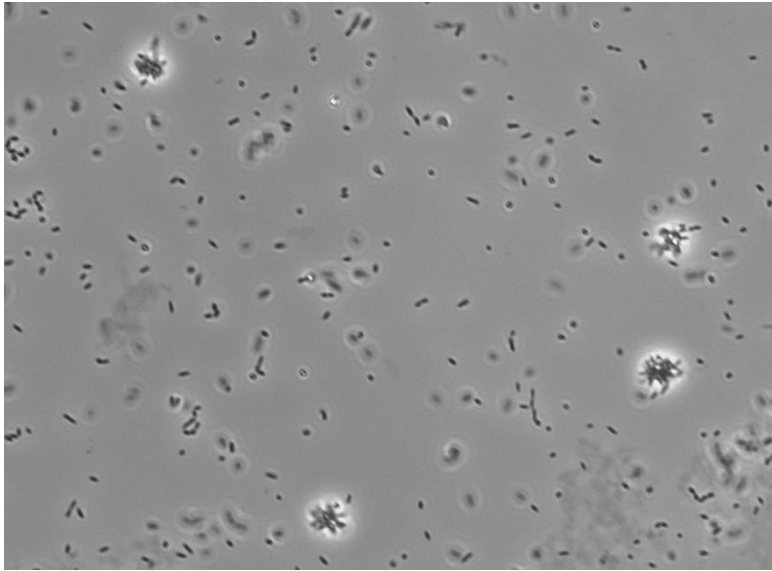


**Figure 6.** Biofilm formation in glass tubes by *A. crassostreae* in YP30 with various amounts of pallial fluid (opf #1) added. Glass tubes contain a total volume of 2 ml of either YP30 or YP30 supplemented with various amounts of pallial fluid and were incubated for 24 h at 27°C under static conditions. Data represent the average values of four biological replicates that were tested in duplicate and optical densities were taken in triplicate for each tube. Error bars equal one standard deviation.

A.



B.

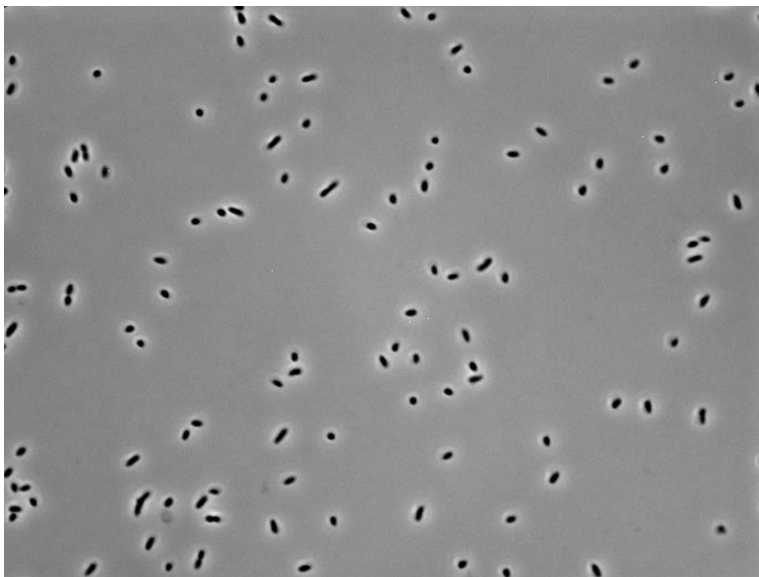


**Figure 7.** *A. crassostreae* cells (400× magnification) when grown statically in oyster pallial fluid in glass tubes form rosette-like structures. Cultures were incubated at 27°C for 24 h and reached a density of  $\sim 4 \times 10^8$  CFU/ml (A). In comparison, stationary phase *A. crassostreae* cells (1000× magnification) grown in YP30 at 27°C under shaking conditions (175 rpm) do not display any rosette-like structures (B).

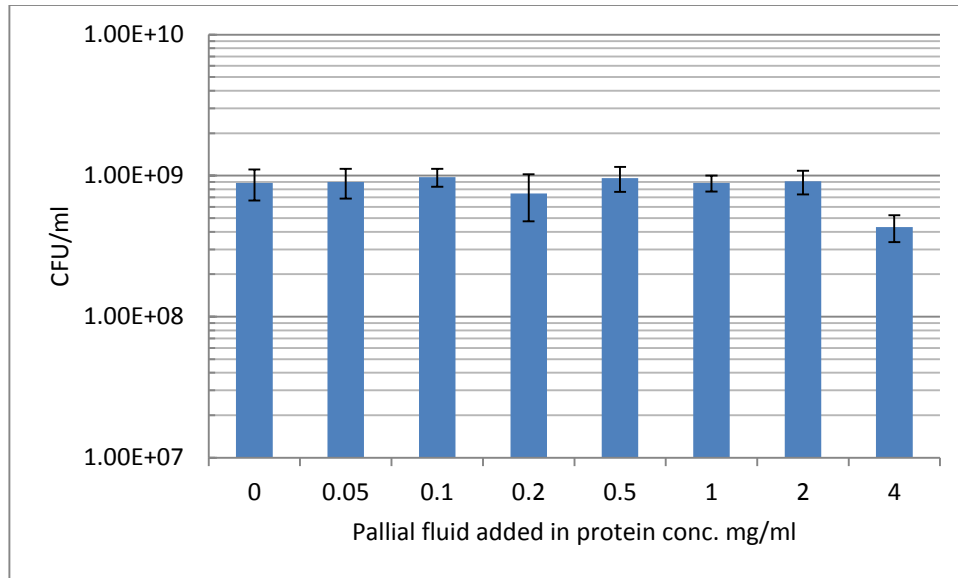


**Figure 8.** Planktonic cell densities of *A. crassostreae* during biofilm formation in glass tubes with various amounts of pallial fluid (opf #1) added. Glass tubes contain a total volume of 2 ml of YP30 or YP30 supplemented with various amounts of pallial fluid (opf #1). Tubes were incubated for 24 h under static conditions. Data represent four biological replicates. Three of these replicates were tested in duplicate and all samples were spot plated (10  $\mu$ l) in triplicate. Error bars equal one standard deviation.

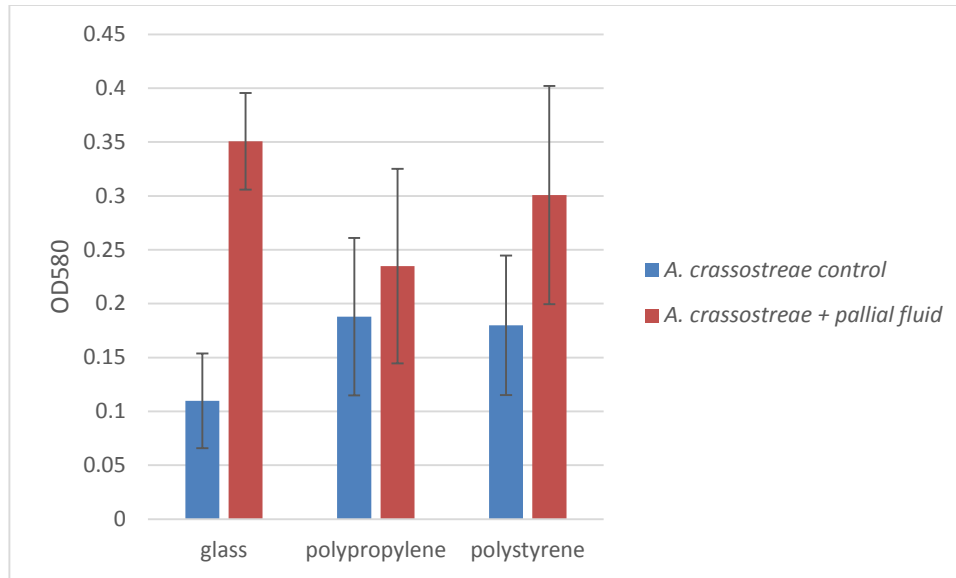


**Figure 9.** Effects of oyster pallial fluid on biofilm formation by *A. crassostreae* in glass, polypropylene, and polystyrene tubes. Protein concentration of pallial fluid (opf #1) added to growth medium for treatment groups was 0.5 mg/ml. Total culture volumes in tubes were 2 ml and all tubes were incubated for 24 h at 27°C under static conditions. Controls were grown in YP30 without the addition of pallial fluid. Data show the average values for three biological replicates that were tested in duplicate and OD<sub>580</sub> readings are averages of values taken in triplicate. Error bars equal one standard deviation. A significant increase in biofilm formation was observed for *A. crassostreae* grown in glass tubes ( $p=0.0027$ ). No significant difference in biofilm formation in polypropylene and polystyrene tubes was detected when growth medium was supplemented with pallial fluid versus un-supplemented YP30.



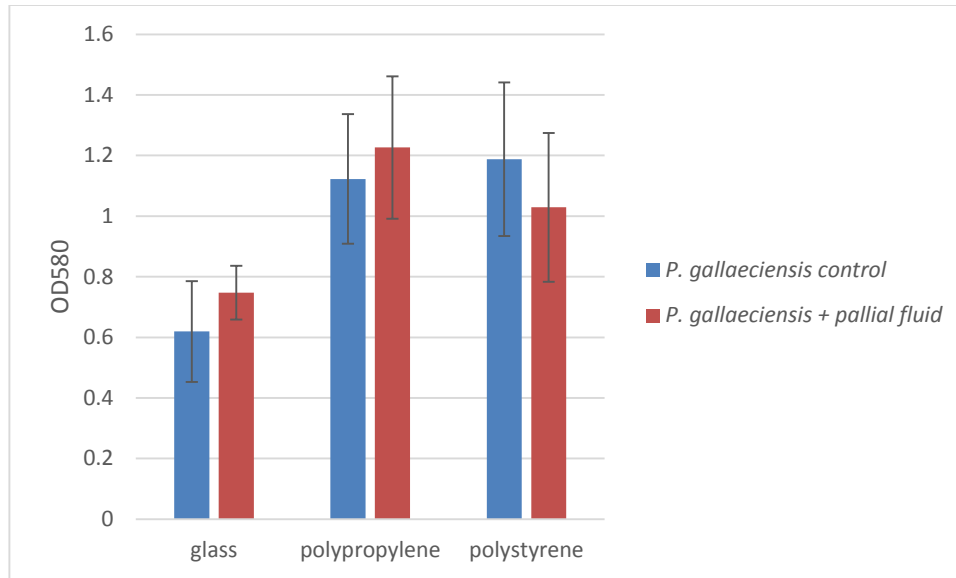


**Figure 10.** Effects of oyster pallial fluid on biofilm formation by *P. gallaeciensis*.

Protein concentration of pallial fluid added to growth medium was 0.5 mg/ml (opf #1).

Controls were grown in YP30 without added pallial fluid. Total culture volumes in tubes were 2 ml and all tubes were incubated for 24 h at 27°C under static conditions.

Data are averages of three biological replicates that were tested in duplicate. OD<sub>580</sub> readings of each tube were taken in triplicate. Error bars equal one standard deviation.

Biofilm formation of *P. gallaeciensis* was significantly increased in glass tubes when grown in YP30 alone ( $p=0.027$ ) or when supplemented with pallial fluid ( $p=0.006$ ) compared to biofilm formation of *A. crassostreae* under the same culture conditions. *P. gallaeciensis* also formed a significantly increased amount of biofilm in polystyrene and polypropylene tubes (unsupplemented YP30 and YP30 supplemented with pallial fluid) compared to biofilm formation of *A. crassostreae* under the same culture conditions.

## DISCUSSION

Our study shows that oyster pallial fluid is likely to contribute to the initial colonization of *A. crassostreae* or *P. gallaeciensis* in the oyster in two ways – by promoting positive chemotaxis and growth. Additionally, pallial fluid seems to promote colonization of *A. crassostreae* by stimulating biofilm formation. O’Toole et al. (1996) showed that chemotaxis is required for *V. anguillarum* to infect fish (35). Furthermore, the soilborne plant pathogen *Ralstonia solanacearum* requires chemotactic abilities to invade host plants (24). We demonstrate that pallial fluid serves as a chemoattractant, able to attract these microorganisms towards or into the pallial cavity of oysters. Filter-feeding may enhance colonization once these microorganisms are in the proximity of oysters. We have shown that the molecule/s of interest that elicits this chemotactic response is  $>10$  kDa in mass. Further studies will be necessary to identify the molecule/s.

In order to capture nutrients from ocean waters, one oyster is capable of processing over 100 L of seawater per day (36). This filter-feeding behavior exposes the animal to many microorganisms that are present in the ocean including the pathogen *A. crassostreae* (36, 37). During this filter-feeding process and during ejection of pseudofeces microorganisms come in contact with pallial fluid which could promote colonization of the oyster. However, the exact route of infection by *A. crassostreae* still remains to be discovered.

Virulence factors in other marine pathogens are up-regulated when exposed to mucus found in the natural host (10, 13, 21). For instance, genes that affect apoptosis and immunity in invertebrates, proteases and other genes are up-regulated in the oyster pathogen *P. marinus* when exposed to oyster pallial mucus (13). Additionally, growth rates of *P. marinus* were faster when media was supplemented with mantle mucus from *C. virginica* (21). However, our data show that *A. crassostreae* remains non-hemolytic even when challenged with nutrient poor conditions or the addition of oyster pallial fluid. That no hemolytic activity was observed when blood agar plates were supplemented with pallial fluid strongly suggests that *A. crassostreae* either does not produce extracellular hemolysins or that potential hemolysins do not express hemolytic activity against fish erythrocytes. If *A. crassostreae* secretes hemolysins – as indicated by studies from Gomez-Leon et al. (2008) (15) – they may be specific to oyster hemocytes. The phosphatidylcholine-specific phospholipase Plp in *V. anguillarum* for example causes hemolysis specifically in fish erythrocytes, but not in sheep erythrocytes while the other two hemolysins in *V. anguillarum*, Vah1 and RtxA, are capable of causing lysis of both sheep and fish erythrocytes (40, 41). Hemolysins

by *A. crassostreae* may not be able to affect fish erythrocytes, but may only specifically degrade oyster hemocytes. Additionally, *A. crassostreae* did not produce any extracellular protease that could serve as a virulence factor.

Our research demonstrates that *A. crassostreae* can rapidly multiply in oyster pallial fluid. However, *A. crassostreae* grew more slowly in pallial fluid than YP30 immediately after inoculation. This may be due to immune molecules with antimicrobial activity that are present in oyster pallial fluid. Oysters do not have an innate immune system, but rather rely on humoral and cellular defense mechanisms to protect themselves from invading pathogenic organisms (38). While hemocytes are the primary immunogenic cells that circulate in hemolymph and are capable of phagocytosis (38), humoral factors present in oyster hemolymph include lectins, toxic oxygen intermediates, lysozyme, as well as antimicrobial peptides (38). The presence of antimicrobial peptides has also been confirmed in oyster gill extract (42) and mantle tissue (43). Thus, the initial lag in growth could be due to antimicrobial peptides or other humoral defense factors in pallial fluid. Alternatively, this lag may be explained by the fact that *A. crassostreae* cells were initially grown in YP30 and must adapt to a new environment when placed in pallial fluid. Despite this initial lag phase, pallial fluid can serve as a nutrient source for *A. crassostreae* allowing these bacteria to grow rapidly and multiply within the oyster. Oyster pallial fluid is not only an excellent growth medium for *A. crassostreae*, but *P. gallaeciensis* is also capable of growth in oyster pallial fluid. Similar to the results obtained with *A. crassostreae*, *P. gallaeciensis* initially grew a little slower in pallial fluid than YP30. Again, this could

be due to the fact that the cells were introduced to a new medium (pallial fluid) or because the organism was overcoming humoral defense factors that are present in oyster pallial fluid.

Studies by Boardman et al. (7, 44) have shown that *A. crassostreae* colonizes the inner shell surface and attaches to conchiolin deposits via its the polar end. The observations that pallial fluid increases biofilm formation on glass surfaces by *A. crassostreae* (Figure 6 and 9) suggest that pallial fluid within the oyster promotes surface attachment of *A. crassostreae* to the inner shell surface. In addition, rosette-like morphologies were observed when *A. crassostreae* was grown statically in pallial fluid alone (Figure 7). Induction of rosette-like formations correlate with an increase in biofilm formation with increased amounts of pallial fluid. An increase in biofilm formation was observed until a saturation point of 0.5 mg/ml of protein from pallial fluid was reached. An increase in variation was observed when more pallial fluid was added. This increase in variation with more than 0.5 mg/ml protein from pallial fluid added may be due to humoral defensins, e.g. antimicrobial peptides, present in pallial fluid. With an increased amount of pallial fluid an increased amount of antimicrobial peptides is added to the test tubes, which could counteract the biofilm-enhancing properties. Additionally, a lower density of planktonic *A. crassostreae* cells was observed during biofilm formation in pallial fluid alone (Figure 8). This reduced cell concentration again could be due to antimicrobial peptides and other humoral factors present in pallial fluid or the fact that the inoculum was grown in YP30, which could have caused an extended lag phase. The planktonic concentration of *A. crassostreae* would most likely increase with prolonged incubation times. Further studies utilizing

oyster shells instead of glass as a surface for attachment are needed to confirm whether biofilm enhancement by pallial fluid occurs in oysters.

*P. gallaeciensis* is a probiotic organism that protects oyster larvae and increases their survival rates when challenged with *A. crassostreae* (18). Like *A. crassostreae*, *P. gallaeciensis* exhibits positive chemotaxis to oyster pallial fluid. Pallial fluid also provides an excellent growth medium for this organism. Colonization by *P. gallaeciensis* appears to benefit larval oysters by reducing mortality caused by pathogens including *A. crassostreae* or *V. coralliilyticus* RE22 (18). However, our study shows that pallial fluid does not promote surface attachment of *P. gallaeciensis* as it does with *A. crassostreae* (Figure 10). This study and previous research on Phaeobacters (17, 45, 46) demonstrate that these bacteria are excellent biofilm formers and readily attach to various surfaces. Despite an increase in biofilm by *A. crassostreae* when supplemented with pallial fluid, *P. gallaeciensis* still grows a thicker biofilm. For example, the highest average OD<sub>580</sub> value for *P. gallaeciensis* in this study was 1.2 (observed in polypropylene tubes treated with pallial fluid), whereas the highest average OD<sub>580</sub> value for *A. crassostreae* was observed to be 0.6 (detected in glass tubes when YP30 was supplemented with 0.5, 1.0, and 4 mg/ml protein from pallial fluid) (Figures 6 and 10). Thus, at a minimum, *P. gallaeciensis* biofilm formation is 2-fold greater than biofilm formation by *A. crassostreae*. The same was observed between *A. crassostreae* biofilm in glass tubes supplemented with pallial fluid and *P. gallaeciensis* biofilm in glass tubes; *P. gallaeciensis* formed >2-fold biofilm on glass than *A. crassostreae* (Figures 9 and 10). This correlates with the results of biofilm competition assays performed by Zhao et al. (2014), which show

that glass coverslips pre-colonized with *P. gallaeciensis* significantly inhibit colonization of *V. coralliilyticus* RE22 (20). Thus, inhibition of colonization of pathogens is most effective, when surfaces are pre-colonized with *P. gallaeciensis* (20).

In conclusion, oyster pallial fluid is rich in free amino acids and other nutrients and serves as an excellent growth medium for both *A. crassostreae* and *P. gallaeciensis*. Pallial fluid promotes biofilm formation by *A. crassostreae* and is a chemoattractant to both *A. crassostreae* and *P. gallaeciensis*. In the absence of *P. gallaeciensis*, pallial fluid would not only promote chemotaxis of *A. crassostreae* toward oysters, but promote growth and colonization of the pathogen. Further studies like differential gene expression in *A. crassostreae* in the absence and presence of pallial fluid would help identify potential virulence factors.

## REFERENCES

1. **Maloy AP, Ford SE, Karney RC, Boettcher KJ.** 2007. *Roseovarius crassostreae*, the etiological agent of Juvenile Oyster Disease (now to be known as *Roseovarius* Oyster Disease) in *Crassostrea virginica*. *Aquaculture* **269**:71-83.
2. **Davis CV, Barber BJ.** 1999. Growth and survival of selected lines of eastern oysters, *Crassostrea virginica* (Gmelin 1791) affected by juvenile oyster disease. *Aquaculture* **178**:253-271.
3. **Bricelj VM, Ford ES, Borrero FJ, Perkins FO, Rivara G, Hillman RE, Elston RA, Chang J.** 1992. Unexplained mortalities of hatchery-reared, juvenile oysters, *Crassostrea virginica* (Gmelin). *J Shellfish Res* **11**:331-347.
4. **Davis CV, Barber BJ.** 1994. Size-dependent mortality in hatchery-reared populations of oysters, *Crassostrea virginica*, Gmelin 1791, affected by Juvenile Oyster Disease. *J Shellfish Res* **13**:137-142.
5. **Ford SE, Borrero FJ.** 2001. Epizootiology and pathology of juvenile oyster disease in the Eastern oyster, *Crassostrea virginica*. *J Invertebr Pathol* **78**:141-154.
6. **Maloy AP, Barber BJ, Boettcher KJ.** 2007. Use of the 16S-23S rDNA internal transcribed spacer of *Roseovarius crassostreae* for epizootiological studies of juvenile oyster disease (JOD). *Dis Aquat Org* **76**:151.
7. **Boardman CL, Maloy AP, Boettcher KJ.** 2008. Localization of the bacterial agent of juvenile oyster disease *Roseovarius crassostreae* within affected eastern oysters *Crassostrea virginica*. *J Invertebr Pathol* **97**:150-158.
8. **Sunila I.** *Roseovarius* Oyster Disease. <http://www.ct.gov/doag/lib/doag/aquaculture/rod.pdf>. Accessed 3-12-15.
9. **Boettcher KJ, Geaghan KK, Maloy AP, Barber BJ.** 2005. *Roseovarius crassostreae* sp. nov., a member of the *Roseobacter* clade and the apparent cause of juvenile oyster disease (JOD) in cultured Eastern oysters. *Int J Syst Evol Microbiol* **55**:1531-1537.
10. **Denkin SM, Nelson DR.** 1999. Induction of protease activity in *Vibrio anguillarum* by gastrointestinal mucus. *Appl Environ Microbiol* **65**:3555-3560.
11. **Rock JL, Nelson DR.** 2006. Identification and characterization of a hemolysin gene cluster in *Vibrio anguillarum*. *Infect Immun* **74**:2777-2786.
12. **Spinard EK, L; Gomez-Chiarri, M; Rowley, D; Nelson, D.** 2015. Draft genome of the marine pathogen *Vibrio coralliilyticus* RE22 Genome Announc **3**.
13. **Pales Espinosa E, Corre E, Allam B.** 2014. Pallial mucus of the oyster *Crassostrea virginica* regulates the expression of putative virulence genes of its pathogen *Perkinsus marinus*. *Int J Parasitol* **44**:305-317.
14. **Peyre JFL, Schafhauser DY, Rizkalla EH, Faisal M.** 1995. Production of Serine Proteases by the Oyster Pathogen *Perkinsus marinus* (*Apicomplexa*) *In Vitro*. *J Eukaryot Microbiol* **42**:544-551.
15. **Gomez-Leon J, Villamil L, Salger SA, Sallum R, Remacha-Trivino A, Leavitt DF, Gomez-Chiarri M.** 2008. Survival of eastern oysters *Crassostrea*



- virginica* from three lines following experimental challenge with bacterial pathogens. J Shellfish Res **32**:401-408.
16. **Chatterji D, Ojha AK.** 2001. Revisiting the stringent response, ppGpp and starvation signaling. Curr Opin Microbiol **4**:160-165.
  17. **Bruhn JB, Nielsen KF, Hjelm M, Hansen M, Bresciani J, Schulz S, Gram L.** 2005. Ecology, inhibitory activity, and morphogenesis of a marine antagonistic bacterium belonging to the *Roseobacter* clade. Appl Environ Microbiol **71**:7263-7270.
  18. **Karim M, Zhao W, Rowley D, Nelson D, Gomez-Chiarri M.** 2013. Probiotic Strains for Shellfish Aquaculture: Protection of Eastern Oyster, *Crassostrea virginica*, Larvae and Juveniles Against Bacterial Challenge. J Shellfish Res **32**:401-408.
  19. **Dang H, Lovell CR.** 2000. Bacterial primary colonization and early succession on surfaces in marine waters as determined by amplified rRNA gene restriction analysis and sequence analysis of 16S rRNA genes. Appl Environ Microbiol **66**:467-475.
  20. **Zhao W.** 2014. Characterization of the Probiotic Mechanism of *Phaeobacter gallaeciensis* S4 Against Bacterial Pathogens University of Rhode Island.
  21. **Espinosa EP, Winnicki S, Allam B.** 2013. Early host–pathogen interactions in a marine bivalve: *Crassostrea virginica* pallial mucus modulates *Perkinsus marinus* growth and virulence. Dis Aquat Org **104**:237-247.
  22. **Olsson JC, Westerdahl A, Conway PL, Kjelleberg S.** 1992. Intestinal colonization potential of turbot (*Scophthalmus maximus*)-and dab (*Limanda limanda*)-associated bacteria with inhibitory effects against *Vibrio anguillarum*. Appl Environ Microbiol **58**:551-556.
  23. **Bordas MA, Balebona MC, Rodriguez-Maroto JM, Borrego JJ, Moriñigo MA.** 1998. Chemotaxis of Pathogenic *Vibrio* Strains towards Mucus Surfaces of Gilt-Head Sea Bream (*Sparus aurata* L.). Appl Environ Microbiol **64**:1573-1575.
  24. **Yao J, Allen C.** 2006. Chemotaxis is required for virulence and competitive fitness of the bacterial wilt pathogen *Ralstonia solanacearum*. J Bacteriol **188**:3697-3708.
  25. **Boettcher KJ, Barber BJ, Singer JT.** 1999. Use of antibacterial agents to elucidate the etiology of juvenile oyster disease (JOD) in *Crassostrea virginica* and numerical dominance of an  $\alpha$ -Proteobacterium in JOD-affected animals. Appl Environ Microbiol **65**:2534-2539.
  26. **Espinosa EP, Perrigault M, Ward JE, Shumway SE, Allam B.** 2009. Lectins associated with the feeding organs of the oyster *Crassostrea virginica* can mediate particle selection. Biol Bull **217**:130-141.
  27. **Crenshaw MA.** 1972. The Inorganic Composition of Molluscan Extrapallial Fluid. Biol Bull **143**:506-512.
  28. **Allam B, Paillard C.** 1998. Defense factors in clam extrapallial fluids. Dis Aquat Org **33**:123-128.
  29. **Masuko T, Minami A, Iwasaki N, Majima T, Nishimura S, Lee YC.** 2005. Carbohydrate analysis by a phenol-sulfuric acid method in microplate format. Anal Biochem **339**:69-72.

30. **Mårdén P, Tunlid A, Malmcrona-Friberg K, Odham G, Kjelleberg S.** 1985. Physiological and morphological changes during short term starvation of marine bacterial isolates. *Arch Microbiol* **142**:326-332.
31. **Neidhardt FC, Bloch PL, Smith DF.** 1974. Culture Medium for Enterobacteria. *J Bacteriol* **119**:736-747.
32. **Adler J.** 1973. A method for measuring chemotaxis and use of the method to determine optimum conditions for chemotaxis by *Escherichia coli*. *J Gen Microbiol* **74**:77-91.
33. **Belas R, Horikawa E, Aizawa S-I, Suvanasuthi R.** 2009. Genetic determinants of *Silicibacter* sp. TM1040 motility. *J Bacteriol* **191**:4502-4512.
34. **Mesibov R, Adler J.** 1972. Chemotaxis toward amino acids in *Escherichia coli*. *J Bacteriol* **112**:315-326.
35. **O'Toole R, Milton DL, Wolf-Watz H.** 1996. Chemotactic motility is required for invasion of the host by the fish pathogen *Vibrio anguillarum*. *Mol Microbiol* **19**:625-637.
36. **Allam B, Carden WE, Ward JE, Ralph G, Winnicki S, Pales Espinosa E.** 2013. Early host-pathogen interactions in marine bivalves: Evidence that the alveolate parasite *Perkinsus marinus* infects through the oyster mantle during rejection of pseudofeces. *J Invertebr Pathol* **113**:26-34.
37. **Ben-Horin T, Bidegain G, Huey L, Narvaez DA, Bushek D.** 2015. Parasite transmission through suspension feeding. *J Invertebr Pathol* **131**:155-176.
38. **Canesi L, Gallo G, Gavioli M, Pruzzo C.** 2002. Bacteria-hemocyte interactions and phagocytosis in marine bivalves. *Microsc Res Tech* **57**:469-476.
39. **Kennedy V, Newell R, Eble A.** 1996. The Eastern Oyster - *Crassostrea virginica*. Maryland Sea Grant College, University of Maryland System, College Park.
40. **Li L, Mou X, Nelson DR.** 2013. Characterization of Plp, a phosphatidylcholine-specific phospholipase and hemolysin of *Vibrio anguillarum*. *BMC Microbiol* **13**:271.
41. **Li L, Rock JL, Nelson DR.** 2008. Identification and characterization of a repeat-in-toxin gene cluster in *Vibrio anguillarum*. *Infect Immun* **76**:2620-2632.
42. **Seo JK, Crawford JM, Stone KL, Noga EJ.** 2005. Purification of a novel arthropod defensin from the American oyster, *Crassostrea virginica*. *Biochem Biophys Res Commun* **338**:1998-2004.
43. **Gueguen Y, Herpin A, Aumelas A, Garnier J, Fievet J, Escoubas JM, Bulet P, Gonzalez M, Lelong C, Favrel P, Bachere E.** 2006. Characterization of a defensin from the oyster *Crassostrea gigas*. Recombinant production, folding, solution structure, antimicrobial activities, and gene expression. *J Biol Chem* **281**:313-323.
44. **Boardman C.** 2005. Host-pathogen interactions between Eastern oysters (*Crassostrea virginica*) and the bacterial agent of juvenile oyster disease (*Roseovarius crassostreae*) The University of Maine.
45. **Zhao W.** 2015. Contributions of tropodithietic acid and biofilm formation to the probiotic activity of *Phaeobacter gallaeciensis* University of Rhode Island.

46. **Bruhn JB, Gram L, Belas R.** 2007. Production of antibacterial compounds and biofilm formation by *Roseobacter* species are influenced by culture conditions. *Appl Environ Microbiol* **73**:442-450.

## Manuscript II

**Publication Status:** Preparing to submit short version to Genome Announcements, 2015

**Title:** Draft genome sequence of *Aliiroseovarius crassostreae* CV919-312<sup>T</sup>Sm, the causative agent of Roseovarius Oyster Disease (formerly Juvenile Oyster Disease)

**Authors:** Linda Kessner<sup>a</sup>, Edward Spinard<sup>a</sup>, Marta Gomez-Chiarri<sup>b</sup>, David C. Rowley<sup>c</sup>, David R. Nelson<sup>a#</sup>

**Author Affiliations:** <sup>a</sup>Department of Cell and Molecular Biology, University of Rhode Island, Kingston, RI, USA; <sup>b</sup>Department of Fisheries, Animal and Veterinary Sciences, University of Rhode Island, Kingston Rhode Island, USA; <sup>c</sup>Department of Biomedical and Pharmaceutical Sciences, University of Rhode Island, Kingston, Rhode Island, USA

**Running Head:** Draft genome of *Aliiroseovarius crassostreae*

#Address correspondence to: David R. Nelson, dnelson@uri.edu

## ABSTRACT

*Aliiroseovarius crassostreae* CV919-312<sup>T</sup> is a Gram-negative marine  $\alpha$ -Proteobacterium and the causative agent of *Roseovarius* Oyster Disease. Hatchery raised eastern oysters suffer high mortality rates caused by *Roseovarius* Oyster Disease which results in significant economic losses to the aquaculture industry on the northeastern coast of the United States. In this investigation we announce the first draft genome of *A. crassostreae* consisting of 27 contigs including one complete plasmid. After annotation with IMG/ER as well as RAST, multiple putative virulence genes have been identified. Numerous putative cytotoxins including a serralyisin peptidase and RTX related Ca<sup>2+</sup>-binding proteins were detected. Additionally, two *tad/flp* gene clusters responsible for *flp*-pili formation that are most likely involved in surface attachment have been identified. A type 1 secretion system responsible for the transport of a putative adhesin was located. A type 4A secretion system and a partial type 4B secretion system were identified. Multiple genes that are predicted to encode proteins involved in surface adhesion and host colonization were discovered. The discovery of numerous putative virulence genes will provide the basis for insight into the mechanisms of pathogenesis of *A. crassostreae*.

## INTRODUCTION

*Aliiroseovarius crassostreae*, formerly known as *Roseovarius crassostreae*, is the causative agent of *Roseovarius* Oyster Disease (ROD), which results in high mortality rates in hatchery raised juvenile eastern oysters in the Northeast United States (1-3). This Gram-negative  $\alpha$ -Proteobacterium is a strict aerobe and a member of the *Roseobacter* clade (4). Previously sequenced genomes of this clade reveal that their genome size ranges between 3.5 and 5.0 Mbp. Clade members often carry a plasmid that can range from 3.4 to 821.7 Kbp in size and can comprise up to 20% of the entire genome (5).

Clinical signs of ROD in juvenile oysters appear as cessation of growth, conchiolin deposits on the inner shell surface, tissue lesions, uneven valve margins, and excessive cupping of the left valve (1, 2, 6-8). Previous research shows that the organisms colonize the inner shell surface and conchiolin deposits over any other part of the oyster (9). Oysters less than 25 mm in shell length are more heavily impacted by the disease than fully grown adults (1, 2, 8). The onset of ROD occurs seasonally as water temperatures reach 20°C (1, 2, 8). Mortalities start 1-2 weeks after the first clinical signs of disease are apparent (6).

Strain CV919-312<sup>T</sup> was isolated by Boettcher et al. (4) from the tissues of an infected oyster from the Damariscotta River in Maine. Formerly classified as a member of the genus *Roseovarius*, recent phylogenetic analysis of the 16S ribosomal gene revealed less than 95% identity to other members of the genus (10). This led to the reclassification of the organism to *Aliiroseovarius crassostreae* in 2015 (10).

Virulence mechanisms of the organism remain to be uncovered. Prior to this study, no genome sequence besides the 16S rRNA gene sequence and the internal transcribed spacer region were publically available. This draft genome of *A. crassostreae* CV919-312<sup>T</sup>Sm, a spontaneous streptomycin resistant mutant, will help elucidate the mechanisms of virulence by this bacterium to cause *Roseovarius* Oyster Disease. Selected genes or gene clusters will be discussed that are putative virulence genes involved in either oyster colonization or pathogenicity.

## **MATERIALS AND METHODS**

### **Growth Conditions and DNA Extraction**

Prior to sequencing, a spontaneous streptomycin resistant mutant was isolated by growing the organism on media with increasing concentrations of streptomycin. A single colony of *A. crassostreae* CV919-312<sup>T</sup>Sm was grown overnight at 27°C (shaking, 175 rpm) in yeast-peptone broth supplemented with 3% artificial sea salts (YP3, Karim et al. (11)) . Genomic DNA was isolated using the Promega Wizard Genomic DNA purification kit according to manufacturer's recommendations with the exception that DNA was resuspended in 2 mM Tris-HCl Buffer (Bio Basic) instead of the buffer provided with the kit. The integrity of genomic DNA was confirmed by gel electrophoresis and compared to Lambda DNA/HindIII markers (Promega). Paired-end and mate-pair sequencing was performed at the Rhode Island Genomics and Sequencing Center using the Illumina MiSeq benchtop instrument.

## **Sequence Trimming, Genome Assembly, and Annotation**

Sequence trimming and *de novo* assembly was performed using the CLC Genomics Workbench (v8.0.1). Sequences from paired end and mate pair sequencing were trimmed and sequences with an average coverage above 100 were used for *de novo* assembly with the CLC Genomics Workbench. Trimmed reads were also assembled with SPAdes Genomic Assembler (v3.1.1). Resulting contigs from both CLC Genomics workbench and SPAdes Genomic Assembler were joined using the CLC Microbial Genome Finishing module.

## **Bioinformatics Tools for Genomic Analysis**

Gene annotation was performed with Rapid Annotations using Subsystems Technology (RAST) (12-14). In addition, the draft genome was submitted to and annotated by Integrated Microbial Genomes/Expert Review (IMG/ER) (15). When these annotation pipelines identified open reading frames without any functional annotation, NCBI's Basic Local Alignment Search Tool (BLAST) (16-19) search tool was used to help identify homologous proteins in other organisms and to compare amino acid sequences to sequence databases. BLAST was also used to detect conserved regions within sequences that could help identify the functional role of a hypothetical protein and/or characterize members of protein families.



## RESULTS AND DISCUSSION

### Overview and Statistics

The draft genome consists of 26 contigs with a total sequence length of 3,706,831 bp and G+C content of 57.4% plus one complete plasmid of 18,548 bp with G+C content of 58.3%.

According to IMG/ER the draft genome contains 3763 total ORFs including 3694 protein encoding genes (15). RAST detected 3812 protein encoding ORFs and 59 features encoding tRNA or rRNA (12-14). IMG/ER assigned a predicted function to almost 74% of protein encoding genes (15). The number of genes identified as encoding tRNAs is 50 and while minimally one 16S, one 5S, and one 23S rRNA gene is required, three 16S, three 5S, and three 23S rRNA genes have been annotated (15). In order to simplify references of gene loci to certain contigs in this study, the 26 *A. crassostreae* contigs were numbered and matched to individual GenBank sequence accession numbers. Contig numbers and associated GenBank sequence accessions are displayed in Table 1.

### *Tad/flp* Gene Clusters

Previous research by Boardman et al. (2008) revealed that *A. crassostreae* prefers to colonize the inner shell surface of oysters (9). *A. crassostreae* was isolated from challenged culture-positive oysters from the left or right valves 89% and 95% of the time, respectively (9). In only 21% and 47% of culture positive oysters was the organism identified in pallial fluid or soft tissue samples, respectively (9). The percent

**Table 1.** Contig numbers used in this study and associated GenBank accession numbers.

<b>Contig</b>	<b>GenBank accession number</b>	<b>Size</b>
1	LKBA01000001.1	353,615 bp
2	LKBA01000002.1	6912 bp
3	LKBA01000003.1	39,923 bp
4	LKBA01000004.1	828,384 bp
5	LKBA01000005.1	5,774 bp
6	LKBA01000006.1	784,730 bp
7	LKBA01000007.1	105,512 bp
8	LKBA01000008.1	101,234 bp
9	LKBA01000009.1	94,398 bp
10	LKBA01000010.1	47,167 bp
11	LKBA01000011.1	32,559 bp
12	LKBA01000012.1	28,934 bp
13	LKBA01000013.1	24,700 bp
14	LKBA01000014.1	20,992 bp
15	LKBA01000015.1	13,351 bp
16	LKBA01000016.1	12,746 bp
17	LKBA01000017.1	3,412 bp
18	LKBA01000018.1	2,566 bp
19	LKBA01000019.1	625,830 bp
20	LKBA01000020.1	2,314 bp
21	LKBA01000021.1	1,130 bp
22	LKBA01000022.1	955 bp
23	LKBA01000023.1	226,010 bp
24	LKBA01000024.1	209,228 bp
25	LKBA01000025.1	133,486 bp
26	LKBA01000027.1	969 bp

colony forming units (CFU) of *A. crassostreae* was ~6 times higher for the inner shell surface than in tissue and pallial fluid samples (9). Boettcher et al. (2005) have shown that *A. crassostreae* produces a polar tuft of fimbriae (3). These polar fimbriae are most likely involved in polar surface attachment by the organism (20). Scanning electron microscopy images have shown that *A. crassostreae* attaches to the inner shell surface and to conchiolin deposits by its polar end (9). This indicates that the polar tuft of fimbriae is most likely involved in surface attachment to the oyster's inner shell surface. Annotation by both IMG/ER as well as RAST revealed multiple clusters of genes involved in *flp* (fimbrial low-molecular weight protein) pilus assembly which may be responsible for the fimbriae formation observed in *A. crassostreae* and, in turn, may play an important role in inner shell surface attachment. This cluster of genes, referred to as the *tad* gene cluster (*t*ight *a*dherence), has previously been associated with tenacious biofilm formation and virulence in multiple organisms and more recently with the uptake of external DNA into the cell (21). *Flp* pili have been associated with adherence, colonization, biofilm formation and pathogenesis in various bacteria including *Aggregatibacter actinomycetemcomitans*, *Pasteurella multocida*, *Burkholderia pseudomallei*, and *Pseudomonas aeruginosa* (22). Mutations within the *tad* gene cluster resulted in either attenuation or significantly reduced pathogenicity (22). *Flp/tad* pili seem to also be involved in virulence of *Pectobacteria* which cause soft rot disease in potatoes (23). The *flp/tad* gene cluster has been extensively studied in *A. actinomycetemcomitans* where it is required for tight adherence and biofilm formation on solid surfaces including glass and plastics (24) (see Figure 1 for hypothetical structure of *flp* pilus machinery). Mutagenesis studies

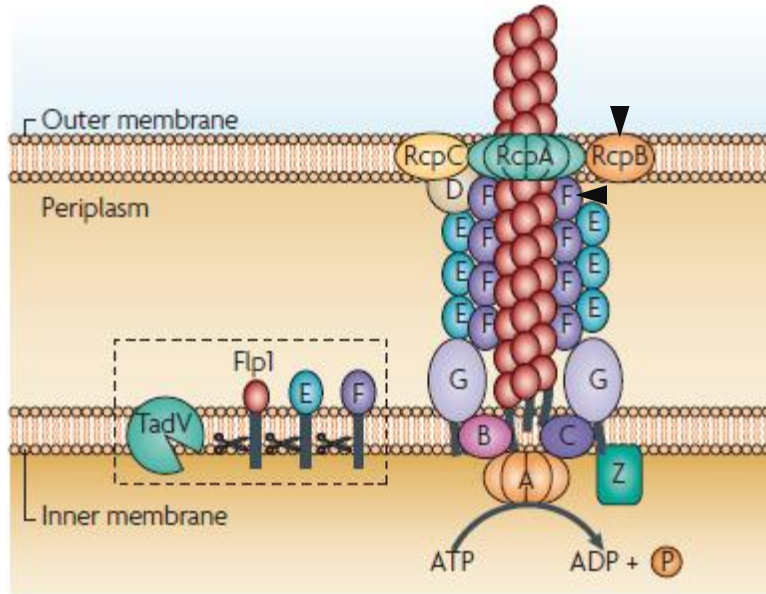


**Figure 1.** Hypothetical model of Tad/Flp secretion. This structure is based on functions of homologous proteins found in other prokaryotic secretion systems. Tad proteins are marked with their corresponding fourth letter (22). TadF and RcpB (indicated by arrowhead) are absent in the *A. crassostreae* genome. Figure from Tomich et al. (2007) (22).

revealed that *flp-1*, *rcpA*, *rcpB*, *tadB*, *tadD*, *tadE*, and *tadF* are necessary for the expression of fimbriae in *Aggregatibacter actinomycetemcomitans* (25). A locus homologous to *flp/tad* has also been described in the non-pathogenic *Caulobacter crescentus* and is responsible for the formation of polar pili by that bacterium (22). Instead of *flp* prepilin, *C. crescentus* encodes for *pilA* as a prepilin and *cpaABCEF* are homologous to the *tadV-rcpCA-tadZA* genes in *A. actinomycetemcomitans* (22). Many organisms contain two (sometimes three) distinct loci of the *flp/tad* gene cluster (22). While some of the involved genes are homologous to genes found in type 2 or type 4 secretion systems, many of the genes associated with the *flp/tad* locus in other organisms like *A. actinomycetemcomitans* are entirely novel, including *rcpC*, *rcpB*, *tadZ*, *tadD*, and *tadG* (22, 26).

With the exception of *tadF* and *rcpB* all of the genes associated with *flp*-fimbriae biogenesis have been located in the draft genome of *A. crassostreae* CV919-312<sup>T</sup> (Figures 2, 3, 4). Most of these genes are located in two distinct clusters on contig 6 and contig 19 (Figure 2, 3). Two more loci were detected that contain a gene encoding TadG and a gene encoding a TadE-like protein. TadG appears to be essential for complete fimbriae expression; it is thought to anchor the pili/fimbriae by a transmembrane domain to the inner (cytoplasmic) membrane (22, 25, 27). Tomich et al. (22) suggest that these genes might be paralogues because TadE is 22% identical to the amino acid sequence of TadF. TadE and TadF are pili-like proteins that are not assembled into the *flp*-fimbriae, but appear to form a pilus-like structure in the periplasm that is anchored to the inner (cytoplasmic) membrane and may assist in

extrusion of fimbriae (22). TadE and TadF are thought to interact with each other in the assembly of this extrusion mechanism (22).

One cluster containing 15 genes involved in *flp*-fimbriae biogenesis is located on contig 6 (Figure 2) (12-15). *RcpB*, *tadE*, *tadF*, and *tadG* are missing from this cluster; RcpB, along with RcpA, RcpC and TadD, are outer membrane components of the secretion apparatus (22, 26). RcpA is a secretin that is thought to form a pore in the outer membrane through which the pilus structure is secreted (22, 26) and RcpB may stabilize the secretion apparatus and maintain the integrity of the outer membrane (26). The role of RcpC remains to be elucidated (26); however, it has been proposed that RcpC may post-translationally modify the pilus structure, or bind to peptidoglycan as a scaffolding protein (22).

TadD is a lipoprotein containing a tetratricopeptide repeat and due to its homology with lipoproteins in T4SS and T2SS is thought to assist in integration or polymerization of RcpA (22, 26). Tetratricopeptide repeat motifs facilitate protein-protein interactions and are often associated with the assembly of multiprotein complexes (28, 29). Interestingly, *rcpA*, *rcpB*, and *tadD* are not found in Gram-positive bacteria, suggesting that they localize to the outer membrane in Gram-negative organisms (22, 26). The cluster of *flp/tad* genes on contig 6 encodes for three *flp* prepilins (12-14). In *A. actinomycetemcomitans* Flp-1 is the major pilin subunit while Flp-2 seems to be a homologue of Flp-1 (22, 30). Figurski et al. (2013) showed that Flp-1 is a glycoprotein in *A. actinomycetemcomitans* (31). While most organisms contain either one or two *flp* genes, three or even more *flp* genes have been found in a few organisms (22). *A. crassostreae* is one of those exceptions as it carries three *flp*

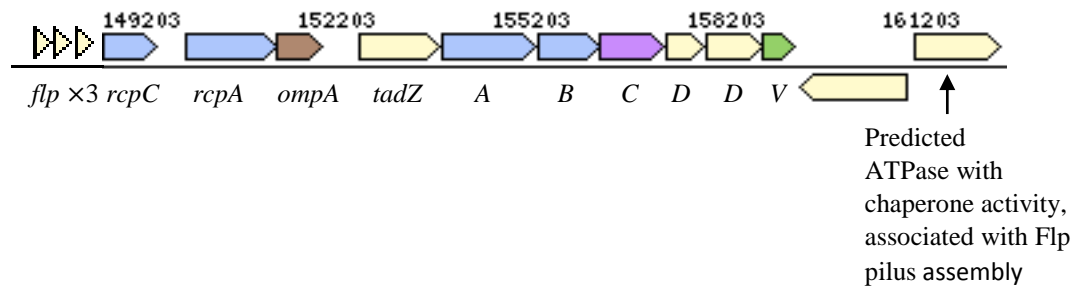


**Figure 2.** *A. crassostreae tad* gene cluster on contig 6. The functional role of unlabeled ORFs remains to be determined (12-15).

prepilin genes on contig 6 (12-14). These major structural units of the pili/fimbriae are usually 50 to 80 amino acids in size and are cleaved by TadV, the prepilin peptidase, into mature pilus subunits (22, 31). TadV also required for maturation of pseudopilins TadE and TadF (22). All three Flp prepilins located on contig 6 in *A. crassostreae* are 65 amino acids in length (pre-modification). The genes for RcpC and RcpA are found downstream of the Flp-prepilins followed by a gene encoding the outer membrane protein A (OmpA) (12-15). The *ompA* gene is usually not part of the traditional *flp/tad* gene cluster and its role in this gene cluster has not been identified. However, studies in *A. actinomycetemcomitans* suggest that OmpA might be involved in pathogenicity or immune responses in host organisms (24, 32). Further downstream from *ompA* the pilus assembly gene *tadZ* is found (12-15). TadZ belongs to the *parA/minD* superfamily (33). ParA and MinD are proteins that localize to a specific region within the bacterial cell and facilitate localization of other proteins (33). MinD is required for proper cell division while ParA is required for accurate DNA segregation in bacteria (33). TadZ appears to localize the *flp/tad* secretion apparatus to the polar end of the cell (22, 33). Immediately downstream of *tadZ* are *tadABC* (Figure 1) (12-15). TadA is an ATPase that powers pilus biogenesis (22, 34). TadB and TadC are inner membrane components of the pilus assembly apparatus with high similarity in amino acid sequence and homology to proteins involved in type 2 secretion (22, 26). However, their exact role in pilus biogenesis has not been elucidated. It has been proposed that TadB and TadC are molecular pistons that transfer energy from TadA in order to utilize it in *flp*-polymerization or the two genes are merely involved in scaffolding of the apparatus in the inner membrane (22). The cluster encodes for two



TadD molecules that immediately follow one another (12-14). As previously mentioned, TadD assists in assembly of RcpA into the outer membrane (22). *TadV* is located immediately downstream of *tadD* (12-15) and responsible for modifying the Flp prepilin into mature pilin subunits (22). According to RAST, a predicted ATPase with chaperone activity that is associated with Flp pilus assembly is also located near the *tad* gene cluster on contig 6 (Figure 2) (12-14). BLASTX results confirmed this gene to be an ATPase with multiple hits that have an E-value of 0 and a query cover of 99%. One of the hits aligned to a putative ATPase with chaperone activity, associated with Flp pilus assembly in *Celeribacter marinus* (99% query cover, E-value = 0, 73% identity). A hypothetical protein encoded by 1644 bp is located on the negative strand (opposite of the other genes in the *tad* cluster) between the *tad* gene cluster and this Flp pilus assembly associated ATPase (Figure 2) (12-15). BLASTX results did not reveal any functional properties besides a conserved region (PHA03307) spanning the first 29-457 bp with an E-value of  $5 \times 10^{-5}$  proposing the location of a transcriptional regulator (16-19).

Contig 19 encodes for another *flp/tad* gene cluster (12-15). The ORF at the 5' end of the gene cluster has been annotated as a tetratricopeptide repeat-containing (TRP) protein by both IMG/ER and RAST (Figure 3) (12-15). BLASTX results confirmed that the protein contains a TRP site, but also revealed the conserved domain 'Flp pilus assembly protein TadD, contains TPR repeats' (COG5010, E-value =  $7.43 \times 10^{-17}$ ) (16-19). Downstream of this putative *tadD* the cluster encodes a prepilin peptidase CpaA (15) which is a homologue of TadV (22). While RAST annotated the next 1629 bp long ORF as a hypothetical protein (12-14), IMG/ER annotated a

putative Flp pilus-assembly TadE/G-like protein (15). However, judging by the length of the gene, this ORF (1629 bp) seems to rather encode for TadG than TadE since *tadG* is usually greater than 1 kb in size and *tadE* approximates 0.5kb (22).

Additionally, a BLASTX search resulted in similarity to Flp pilus assembly protein TadG in the organism *Labrenzia alba* with an E-value of  $1 \times 10^{-42}$  (99% query coverage and 32% identity, accession CTQ52072.1) (35). *TadG* is followed by an *flp* gene encoding a 73 amino acid Flp prepilin (15). *RcpC* and *rcpA* are also part of this cluster followed by a 65 amino acid long hypothetical protein (12-15). BLASTX results suggest that this gene may encode for another Flp prepilin ('pilus assembly protein' in *Ensifer sojiae*, 89% query coverage, 49% identity, E-value =  $3 \times 10^{-8}$ , accession WP\_034855966.1) (35).

Downstream of this putative *flp* gene are two ORFs annotated as hypothetical proteins and TadE-like proteins by RAST and IMG/ER, respectively (12-15). BLASTX results confirm that both genes are indeed *tadE* or *tadE*-like (Table 2) (35). This gene cluster on contig 19 also contains sequences for *tadZ*, *tadA*, *tadB*, and *tadC* (12-15). However, a gene (558 bp) encoding a protein that is 185 amino acids long is located within the cluster and was annotated as 'L,D-transpeptidase catalytic domain' by IMG/ER (15) and as 'ErfK/YbiS/YcfS/YnhG' by RAST (12-14). Both annotations were confirmed by BLASTX as conserved regions were revealed for ErfK, a lipoprotein-anchoring transpeptidase (COG1376, E-value =  $4.77 \times 10^{-32}$ ), the YkuD L,D-transpeptidase catalytic domain (pfam03734, E-value =  $3.31 \times 10^{-6}$ ), and a provisional L,D-transpeptidase (PRK10260, E-value =  $2.86 \times 10^{-17}$ ) (16-19). According

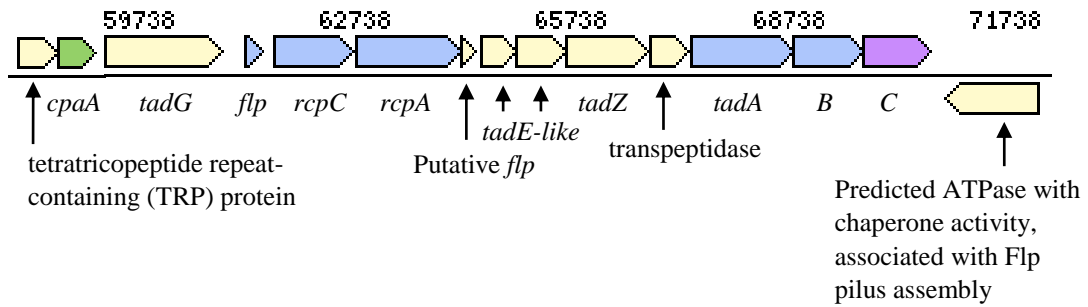


**Figure 3.** The *tad/flip* gene cluster on contig 19. Annotations were performed by IMG/ER and RAST and a putative *flp* gene was identified by BLASTX (12-15, 35).

**Table 2.** BLASTX results of two *tadE*-like genes located on contig 19 (35).

Contig	Locus	IMG/ER Description	BLASTX hit with lowest E-value	Query cover	E-value	% ID	Accession
19	64982..65461 (+)(480bp)	TadE-like protein	pilus biosynthesis protein TadE [ <i>Rhizobium leguminosarum</i> ]	92%	5.0E-41	46%	WP_018493559.1
19	65455..66117 (+)(663bp)	TadE-like protein	pilus assembly protein TadE [ <i>Rhizobium</i> sp. CF097]	94%	3.0E-55	48%	WP_037121181.1

to NCBI, this type of transpeptidase is an alternative pathway for peptidoglycan cross-linking (16-19).

While all the genes described so far in this gene cluster on contig 19 are encoded on the same strand, one gene that is located immediately downstream of the cluster is encoded on the opposite strand. This gene has been annotated as ‘Predicted ATPase with chaperone activity, associated with Flp pilus assembly’ by RAST (12-14). This prediction was confirmed by BLASTX with multiple alignments to ATPases in other organisms including an ‘ATPase with chaperone activity, associated with Flp pilus assembly *Loktanella cinnabarina*’ (96% query cover, E-value =  $9 \times 10^{-107}$ , 41% identity) (35).

In addition to these two *tad* gene clusters two loci that each contain a *tadE*-like gene and *tadG* have been detected (15) (Figure 4). One of them is localized to contig 23, while the other one is located on contig 19, approximately 315 kb downstream of the cluster of *tad* genes that are located on contig 19 (Figure 4).

BLAST alignments of the two TadE-like proteins revealed some similarities with an E-value of  $8 \times 10^{-7}$  while the two *tadG* loci also revealed minor similarity at the amino acid level (E-value =  $4 \times 10^{-11}$ , 58% query cover) (35). These genes are most likely orthologs. As previously mentioned, TadE and TadF are homologous to each other (22). These TadE-like proteins might actually be TadF proteins or may have taken on the role of TadF in the pilus assembly machinery.

The *flp/tad* gene cluster has been described in many prokaryotes and seems to be a mobile genomic island, which has been labeled as a ‘widespread colonization island’ (22). While the G+C content of the *tad/flp* gene cluster on contig 6 is 58.2%,

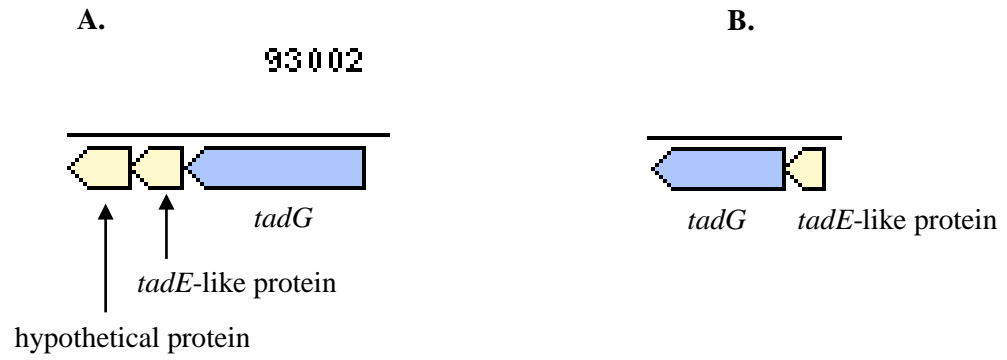


**Figure 4.** TadE-like protein and TadG are encoded in duplicate at two different loci.

**A.** illustrates the genes encoded on contig 23, **B.** illustrates the locus on contig 19 (15).

the G+C content of the 5 kb upstream and downstream region of this gene cluster was 60% and 59%, respectively. The G+C content of the *flp/tad* cluster on contig 19 was 55.6% and the 5 kb upstream region GC content was 57.5% and the downstream region G+C content was determined to be 56%. While the *tad/flp* gene clusters appear to have a slightly lower G+C content than the surrounding regions, it does not necessarily indicate a recent horizontal gene transfer. Phylogenetic analyses by Tomich et al. (2007) show that *tad/flp* gene clusters have not just undergone horizontal gene transfer, but also duplication, loss, and gene shuffling between distant prokaryotic relatives (22).

### **Genes Containing Conserved Regions Associated with RTX Toxin-Related Ca<sup>2+</sup>-Binding Proteins**

Extracellular proteins produced by *A. crassostreae* CV919-312<sup>T</sup> are capable of eliciting a similar mortality rate in oyster hemocytes as hemocytes treated with the organism itself (36). This indicates that extracellular proteins, potentially hemolysin/leukotoxin type toxins, play a role in pathogenicity (36). Furthermore, it has been suggested that the etiological agent of ROD most likely produces a toxin as a virulence factor (1, 8, 37).

The genome of *A. crassostreae* contains 11 open reading frames with conserved regions associated with RTX toxins and related Ca<sup>2+</sup>-binding (Table 3) (12-15). Additionally, one ORF on contig 23 has been annotated as a RTX toxin and related Ca<sup>2+</sup>-binding protein by IMG/ER (Table 3) (15). However, according to BLAST this gene does not contain any conserved domains related to RTX toxins and

related Ca<sup>2+</sup>-binding (35). Repeats-in-Toxins (RTX) is a family of proteins that is secreted by Gram-negative bacteria (38, 39). RTX proteins have characteristic glycine and aspartate rich nonapeptide repeats near the carboxyl terminal end of proteins (38, 39). These repeats are known to bind Ca<sup>2+</sup> ions upon secretion to promote proper folding of the protein into its functional conformation (39).

All known RTX proteins are secreted via a type I secretion system (T1SS) and have a wide range of functions (38, 39). Since the secretion signal is located at the carboxyl- terminal end of the protein, only fully translated proteins are secreted (38, 39). The T1SS consists of an ATPase localized to the inner membrane (ABC transporter), a membrane fusion protein (MFP), and a TolC-like outer membrane protein (OMP) (Figure 5) (38, 39).

The  $\alpha$ -hemolysin of *E. coli* (HlyA) and its secretion apparatus is one of the most extensively studied RTX toxins (40). Like many other RTX loci, this toxin along with the toxin activating protein (HlyC), the ABC transporter (HlyB), and the MFP (HlyD) are encoded within the same operon while the OMP (TolC) is located outside the *hly* operon (39, 40). The toxin activating protein HlyC is an acyltransferase that post-translationally activates the protoxin by attaching a fatty acyl residue to the protein (39, 40). Pore-forming RTX cytotoxins include hemolysins as well as leukotoxins, many of which are considered to be species and cell specific (39). While IMG/ER annotated most of the 11 ORFs in *A. crassostreae* as RTX toxins and related Ca<sup>2+</sup>-binding proteins or hemolysins, one ORF on contig 10 has been identified as a hypothetical protein (Table 3) (15). BLASTX revealed that this gene contains a

**Table 3.** Predicted ORFs in *A. crassostreae* draft genome that were annotated as RTX toxins and related Ca<sup>2+</sup> binding proteins or have conserved regions associated with RTX toxins and related Ca<sup>2+</sup> binding proteins (15-19, 35).

Contig/ Node	Locus	Description IMG/ER	BLASTX hit with lowest E-value	Query cover	E-value	%Identity	Accession number	Putative conserved domains with E- value <1E-05
Contig 10	33924..36203 (-)(2280bp)	Hemolysin- type calcium- binding repeat- containing protein	hypothetical protein [ <i>Roseobacter</i> sp. SK209-2-6]	84%	6.00E-113	40%	WP_008209620.1	COG2931, pfam08548
Contig 10	2154..10067 (+)(7914bp)	hypothetical protein	RTX toxins determinant A and related Ca <sup>2+</sup> -binding proteins [ <i>Vibrio maritimus</i> ]	58%	3.00E-108	41%	GAL22704.1	COG2931, pfam08548
Contig 19	587728..592248 (-)(4521bp)	Ca <sup>2+</sup> -binding protein, RTX toxin-related	Hemolysin-type calcium-binding region [ <i>Rhodobacter</i> sp. SW2]	58%	9.00E-144	69%	WP_008028071.1	pfam13403, COG2931, pfam13448, PRK15319, TIGR04225
Contig 4	1502..7750 (-)(6249bp)	Ca <sup>2+</sup> -binding protein, RTX toxin-related	Hemolysin-type calcium-binding region [ <i>Paracoccus denitrificans</i> PD1222]	30%	1.00E-30	30%	ABL68672.1	COG2931, pfam08548
Contig 3	10961..16465 (-)(5505bp)	Ca <sup>2+</sup> -binding protein, RTX toxin-related	hypothetical protein C-sp_D33230 [ <i>Curvibacter</i> putative symbiont of <i>Hydra magnipapillata</i> ]	82%	0	46%	CBA32654.1	COG2931, pfam08548



Contig 23	104519..106723 (+)(2205bp)	Ca <sup>2+</sup> -binding protein, RTX toxin-related	hypothetical protein [ <i>Sulfitobacter mediterraneus</i> ]	99%	1.00E-171	44%	WP_025050013.1	pfam13403, COG2931, pfam08548, PRK15319
Contig 6	718142..721957 (-)(3816bp)	Ca <sup>2+</sup> -binding protein, RTX toxin-related	hypothetical protein [ <i>Falsirhodobacter sp. alg1</i> ]	38%	1.00E-81	54%	WP_045392820.1	pfam13403, COG2931
Contig 24	49798..51039 (-)(1242bp)	Hemolysin- type calcium- binding repeat- containing protein	hypothetical protein [ <i>Maritimibacter alkaliphilus</i> ]	93%	1.00E-56	40%	WP_008331985.1	COG2931, pfam08548
Contig 19	617714..618508 (-)(795bp)	Hemolysin- type calcium- binding repeat- containing protein	hypothetical protein [ <i>Actibacterium mucosum</i> ]	58%	5.00E-11	48%	WP_035255897.1	COG2931
Contig 19	618647..619330 (-)(684bp)	Hemolysin- type calcium- binding repeat- containing protein	type I secretion target repeat protein [ <i>Roseobacter</i> sp. SK209-2-6]	33%	6.00E-06	40%	WP_008204875.1	COG2931
Contig 10	30208..32586 (-)(2379bp)	serralysin	M10 family peptidase [ <i>Citricella</i> sp. 357]	81%	7.00E-112	48%	WP_009506811.1	cd04277, COG2931, pfam08548
Contig 23	106871..108871 (+)(2001bp)	Ca <sup>2+</sup> -binding protein, RTX toxin-related	type I secretion protein [ <i>Leisingera aquimarina</i> ]	91%	7.00E-117	51%	WP_027258536.1	pfam13403

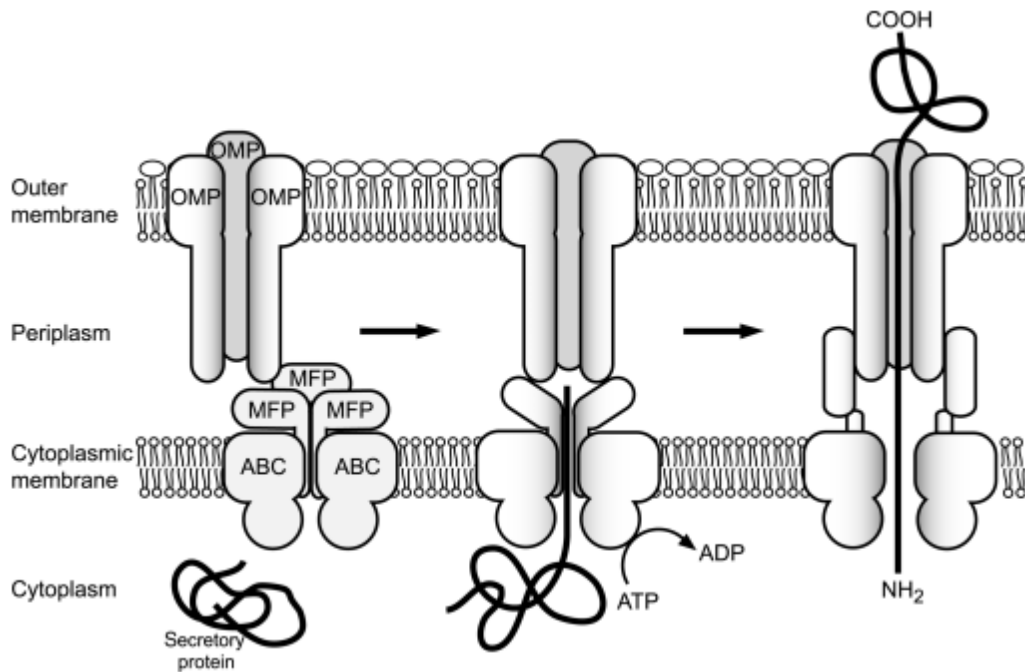


**Figure 5.** Assembly and schematic operation of a T1SS. The ABC transporter recognizes the C-terminal secretion signal on a RTX protein substrate and provides the energy to activate the channel-tunnel assembly. This assembly consists of the ABC transporter, the MFP, and the OMP. The channel spans the entire cell envelope through which the RTX protein can then be translocated directly from the cytoplasm to the exterior of the cell. A higher  $\text{Ca}^{2+}$  concentration outside the cell compared to the cytoplasm promotes correct protein folding and allows the protein to become biologically active (39).

conserved region associated with RTX toxin related  $\text{Ca}^{2+}$ -binding proteins (16-19). This gene (contig 10) is encoded by 7914 bp and an acyltransferase is located directly adjacent to it (Figure 6) (15). However, a T1SS that could potentially be involved in secretion of this protein has not been detected at this locus and could be located elsewhere on the genome.

A second RTX toxin related  $\text{Ca}^{2+}$ -binding protein with a cytolysin-activating acyltransferase immediately following has been located on contig 3 (15). Again, a T1SS is absent. In addition to these two cytolysin-activating acyltransferases that are located immediately next to a RTX toxin related  $\text{Ca}^{2+}$ -binding protein, one other putative cytolysin-activating acyltransferase was identified that is not located near a potential cytolysin gene (Table 4).

Linhartova et al. (2010) mention that recent studies revealed a weak lectin activity of some well-studied cytolytic pore-forming RTX proteins which suggests the possibility that initial binding of RTX proteins to host cells may be facilitated by recognition of glycoproteins on the host cell surface (39).

While many of the known RTX proteins are mostly known for their pore-forming cytotoxin activity as hemolysins and leukotoxins, this family of proteins also includes proteases, lipases, adenylate cyclases, bacteriocins, and S-layers (38-40). Out of the 11 RTX toxin related  $\text{Ca}^{2+}$ -binding proteins in the draft genome 7 contain conserved domains that are linked to serralyisin peptidases (pfam08548) (Table 3) (16-19). One of the 7 genes in particular has been annotated as serralyisin by IMG/ER and in addition to having a conserved domain found in serralyisins (pfam08548), the gene

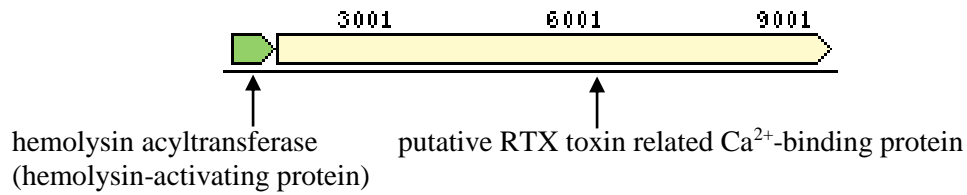


**Figure 6.** Putative RTX toxin on contig 10 of *A. crassostreae* genome with a cytolysin activating acyltransferase located immediately upstream (15). Although IMG/ER annotated this putative RTX toxin as a hypothetical protein, BLASTX revealed that this gene contains a conserved region associated with RTX toxin related Ca<sup>2+</sup>-binding proteins (16-19).

**Table 4.** Putative cytolysin activating acyltransferases encoded on the *A. crassostreae* CV919-312<sup>T</sup> draft genome (12-15). Conserved domains were identified by BLASTX (16-19). A key for conserved domain descriptions can be found in the appendix.

Contig/ Node	Locus	Description IMG/ER	Description RAST	Conserved domains with E-value <1E-05
Contig 10	1495..2109 (+)(615bp)	ACP:hemolysin acyltransferase (hemolysin-activating protein)	-	pfam02794, COG2994
Contig 3	10445..10954 (-)(510bp)	cytolysin-activating lysine-acyltransferase	RTX toxin activating lysine-acyltransferase	pfam02794, COG2994
Contig 6	38280..39065 (-)(786bp)	ornithine-acyl (acyl carrier protein) N-acyltransferase	Putative hemolysin	COG3176, pfam13444, c117185

carries a second conserved domain found in Zinc-dependent metalloproteases belonging to a serralysin-like subfamily (cd04277) (16-19). According to NCBI, this family of proteins contains a calcium-binding carboxyl-terminal domain that forms a beta role potentially involved in translocation (16-19). All these conserved domains within this gene confirm the annotation by IMG/ER. Serralysin is an important virulence factor of *Serratia marcescens* (41). According to Stocker et al. (1995), a C-terminal  $\beta$ -sandwich structure binds calcium ions in order to activate serralysin peptidases (42). Serralysin-type protease PrtA of the insect-pathogenic bacterium *Photorhabdus luminescens* has been shown to digest proteins in hemolymph of *Manduca sexta* that have immune-related functions like immune recognition and signaling (43). These results suggest that the substrate specificity of serralysins may be directed towards components of the innate immune system (43). Additionally, bacterial proteases have the ability to degrade numerous antimicrobial peptides (41, 44, 45). Since antimicrobial peptides are present in oysters as part of their innate immune system, a serralysin peptidase could help in the infectious process of ROD by hydrolyzing these innate immune antimicrobial peptides.

Members of a newly discovered subgroup of RTX proteins function as adhesins or biofilm associated proteins (38). Some of the genes with conserved RTX toxin  $\text{Ca}^{2+}$ -binding protein domains in the *A. crassostreae* genome might be involved in surface attachment rather than cytolytic activities. RTX adhesins can promote inter-bacterial interaction or interaction between bacteria and their host (38). LapA for example is a RTX protein found in *Pseudomonas putida* and *Pseudomonas fluorescens* and is required for biofilm formation in these organisms (38). BapA

(biofilm associated protein) is a protein found in *Salmonella enterica* that shows homology to RTX proteins and promotes cell-cell interaction (46). FrhA is a RTX protein in *Vibrio cholera* and associated with hemagglutination, adherence to epithelial cells, biofilm formation as well as chitin binding (38). Similarly, RtxA is thought to promote contact to phagocytic host cells in the intracellular pathogen *Legionella pneumophila* in order to facilitate entry and promote pathogenesis (38). Furthermore, an RTX related protein in *Shewanella oneidensis* (BpfA) is known to be secreted by a T1SS and aids in the formation of biofilm (47). BpfA is positively regulated by the availability of calcium ions (47). Calcium concentration is known to influence biofilm formation in bacteria (48). Increased calcium concentrations also promote biofilm formation and affect protein expression in *Pseudoalteromonas* sp. 1398 (49). Some of the RTX proteins present in the draft genome of *A. crassostreae* may have similar functions as the aforementioned RTX proteins that are involved in surface-attachment. These putative adhesins may also be regulated by calcium concentration. The oyster shell is primarily made up of calcium carbonate. Potential shell degradation and an increase in calcium content in the surrounding environment may promote surface-colonization of the organism to the inner shell surface. Boardman et al. (2008) have shown that *A. crassostreae* prefers to colonize the oyster's inner shell surface over any other part of the oyster (9). This has been confirmed by electron microscopy and immunofluorescent labeling which shows *A. crassostreae* cells attached to the inner shell surface and conchiolin deposits of oysters affected by ROD (9, 36).

It should be noted that while IMG/ER predicted most of the RTX toxin related  $\text{Ca}^{2+}$ -binding proteins and hemolysin activating proteins, RAST annotated many of these genes as alkaline phosphatases.

### **Putative Hemolysins/Leukotoxins Other than RTX Related Proteins**

In addition to all of the above-mentioned RTX related proteins, a putative ‘hemolysin III’ has been annotated by both IMG/ER and RAST (Table 5) (12-15). This cytolysin contains multiple conserved domains with E-values  $<1 \times 10^{-5}$  (PRK15087, COG1272, TIGR01065, pfam03006), all of which suggest that this gene indeed encodes for a hemolysin (16-19). NCBI’s description of these domains can be found in the appendix.

In addition, one gene on contig 4 has been annotated as a putative hemolysin (Table 3) (12-15). BLASTX confirmed this function by detecting a putative hemolysin conserved domain (COG3176, E-value =  $5.31 \times 10^{-6}$ ), but it also identified a conserved region associated with lysophospholipid acyltransferases (cd07986, E-value =  $7.54 \times 10^{-41}$ ) (Table 5) (16-19). In addition, almost all BLASTX hits were aligning the protein to acyltransferases in other organisms with E-values as low as  $1 \times 10^{-147}$  (35).

### **Conserved Hint Domains**

While 11 genes have conserved regions related to RTX toxin related  $\text{Ca}^{2+}$ -binding proteins, one gene on contig 23 has been annotated by IMG/ER (15) as ‘ $\text{Ca}^{2+}$ -binding protein, RTX toxin-related’ without showing any of such conserved regions in BLASTX (35) (Table 3). The only conserved region associated with this gene is a Hint

**Table 5.** Putative hemolysins encoded by draft genome of *A. crassostreae* (12-19).

<b>Contig/Node</b>	<b>Locus</b>	<b>Description IMG/ER</b>	<b>Description RAST</b>	<b>Conserved domains with E-value &lt;1E- 05</b>
Contig 6	33612..34253 (+)(642bp)	hemolysin III	Predicted membrane protein hemolysin III homolog	PRK15087, COG1272, TIGR01065, pfam03006
Contig 4	204213..205076 (+)(864bp)	Putative hemolysin	Putative hemolysin	cd07986, COG3176



domain (pfam13403) that is usually found in inteins (16-19). BLASTX results show that this protein is most likely connected to a T1SS (Table 3). Interestingly, three of the above mentioned genes that have been annotated as RTX toxins and related  $\text{Ca}^{2+}$ -binding proteins by IMG/ER and contain RTX toxin conserved domains also contain the same type of conserved Hint domain. Inteins are genetic elements that are transcribed and translated with the host gene (50). After translation these self-splicing elements cleave themselves from the host protein and the host protein is joined again by a peptide bond leaving the protein completely intact and functional (50). This Hint domain has first been observed in Hedgehog proteins (belonging to the family of Hog proteins) and inteins (51, 52). While inteins are found in archaea as well as in bacteria, plastids, and viruses, Hog proteins are usually found in multicellular eukaryotes (50, 52). Traditional inteins are usually found in conserved proteins that are involved in nucleic acid metabolism and DNA replication (50). However, Amitai et al. (2003) have found that new bacterial intein-like domains are usually found in variable protein regions and are flanked by regions that are found in secreted proteins (52). These flanking domains include calcium binding RTX repeats (52). Since most bacterial intein-like domains are found in secreted proteins, it has been proposed that Hint domains in bacteria may enhance variability in secreted proteins (52).

### **Putative Adhesin**

While no complete T1SS is located near any of the above described RTX toxin and related  $\text{Ca}^{2+}$ -binding proteins, a surface protein that seems to be involved in adhesion is separated by 73 bp from a complete T1SS on contig 4 (12-15). According

to IMG/ER annotation, this T1SS may be responsible for the secretion of the adhesin that is located upstream (Figure 7). This surface protein has been annotated as 'Ig-like domain (group 3)' and 'T1SS secreted agglutinin RTX' by IMG/ER and RAST, respectively (12-15). NCBI's conserved domain database confirms this annotation showing conserved domains containing an Ig-like fold. This family of proteins is found to be surface associated in other bacteria (pfam13754) (16-19). While the majority of BLASTX hits are hypothetical proteins, one hit was aligned to "RTX family exoprotein (*Tateyamaria* sp. ANG-S1)" (90% query cover, E-value =  $2 \times 10^{-75}$ , 35% identity, accession: WP\_039682725.1) (35).

An outer membrane protein, an ATP-binding cassette, and a membrane fusion protein are all encoded in an operon-like structure (Figure 7). IMG/ER annotated the ATPase that is part of the T1SS as "ATP-binding cassette, subfamily C, LapB" while RAST annotated the outer membrane protein as "Type I secretion system, outer membrane component LapE" (Table 6) (12-15).

As mentioned earlier, LapA is a RTX protein found in *Pseudomonas fluorescens* and is required for biofilm formation in this organism (38, 53). In this T1SS system, LapB is a cytoplasmic membrane-localized ATPase, LapC is a membrane fusion protein, and LapE is an outer membrane protein (53). These annotations confirm that this T1SS is associated with the secretion of a molecule involved in surface-attachment. The SiiE protein in *Salmonella enterica* has 53 copies of an immunoglobulin (Ig)-like repeat and is important for adhesion to epithelial cells (38). This suggests that this protein is indeed a surface associated protein that

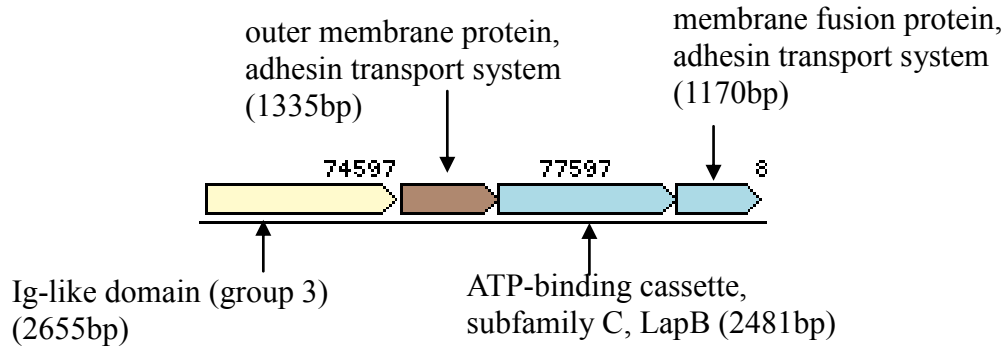


**Figure 7.** IMG/ER annotation of adhesin biogenesis and T1SS gene cluster on contig 4 (15).

**Table 6.** Annotation results of gene cluster on contig 4 involved in secretion of putative adhesion molecule from IMG/ER and RAST (12-15).

<b>Locus</b>	<b>Description IMG/ER</b>	<b>Description RAST</b>
72954..75608 (+)(2655bp)	Ig-like domain (group 3)	T1SS secreted agglutinin RTX
75681..77015 (+)(1335bp)	outer membrane protein, adhesin transport system	Type I secretion system, outer membrane component LapE
77012..79492 (+)(2481bp)	ATP-binding cassette, subfamily C, LapB	Probable ATP-binding/permease fusion ABC transporter
79492..80661 (+)(1170bp)	membrane fusion protein, adhesin transport system	HlyD family secretion protein

facilitates surface attachment to host cells. This molecule could enhance surface attachment of *A. crassostreae* to oyster hemocytes or epithelial cells of oysters and facilitate colonization of the animal.

#### **Type 4 Secretion Systems**

T4SSs are found in Gram-negative bacteria and are related to the bacterial conjugation machinery (54). However, T4SSs are also virulence factors in Gram-negative bacteria as they can translocate not only DNA, but also virulence effector molecules into host cells (55, 56). The T4SS can transport substrate molecules by direct cell-to-cell contact (56). T4SSs can be divided into a T4ASS and T4BSS. The T4ASS is based on the structure and subunits found in the *Agrobacterium tumefaciens* VirB/D4 system consisting of 12 genes (*virB1-virB11* and *virD4*) (55, 57) while the T4BSS is based on the model found in the *Legionella pneumophila* Dot/Icm system (57). While almost all of the genes of a T4ASS are present in the draft genome of *A. crassostreae*, a partial T4BSS can also be located.

#### **Type 4A secretion system**

As previously mentioned, a typical T4ASS is composed of 12 proteins (Figure 8), VirB1-VirB11, and VirD4. The T4ASS gene cluster in *A. crassostreae* is missing VirB1 as well as VirB7 in annotations from both RAST and IMG/ER, but encodes all the other proteins that are associated with a T4ASS (Figure 9) (12-15). Two ORFs within the cluster contain lytic murein transglycosylase domains, which are the same class of proteins as VirB1 (56, 59). Lytic transglycosylases degrade peptidoglycan

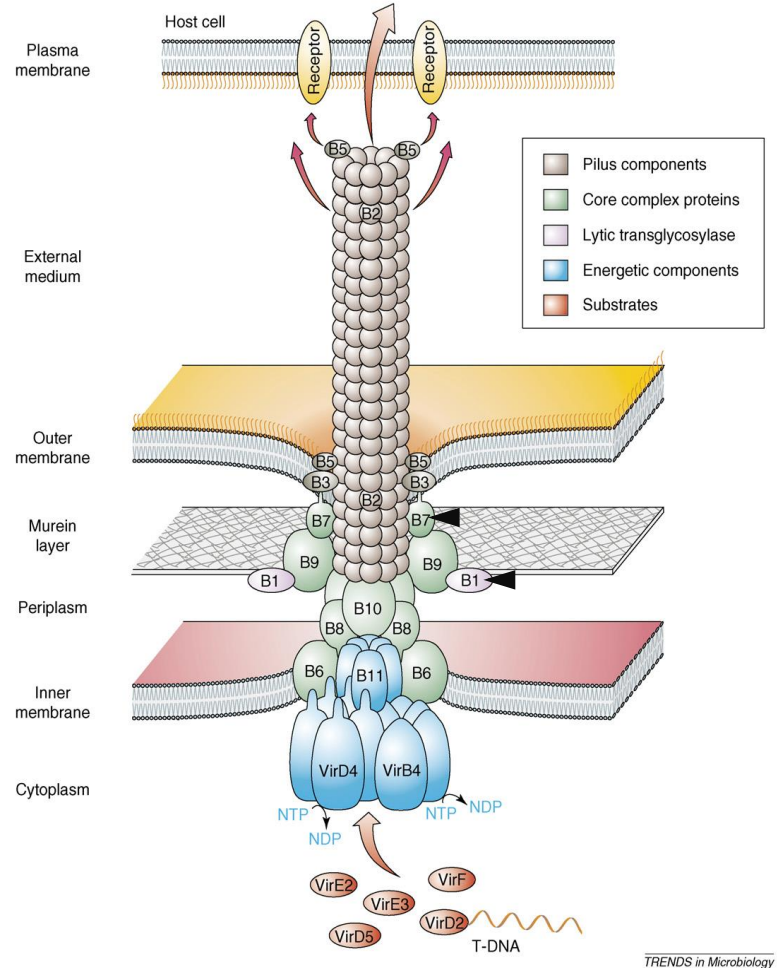


**Figure 8.** Core structure of a typical T4ASS like the one found in *A. tumefaciens*.

Translocation of effector molecules like the VirD2-T-DNA complex are transported directly from the bacterial cytoplasm into target cells. VirB2 and VirB5 are both important pilus components and may function as adhesins that facilitate host cell binding (58). VirB1 and VirB7 were not annotated in *A. crassostreae* genome (indicated by arrowhead). Figure from Backert et al. (2008) (58).

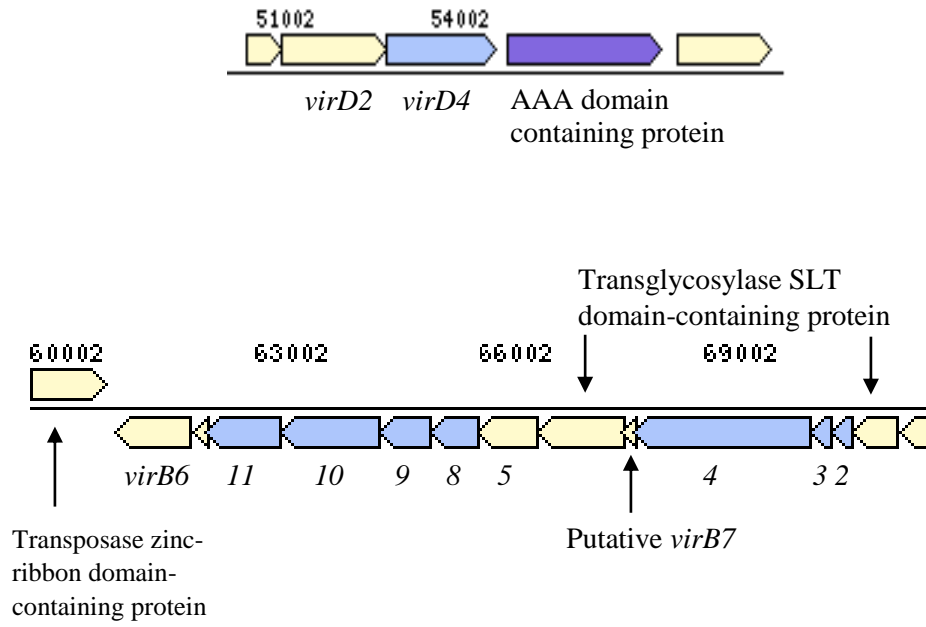


**Figure 9.** T4ASS gene cluster on contig 7 of *A. crassostreae*. Unlabeled ORFs were annotated as hypothetical proteins (12-15).

locally and are essential for the pilus biogenesis of the T4ASS (56, 59). While IMG/ER annotated both ORFs as ‘Transglycosylase SLT domain-containing protein’, RAST annotated them as ‘Membrane-bound lytic murein transglycosylase D precursor’ (12-15). These annotations have been confirmed by conserved domains identified by BLASTX (cd00254, pfam01464, COG0741, PRK11619) and indicate that these genes may have taken on the role of VirB1 (16-19).

While VirB7, together with VirB9 and VirB10, is supposed to form the core complex of the T4ASS that spans the periplasm (56), identification of VirB7 is often challenging since VirB7 has not been described in all T4SSs (54, 59). With 4.5 kDa (60, 61) VirB7 is the smallest of all the proteins that are part of the T4ASS and homologues are sometimes difficult to identify (54). The size for VirB7 ranges from 47 to 69 amino acid residues (54). Two hypothetical proteins are encoded within the *virB* gene cluster that fall within this size range of VirB7, one with 58 amino acids (177bp), and the other with 52 amino acids (159 bp) (12-15). BLASTX results did not reveal any conserved domains (16-19), however IMG/ER linked the 52 amino acid protein to a family of proteins associated with a ‘Prokaryotic membrane lipoprotein lipid attachment site profile’ that can be found in the Swiss Institute of Bioinformatics Resource Portal’s Prosite database (62, 63). Prosite is a database of protein domains, families and functional sites (62, 63). This connection between the 52 amino acid protein encoded on the draft genome and this protein family was confirmed by submitting the 52 amino acid sequence to ScanProsite. ScanProsite matches similarities between the entered amino acid sequence and signature profiles in proteins in order to detect functional and structural domains within a protein (64, 65).

The protein profile detected by Prosite was ‘Prokaryotic membrane lipoprotein lipid attachment site profile’ (accession PS51257) and matched to the first 17 amino acid residues (64, 65). VirB7 is a membrane associated lipoprotein that is thought to anchor and stabilize the pilus complex to the outer membrane (54, 56). This profile match would suggest that the 52 amino acid protein encoded within the *virB* gene cluster is a VirB7 homologue (Figure 9).

Interestingly, VirD2, a protein involved in T-DNA processing and transfer in *Agrobacterium tumefaciens* (66, 67), is encoded just upstream of *virD4* in the draft genome of *A. crassostreae*. In *A. tumefaciens*, oncogenic T-DNA is transferred into plant cells where it is integrated into the nuclear genome and able to modify plant hormonal balance, cell differentiation, transcription, and metabolism leading to tumors (66, 68). VirD2 is the pilot protein that is directly involved in the transfer of T-DNA (68).

A gene located just downstream of *virD4* has been annotated as ‘AAA domain-containing protein’ by IMG/ER (15) while the GenBank annotation service identified this gene as a ‘DNA repair protein’ (35). These annotations correlate with the observation that RecN DNA repair proteins exhibit ATPase activity, which is stimulated by the addition of DNA (16-19, 69). In addition to the genes mentioned above, a second copy of a putative *virB6* gene is located approximately 50 kb upstream of the *virB* gene cluster. This 597 bp gene has been annotated as ‘TrbL/VirB6 plasmid conjugal transfer protein’ by IMG/ER and ‘Inner membrane protein of type IV secretion of T-DNA complex, VirB6’ by RAST (12-15).



## **Type 4B secretion system**

In addition to the T4ASS, a partial T4BSS has been annotated which is often involved in pathogenesis (70) (Figure 10). The T4BSS was first discovered in the human pathogen *Legionella pneumophila* (70). *L. pneumophila* is an intracellular pathogen that multiplies within and kills macrophages (71, 72). The T4BSS seems to contain components that are homologous to proteins found in type 2, type 3, type 4A, and type 6 secretion systems (70). Like the T4ASS, this T4BSS has some similarity to bacterial conjugation systems (70). In *L. pneumophila*, the *dot/icm* genes that encode this T4BSS are necessary for conjugal transfer of IncQ plasmids as well as translocation of effector molecules into host cells (70). Two groups have independently discovered clusters of genes that are responsible for intracellular replication and macrophage killing and while one group named the genes *dot* (defect in organelle trafficking), the other named them *icm* (intracellular multiplication) (70). A typical T4BSS has multiple clusters of genes, one cluster containing *dotD-dotC-dotB*, a second cluster encodes *dotM/icmP-dotL/icmO*, and yet another cluster encodes *dotI/icmL-dotH/icmK-dotG/icmE* (70). Part of the T4BSS is a gene encoding *dotA* and *dotO/icmB* (70) (see Figure 11 for putative assembly and location of proteins associated with T4BSS assembly). Annotations revealed that many of these genes are present in the draft genome of *A. crassostreae* (Figure 10).

Contig 8 encodes *dotL* and *dotA* (12-15). A 6189 bp gene was annotated as ‘C-terminal domain on Strawberry notch homologue’ by IMG/ER while RAST called it a ‘Probably methylase/helicase’ (12-15). BLASTX results show conserved domains

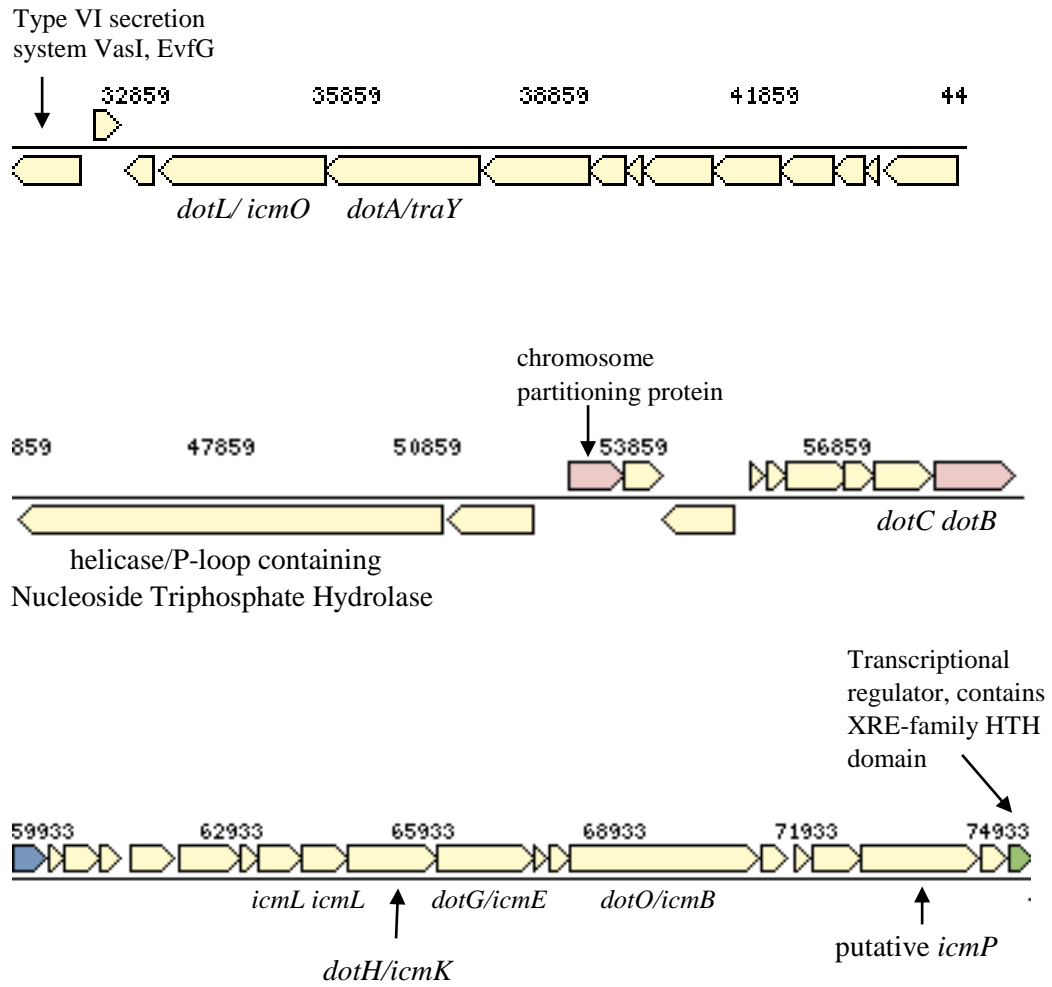


**Figure 10.** Type 4B secretion system in the *A. crassostreae* draft genome. Genes are located on contig 8 and were annotated by IMG/ER and RAST (12-15). ORFs without a gene or functional description were only identified as hypothetical proteins.

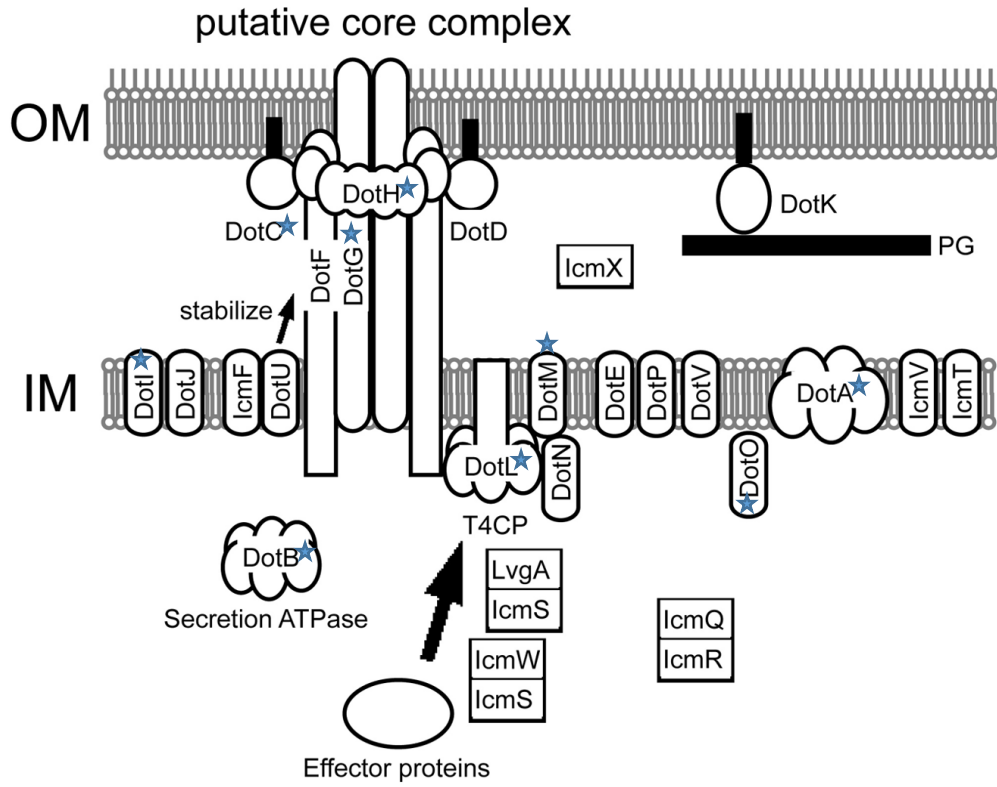


**Figure 11.** Putative core complex assembly of *L. pneumophila* T4BSS proteins and localization of T4BSS associated proteins based on experimental and amino acid sequence prediction data (70). Genes present in *A. crassostreae* genome are indicated by a blue star. Figure from Nagai et al. (2011) (70).

indicating that the gene may indeed encode for a helicase (pfam13871) as suggested by RAST or a 'P-loop containing Nucleoside Triphosphate Hydrolase' (cl21455) (16-19). One of the genes located within this T4BSS cluster of genes was annotated as 'Macrophage killing protein with similarity to conjugation protein' by IMG/ER (15). This annotation was confirmed by BLASTX which detected a conserved domain 'IcmL: Macrophage killing protein with similarity to conjugation protein' (pfam11393) (16-19). According to NCBI's conserved domain database, this conserved region contains two amphipathic beta-sheet regions, which are required for pore formation in the host cell membrane (16-19). Another IcmL (homologue of DotI) protein is encoded immediately downstream containing the same conserved domain (Figure 10) (15).

A protein within this cluster of genes was annotated as 'Putative outer membrane core complex of type IVb secretion' by IMG/ER based on alignments to the protein family 'T4BSS\_DotH\_IcmK' (PF12293) (15). This alignment was confirmed by performing a sequence alignment search with Pfam (73). DotH/IcmK is a transporter protein localized to the outer membrane and is also part of the T4BSS (70).

RAST annotated the gene that is immediately downstream as IcmE/DotG whereas IMG/ER called it 'conjugation TrbI-like protein' (12-15). The Carboxyl-terminal domain of IcmE/DotG is homologous to TrbI (70, 74, 75). TrbI is a protein involved in plasmid DNA transfer (74, 75). In addition, multiple hits with BLASTX showed homology to DotG/IcmE T4BSS protein in other organisms (35). DotG/IcmE

is thought to be an outer membrane protein with a transmembrane helix with high similarity to Virb10 in the T4ASS (70).

DotO/IcmB has been identified by both IMG/ER and RAST (12-15).

DotO/IcmB is a protein that is distantly related to VirB4 proteins and is thought to be localized to the inner membrane (70). However, the exact function of DotO/IcmB as part of the T4BSS remains to be discovered (70).

Many of the proteins encoded in this T4BSS gene cluster in the *A. crassostreae* draft genome have only been identified as hypothetical proteins. This includes a gene containing 1842 bp. While no conserved domains have been identified with BLASTX, multiple hits show homology to IcmP (Best hit: IcmP-like type IV secretion system protein (*Xanthomonas euvesicatoria*), WP\_011345649.1, E-value:  $2 \times 10^{-11}$ ) (35).

While not much is known about the function of DotM/IcmP, this protein seems to be associated with DotL/IcmO which is a member of the type IV coupling protein family and has transmembrane helices and a cytoplasmic domain (70).

A 363 bp gene in this cluster contains a conserved domain of 'Helix-turn-helix XRE-family like proteins,' which are DNA-binding proteins (cd00093) (16-19).

RAST also annotated this gene as a 'putative DNA-binding protein' (12-14) and IMG/ER called it 'Transcriptional regulator, contains XRE-family HTH domain' (15).

While some proteins known to be involved in type 4B secretion are encoded by the draft genome of *A. crassostreae*, many genes associated with type 4B secretion are either missing or remain to be discovered. The exact function of each protein in this secretion system still needs to be elucidated which makes it more difficult to annotate these genes.

## Conclusion

This first publically available draft genome of *A. crassostreae* CV919-312<sup>T</sup> revealed multiple genes that are putatively involved in virulence mechanisms of this organism. Previous research shows that extracellular products of *A. crassostreae* CV919-312<sup>T</sup> are capable of killing oyster hemocytes (36). With the help of annotation services provided by IMG/ER and RAST, we were able to identify genes that are potentially involved in pathogenesis. Multiple genes with conserved regions associated with RTX toxins and related Ca<sup>2+</sup>-binding proteins were detected. Since RTX toxins are often associated with virulence in disease-causing microorganisms, they may play an important role in the pathogenicity of *A. crassostreae*. In order to determine whether any of these genes is involved in pathogenesis further studies would need to be performed including molecular cloning experiments. Targeted mutagenesis to create knockout mutants of selected putative RTX toxin genes and subsequent *in vivo* testing would help identify specific virulence genes. Additionally, multiple genes that are potentially involved in surface-attachment have been identified. Besides the fact that proteins with RTX toxins and related Ca<sup>2+</sup>-binding domains are often associated with surface attachment (38), a putative adhesin protein with the associated T1SS has been identified. Furthermore, the *tad/flp* gene cluster appears to be responsible for fimbriae biogenesis in *A. crassostreae*. Further studies are needed to confirm this hypothesis. A type 4A and partial type 4B secretion system could be involved in pathogenesis by translocation of effector molecules into oyster hemocytes or other host cells. Additional studies at the molecular level would aid in the assignments of functional roles to the genes described in this study. Biofilm assays

of wild type and knockout mutants would reveal whether the putative genes associated with surface attachment that were discussed in this report are indeed involved in oyster shell colonization.

This Whole Genome Shotgun project has been deposited in DDBJ/ENA/GenBank under the accession LKBA00000000. The version described in this paper is version LKBA01000000.

### **FUNDING INFORMATION**

This work was supported by an award from the Rhode Island Science and Technology Advisory Council to Dr. David Nelson and Dr. David Rowley.

### **ACKNOWLEDGEMENTS**

We thank Dr. Katherine Boettcher for providing us with *A. crassostreae* strain CV919-312<sup>T</sup>.

This research is based in part upon work conducted using the Rhode Island Genomics and Sequencing Center which is supported in part by the National Science Foundation under EPSCoR Grants Nos. 0554548 & EPS-1004057.

## REFERENCES

1. **Bricelj VM, Ford ES, Borrero FJ, Perkins FO, Rivara G, Hillman RE, Elston RA, Chang J.** 1992. Unexplained mortalities of hatchery-reared, juvenile oysters, *Crassostrea virginica* (Gmelin). *J Shellfish Res* **11**:331-347.
2. **Davis CV, Barber BJ.** 1994. Size-dependent mortality in hatchery-reared populations of oysters, *Crassostrea virginica*, Gmelin 1791, affected by Juvenile Oyster Disease. *J Shellfish Res* **13**:137-142.
3. **Boettcher KJ, Geaghan KK, Maloy AP, Barber BJ.** 2005. *Roseovarius crassostreae* sp. nov., a member of the *Roseobacter* clade and the apparent cause of juvenile oyster disease (JOD) in cultured Eastern oysters. *Int J Syst Evol Microbiol* **55**:1531-1537.
4. **Boettcher KJ, Barber BJ, Singer JT.** 1999. Use of antibacterial agents to elucidate the etiology of juvenile oyster disease (JOD) in *Crassostrea virginica* and numerical dominance of an  $\alpha$ -Proteobacterium in JOD-affected animals. *Appl Environ Microbiol* **65**:2534-2539.
5. **Brinkhoff T, Giebel H-A, Simon M.** 2008. Diversity, ecology, and genomics of the *Roseobacter* clade: a short overview. *Arch Microbiol* **189**:531-539.
6. **Maloy AP, Ford SE, Karney RC, Boettcher KJ.** 2007. *Roseovarius crassostreae*, the etiological agent of Juvenile Oyster Disease (now to be known as *Roseovarius* Oyster Disease) in *Crassostrea virginica*. *Aquaculture* **269**:71-83.
7. **Sunila I.** *Roseovarius* Oyster Disease. <http://www.ct.gov/doag/lib/doag/aquaculture/rod.pdf>. Accessed 3-12-15.
8. **Ford SE, Borrero FJ.** 2001. Epizootiology and pathology of juvenile oyster disease in the Eastern oyster, *Crassostrea virginica*. *J Invertebr Pathol* **78**:141-154.
9. **Boardman CL, Maloy AP, Boettcher KJ.** 2008. Localization of the bacterial agent of juvenile oyster disease *Roseovarius crassostreae* within affected eastern oysters *Crassostrea virginica*. *J Invertebr Pathol* **97**:150-158.
10. **Park S, Park JM, Kang CH, Yoon JH.** 2015. *Aliiroseovarius pelagivivens* gen. nov., sp. nov., isolated from seawater, and reclassification of three species of the genus *Roseovarius* as *Aliiroseovarius crassostreae* comb. nov., *Aliiroseovarius halocynthiae* comb. nov. and *Aliiroseovarius sediminilitoris* comb. nov. *Int J Syst Evol Microbiol* **65**:2646-2652.
11. **Karim M, Zhao W, Rowley D, Nelson D, Gomez-Chiarri M.** 2013. Probiotic Strains for Shellfish Aquaculture: Protection of Eastern Oyster, *Crassostrea virginica*, Larvae and Juveniles Against Bacterial Challenge. *J Shellfish Res* **32**:401-408.
12. **Aziz RK, Bartels D, Best AA, DeJongh M, Disz T, Edwards RA, Formsma K, Gerdes S, Glass EM, Kubal M, Meyer F, Olsen GJ, Olson R, Osterman AL, Overbeek RA, McNeil LK, Paarmann D, Paczian T, Parrello B, Pusch GD, Reich C, Stevens R, Vassieva O, Vonstein V, Wilke A, Zagnitko O.** 2008. The RAST Server: Rapid Annotations using Subsystems Technology. *BMC Genomics* **9**:75-75.



13. **Overbeek R, Olson R, Pusch GD, Olsen GJ, Davis JJ, Disz T, Edwards RA, Gerdes S, Parrello B, Shukla M, Vonstein V, Wattam AR, Xia F, Stevens R.** 2014. The SEED and the Rapid Annotation of microbial genomes using Subsystems Technology (RAST). *Nucleic Acids Res* **42**:D206-214.
14. **Overbeek R, Begley T, Butler RM, Choudhuri JV, Chuang H-Y, Cohoon M, de Crécy-Lagard V, Diaz N, Disz T, Edwards R, Fonstein M, Frank ED, Gerdes S, Glass EM, Goesmann A, Hanson A, Iwata-Reuyl D, Jensen R, Jamshidi N, Krause L, Kubal M, Larsen N, Linke B, McHardy AC, Meyer F, Neuweger H, Olsen G, Olson R, Osterman A, Portnoy V, Pusch GD, Rodionov DA, Rückert C, Steiner J, Stevens R, Thiele I, Vassieva O, Ye Y, Zagnitko O, Vonstein V.** 2005. The Subsystems Approach to Genome Annotation and its Use in the Project to Annotate 1000 Genomes. *Nucleic Acids Res* **33**:5691-5702.
15. **Markowitz VM, Chen IM, Palaniappan K, Chu K, Szeto E, Grechkin Y, Ratner A, Jacob B, Huang J, Williams P, Huntemann M, Anderson I, Mavromatis K, Ivanova NN, Kyrpides NC.** 2012. IMG: the Integrated Microbial Genomes database and comparative analysis system. *Nucleic Acids Res* **40**:D115-122.
16. **Marchler-Bauer A, Lu S, Anderson JB, Chitsaz F, Derbyshire MK, DeWeese-Scott C, Fong JH, Geer LY, Geer RC, Gonzales NR, Gwadz M, Hurwitz DI, Jackson JD, Ke Z, Lanczycki CJ, Lu F, Marchler GH, Mullokandov M, Omelchenko MV, Robertson CL, Song JS, Thanki N, Yamashita RA, Zhang D, Zhang N, Zheng C, Bryant SH.** 2011. CDD: a Conserved Domain Database for the functional annotation of proteins. *Nucleic Acids Res* **39**:D225-229.
17. **Marchler-Bauer A, Derbyshire MK, Gonzales NR, Lu S, Chitsaz F, Geer LY, Geer RC, He J, Gwadz M, Hurwitz DI, Lanczycki CJ, Lu F, Marchler GH, Song JS, Thanki N, Wang Z, Yamashita RA, Zhang D, Zheng C, Bryant SH.** 2015. CDD: NCBI's conserved domain database. *Nucleic Acids Res* **43**:D222-226.
18. **Marchler-Bauer A, Anderson JB, Chitsaz F, Derbyshire MK, DeWeese-Scott C, Fong JH, Geer LY, Geer RC, Gonzales NR, Gwadz M, He S, Hurwitz DI, Jackson JD, Ke Z, Lanczycki CJ, Liebert CA, Liu C, Lu F, Lu S, Marchler GH, Mullokandov M, Song JS, Tasneem A, Thanki N, Yamashita RA, Zhang D, Zhang N, Bryant SH.** 2009. CDD: specific functional annotation with the Conserved Domain Database. *Nucleic Acids Res* **37**:D205-210.
19. **Marchler-Bauer A, Bryant SH.** 2004. CD-Search: protein domain annotations on the fly. *Nucleic Acids Res* **32**:W327-331.
20. **Boardman C.** 2005. Host-pathogen interactions between Eastern oysters (*Crassostrea virginica*) and the bacterial agent of juvenile oyster disease (*Roseovarius crassostreae*) The University of Maine.
21. **Angelov A, Bergen P, Nadler F, Hornburg P, Lichev A, Ubelacker M, Pachl F, Kuster B, Liebl W.** 2015. Novel Flp pilus biogenesis-dependent natural transformation. *Front Microbiol* **6**:84.

22. **Tomich M, Planet PJ, Figurski DH.** 2007. The *tad* locus: postcards from the widespread colonization island. *Nat Rev Microbiol* **5**:363-375.
23. **Nykyri J, Mattinen L, Niemi O, Adhikari S, Kõiv V, Somervuo P, Fang X, Auvinen P, Mäe A, Palva ET.** 2013. Role and Regulation of the Flp/Tad Pilus in the Virulence of *Pectobacterium atrosepticum* SCRI1043 and *Pectobacterium wasabiae* SCC3193. *PloS one* **8**:e73718.
24. **Kachlany SC, Planet PJ, Bhattacharjee MK, Kollia E, DeSalle R, Fine DH, Figurski DH.** 2000. Nonspecific Adherence by *Actinobacillus actinomycetemcomitans* Requires Genes Widespread in Bacteria and Archaea. *J Bacteriol* **182**:6169-6176.
25. **Wang Y, Chen C.** 2005. Mutation analysis of the *flp* operon in *Actinobacillus actinomycetemcomitans*. *Gene* **351**:61-71.
26. **Clock SA, Planet PJ, Perez BA, Figurski DH.** 2008. Outer membrane components of the Tad (tight adherence) secreton of *Aggregatibacter actinomycetemcomitans*. *J Bacteriol* **190**:980-990.
27. **Li T, Xu Z, Zhang T, Li L, Chen H, Zhou R.** 2012. The genetic analysis of the *flp* locus of *Actinobacillus pleuropneumoniae*. *Arch Microbiol* **194**:167-176.
28. **Blatch GL, Lasse M.** 1999. The tetratricopeptide repeat: a structural motif mediating protein-protein interactions. *Bioessays* **21**:932-939.
29. **Cervený L, Straskova A, Dankova V, Hartlova A, Ceckova M, Staud F, Stulik J.** 2013. Tetratricopeptide Repeat Motifs in the World of Bacterial Pathogens: Role in Virulence Mechanisms. *Infect Immun* **81**:629-635.
30. **Kachlany SC, Planet PJ, DeSalle R, Fine DH, Figurski DH.** 2001. Genes for tight adherence of *Actinobacillus actinomycetemcomitans*: from plaque to plaque to pond scum. *Trends Microbiol* **9**:429-437.
31. **Figurski DH, Perez-Cheeks BA, Fine DH, Hedhli J, Hua J, Kram KE, Xu K, Grosso VW.** 2013. Targeted Mutagenesis in the Study of the Tight Adherence (*tad*) Locus of *Aggregatibacter actinomycetemcomitans*. INTECH Open Access Publisher.
32. **Wilson ME, Hamilton RG.** 1995. Immunoglobulin G subclass response of juvenile periodontitis subjects to principal outer membrane proteins of *Actinobacillus actinomycetemcomitans*. *Infect Immun* **63**:1062-1069.
33. **Perez-Cheeks BA, Planet PJ, Sarkar IN, Clock SA, Xu Q, Figurski DH.** 2012. The product of *tadZ*, a new member of the *parA/minD* superfamily, localizes to a pole in *Aggregatibacter actinomycetemcomitans*. *Mol Microbiol* **83**:694-711.
34. **Bhattacharjee MK, Kachlany SC, Fine DH, Figurski DH.** 2001. Nonspecific adherence and fibril biogenesis by *Actinobacillus actinomycetemcomitans*: TadA protein is an ATPase. *J Bacteriol* **183**:5927-5936.
35. **Altschul SF, Madden TL, Schaffer AA, Zhang J, Zhang Z, Miller W, Lipman DJ.** 1997. Gapped BLAST and PSI-BLAST: a new generation of protein database search programs. *Nucleic Acids Res* **25**:3389-3402.

36. **Gomez-Leon J, Villamil L, Salger SA, Sallum R, Remacha-Trivino A, Leavitt DF, Gomez-Chiarri M.** 2008. Survival of eastern oysters *Crassostrea virginica* from three lines following experimental challenge with bacterial pathogens. *J Shellfish Res* **32**:401-408.
37. **McDowell IC, Nikapitiya C, Aguiar D, Lane CE, Istrail S, Gomez-Chiarri M.** 2014. Transcriptome of American oysters, *Crassostrea virginica*, in response to bacterial challenge: insights into potential mechanisms of disease resistance. *PLoS One* **9**:e105097.
38. **Satchell KJ.** 2011. Structure and function of MARTX toxins and other large repetitive RTX proteins. *Annu Rev Microbiol* **65**:71-90.
39. **Linhartova I, Bumba L, Masin J, Basler M, Osicka R, Kamanova J, Prochazkova K, Adkins I, Hejnova-Holubova J, Sadilkova L, Morova J, Sebo P.** 2010. RTX proteins: a highly diverse family secreted by a common mechanism. *FEMS Microbiol Rev* **34**:1076-1112.
40. **Wiles TJ, Mulvey MA.** 2013. The RTX pore-forming toxin alpha-hemolysin of uropathogenic *Escherichia coli*: progress and perspectives. *Future Microbiol* **8**:73-84.
41. **Kida Y, Inoue H, Shimizu T, Kuwano K.** 2007. *Serratia marcescens* serralyisin induces inflammatory responses through protease-activated receptor 2. *Infect Immun* **75**:164-174.
42. **Stocker W, Bode W.** 1995. Structural features of a superfamily of zinc-endopeptidases: the metzincins. *Curr Opin Struct Biol* **5**:383-390.
43. **Felfoldi G, Marokhazi J, Kepiro M, Venekei I.** 2009. Identification of natural target proteins indicates functions of a serralyisin-type metalloprotease, PrtA, in anti-immune mechanisms. *Appl Environ Microbiol* **75**:3120-3126.
44. **Belas R, Manos J, Suvanasuthi R.** 2004. *Proteus mirabilis* ZapA metalloprotease degrades a broad spectrum of substrates, including antimicrobial peptides. *Infect Immun* **72**:5159-5167.
45. **Schmidtchen A, Frick IM, Andersson E, Tapper H, Bjorck L.** 2002. Proteinases of common pathogenic bacteria degrade and inactivate the antibacterial peptide LL-37. *Mol Microbiol* **46**:157-168.
46. **Lasa I, Penades JR.** 2006. Bap: a family of surface proteins involved in biofilm formation. *Res Microbiol* **157**:99-107.
47. **Theunissen S, De Smet L, Dansercoer A, Motte B, Coenye T, Van Beeumen JJ, Devreese B, Savvides SN, Vergauwen B.** 2010. The 285 kDa Bap/RTX hybrid cell surface protein (SO4317) of *Shewanella oneidensis* MR-1 is a key mediator of biofilm formation. *Res Microbiol* **161**:144-152.
48. **Geesey GG, Wigglesworth - Cooksey B, Cooksey K.** 2000. Influence of calcium and other cations on surface adhesion of bacteria and diatoms: a review. *Biofouling* **15**:195-205.
49. **Patrauchan M, Sarkisova S, Sauer K, Franklin M.** 2005. Calcium influences cellular and extracellular product formation during biofilm-associated growth of a marine *Pseudoalteromonas* sp. *Microbiology* **151**:2885-2897.

50. **Gogarten JP, Senejani AG, Zhaxybayeva O, Olendzenski L, Hilario E.** 2002. Inteins: structure, function, and evolution. *Annual Reviews in Microbiology* **56**:263-287.
51. **Bürglin TR.** 2008. The Hedgehog protein family. *Genome Biol* **9**:241.
52. **Amitai G, Belenkiy O, Dassa B, Shainskaya A, Pietrokovski S.** 2003. Distribution and function of new bacterial intein-like protein domains. *Mol Microbiol* **47**:61-73.
53. **Hinsa SM, Espinosa - Urgel M, Ramos JL, O'Toole GA.** 2003. Transition from reversible to irreversible attachment during biofilm formation by *Pseudomonas fluorescens* WCS365 requires an ABC transporter and a large secreted protein. *Mol Microbiol* **49**:905-918.
54. **Cao TB, Saier MH, Jr.** 2001. Conjugal type IV macromolecular transfer systems of Gram-negative bacteria: organismal distribution, structural constraints and evolutionary conclusions. *Microbiology* **147**:3201-3214.
55. **Fronzes R, Schäfer E, Wang L, Saibil HR, Orlova EV, Waksman G.** 2009. Structure of a Type IV Secretion System Core Complex. *Science* **323**:266-268.
56. **Christie PJ, Whitaker N, González-Rivera C.** 2014. Mechanism and structure of the bacterial type IV secretion systems. *Biochimica et Biophysica Acta (BBA) - Molecular Cell Research* **1843**:1578-1591.
57. **Christie PJ, Atmakuri K, Krishnamoorthy V, Jakubowski S, Cascales E.** 2005. Biogenesis, architecture, and function of bacterial type IV secretion systems. *Annu Rev Microbiol* **59**.
58. **Backert S, Fronzes R, Waksman G.** 2008. VirB2 and VirB5 proteins: specialized adhesins in bacterial type-IV secretion systems? *Trends Microbiol* **16**:409-413.
59. **Gillespie JJ, Ammerman NC, Dreher-Lesnick SM, Rahman MS, Worley MJ, Setubal JC, Sobral BS, Azad AF.** 2009. An anomalous type IV secretion system in *Rickettsia* is evolutionarily conserved. *PLoS One* **4**:e4833.
60. **Sagulenko V, Sagulenko E, Jakubowski S, Spudich E, Christie PJ.** 2001. VirB7 lipoprotein is exocellular and associates with the *Agrobacterium tumefaciens* T pilus. *J Bacteriol* **183**:3642-3651.
61. **Spudich GM, Fernandez D, Zhou XR, Christie PJ.** 1996. Intermolecular disulfide bonds stabilize VirB7 homodimers and VirB7/VirB9 heterodimers during biogenesis of the *Agrobacterium tumefaciens* T-complex transport apparatus. *Proc Natl Acad Sci U S A* **93**:7512-7517.
62. **Sigrist CJ, Cerutti L, Hulo N, Gattiker A, Falquet L, Pagni M, Bairoch A, Bucher P.** 2002. PROSITE: a documented database using patterns and profiles as motif descriptors. *Brief Bioinform* **3**:265-274.
63. **Sigrist CJ, de Castro E, Cerutti L, Cuče BA, Hulo N, Bridge A, Bougueleret L, Xenarios I.** 2013. New and continuing developments at PROSITE. *Nucleic Acids Res* **41**:D344-347.
64. **de Castro E, Sigrist CJ, Gattiker A, Bulliard V, Langendijk-Genevaux PS, Gasteiger E, Bairoch A, Hulo N.** 2006. ScanProsite: detection of PROSITE signature matches and ProRule-associated functional and structural residues in proteins. *Nucleic Acids Res* **34**:W362-365.

65. **Sigrist CJ, De Castro E, Langendijk-Genevaux PS, Le Saux V, Bairoch A, Hulo N.** 2005. ProRule: a new database containing functional and structural information on PROSITE profiles. *Bioinformatics* **21**:4060-4066.
66. **Bako L, Umeda M, Tiburcio AF, Schell J, Koncz C.** 2003. The VirD2 pilot protein of *Agrobacterium*-transferred DNA interacts with the TATA box-binding protein and a nuclear protein kinase in plants. *Proc Natl Acad Sci U S A* **100**:10108-10113.
67. **Mysore KS, Bassuner B, Deng XB, Darbinian NS, Motchoulski A, Ream W, Gelvin SB.** 1998. Role of the *Agrobacterium tumefaciens* VirD2 protein in T-DNA transfer and integration. *Mol Plant Microbe Interact* **11**:668-683.
68. **Guo M, Hou Q, Hew CL, Pan SQ.** 2007. *Agrobacterium* VirD2-binding protein is involved in tumorigenesis and redundantly encoded in conjugative transfer gene clusters. *Mol Plant-Microbe Interact* **20**:1201-1212.
69. **Pellegrino S, Radzimanowski J, de Sanctis D, Erba Elisabetta B, McSweeney S, Timmins J.** 2012. Structural and Functional Characterization of an SMC-like Protein RecN: New Insights into Double-Strand Break Repair. *Structure* **20**:2076-2089.
70. **Nagai H, Kubori T.** 2011. Type IVB Secretion Systems of *Legionella* and Other Gram-Negative Bacteria. *Front Microbiol* **2**:136.
71. **Purcell M, Shuman HA.** 1998. The *Legionella pneumophila* *icmGCDJBF* Genes Are Required for Killing of Human Macrophages. *Infect Immun* **66**:2245-2255.
72. **Brand BC, Sadosky AB, Shuman HA.** 1994. The *Legionella pneumophila* *icm* locus: a set of genes required for intracellular multiplication in human macrophages. *Mol Microbiol* **14**:797-808.
73. **Finn RD, Bateman A, Clements J, Coghill P, Eberhardt RY, Eddy SR, Heger A, Hetherington K, Holm L, Mistry J, Sonnhammer EL, Tate J, Punta M.** 2014. Pfam: the protein families database. *Nucleic Acids Res* **42**:D222-230.
74. **Vogel JP, Andrews HL, Wong SK, Isberg RR.** 1998. Conjugative transfer by the virulence system of *Legionella pneumophila*. *Science* **279**:873-876.
75. **Segal G, Purcell M, Shuman HA.** 1998. Host cell killing and bacterial conjugation require overlapping sets of genes within a 22-kb region of the *Legionella pneumophila* genome. *Proceedings of the National Academy of Sciences of the United States of America* **95**:1669-1674.

## APPENDIX

### Description of conserved domains from NCBI's conserved domain database.

These descriptions are direct citations from the database (1-4):

**pfam13403**: Hint domain. This domain is found in inteins.

**PRK15319**: AIDA autotransporter-like protein ShdA; Provisional

**pfam08548**: Peptidase\_M10\_C. Peptidase M10 serralysin C terminal.

Serralysins are peptidases related to mammalian matrix metalloproteinases (MMPs).

The peptidase unit is found at the N terminal while this domain at the C terminal forms a corkscrew and is thought to be important for secretion of the protein through the bacterial cell wall. This domain contains the calcium ion binding domain pfam00353.

**COG2931**: Ca<sup>2+</sup>-binding protein, RTX toxin-related [Secondary metabolites biosynthesis, transport and catabolism] linked to 3D-structure

**pfam13448**: Domain of unknown function (DUF4114). This is a repeated domain that is found towards the C-terminal of many different types of bacterial proteins. There are highly conserved glutamate and aspartate residues suggesting that this domain might carry enzymic activity.

**TIGR04225**: CshA-type fibril repeat. Many proteins with this repeat are LPXTG-anchored surface proteins of Firmicutes species, but the repeat occurs more broadly. Members include CshA from *Streptococcus gordonii*.

**cd04277**: ZnMc\_serralysin\_like

Zinc-dependent metalloprotease, serralysin\_like subfamily. Serralysins and related proteases are important virulence factors in pathogenic bacteria. They may be secreted into the medium via a mechanism found in gram-negative bacteria, that does not require n-terminal signal sequences which are cleaved after the transmembrane translocation. A calcium-binding domain c-terminal to the metalloprotease domain, which contains multiple tandem repeats of a nine-residue motif including the pattern GGxGxD, and which forms a parallel beta roll may be involved in the translocation mechanism and/or substrate binding. Serralysin family members may have a broad spectrum of substrates each, including host immunoglobulins, complement proteins, cell matrix and cytoskeletal proteins, as well as antimicrobial peptides.

**cl21455**: P-loop\_NTPase Superfamily. P-loop containing Nucleoside Triphosphate Hydrolases. Members of the P-loop NTPase domain superfamily are characterized by a conserved nucleotide phosphate-binding motif, also referred to as the Walker A motif (GxxxxGK{S/T}, where x is any residue), and the Walker B motif (hhhh{D/E}), where h is a hydrophobic residue). The Walker A and B motifs bind the beta-gamma phosphate moiety of the bound nucleotide (typically ATP or GTP) and the Mg<sup>2+</sup> cation, respectively. The P-loop NTPases are involved in diverse cellular functions, and they can be divided into two major structural classes: the KG (kinase-GTPase) class which includes Ras-like GTPases and its circularly permuted YlqF-like; and the ASCE (additional strand catalytic E) class which includes ATPase Binding Cassette (ABC), DExD/H-like helicases, 4Fe-4S iron sulfur cluster binding proteins of NifH family, RecA-like F1-ATPases, and ATPases Associated with a wide variety of

Activities (AAA). Also included are a diverse set of nucleotide/nucleoside kinase families.

**pfam13871**: Helicase\_C-like. Strawberry notch proteins carry DExD/H-box groups and Helicase\_C domains. These proteins promote the expression of diverse targets, potentially through interactions with transcriptional activator or repressor complexes.

**pfam02794**: RTX toxin acyltransferase family. Members of this family are enzymes EC:2.3.1.-. involved in fatty acylation of the protoxins (HlyA) at lysine residues, thereby converting them to the active toxin. Acyl-acyl carrier protein (ACP) is the essential acyl donor. This family show a number of conserved residues that are possible candidates for participation in acyl transfer. Site-directed mutagenesis of the single conserved histidine residue in E. coli hlyC resulted in complete inactivation of the enzyme.

**COG2994**: ACP:hemolysin acyltransferase (hemolysin-activating protein)

[Posttranslational modification, protein turnover, chaperones]

**COG3176**: Putative hemolysin [General function prediction only]

**pfam13444**: Acetyltransferase (GNAT) domain

This family contains proteins with N-acetyltransferase functions.

**cl17185**: Lysophospholipid acyltransferases (LPLATs) of glycerophospholipid biosynthesis. Lysophospholipid acyltransferase (LPLAT) superfamily members are acyltransferases of de novo and remodeling pathways of glycerophospholipid biosynthesis. These proteins catalyze the incorporation of an acyl group from either acylCoAs or acyl-acyl carrier proteins (acylACPs) into acceptors such as glycerol 3-phosphate, dihydroxyacetone phosphate or lyso-phosphatidic acid. Included in this



superfamily are LPLATs such as glycerol-3-phosphate 1-acyltransferase (GPAT, PlsB), 1-acyl-sn-glycerol-3-phosphate acyltransferase (AGPAT, PlsC), lysophosphatidylcholine acyltransferase 1 (LPCAT-1), lysophosphatidylethanolamine acyltransferase (LPEAT, also known as, MBOAT2, membrane-bound O-acyltransferase domain-containing protein 2), lipid A biosynthesis lauroyl/myristoyl acyltransferase, 2-acylglycerol O-acyltransferase (MGAT), dihydroxyacetone phosphate acyltransferase (DHAPAT, also known as 1 glycerol-3-phosphate O-acyltransferase 1) and Tafazzin (the protein product of the Barth syndrome (TAZ) gene).

**PRK15087**: hemolysin; Provisional

**COG1272**: Predicted membrane channel-forming protein YqfA, hemolysin III family  
[Intracellular trafficking, secretion, and vesicular transport]

**TIGR01065**: channel protein, hemolysin III family. This family includes proteins from pathogenic and non-pathogenic bacteria, Homo sapiens and Drosophila. In Bacillus cereus, a pathogen, it has been shown to function as a channel-forming cytolysin. The human protein is expressed preferentially in mature macrophages, consistent with a role cytolytic role.

**pfam03006**: Haemolysin-III related. Members of this family are integral membrane proteins. This family includes a protein with hemolytic activity from Bacillus cereus. It has been proposed that YOL002c encodes a Saccharomyces cerevisiae protein that plays a key role in metabolic pathways that regulate lipid and phosphate metabolism. In eukaryotes, members are seven-transmembrane pass molecules found to encode functional receptors with a broad range of apparent ligand specificities, including

progestin and adipoQ receptors, and hence have been named PAQR proteins. The mammalian members include progesterone binding proteins. Unlike the case with GPCR receptor proteins, the evolutionary ancestry of the members of this family can be traced back to the Archaea.

## REFERENCES

1. **Marchler-Bauer A, Anderson JB, Chitsaz F, Derbyshire MK, DeWeese-Scott C, Fong JH, Geer LY, Geer RC, Gonzales NR, Gwadz M, He S, Hurwitz DI, Jackson JD, Ke Z, Lanczycki CJ, Liebert CA, Liu C, Lu F, Lu S, Marchler GH, Mullokandov M, Song JS, Tasneem A, Thanki N, Yamashita RA, Zhang D, Zhang N, Bryant SH.** 2009. CDD: specific functional annotation with the Conserved Domain Database. *Nucleic Acids Res* **37**:D205-210.
2. **Marchler-Bauer A, Bryant SH.** 2004. CD-Search: protein domain annotations on the fly. *Nucleic Acids Res* **32**:W327-331.
3. **Marchler-Bauer A, Derbyshire MK, Gonzales NR, Lu S, Chitsaz F, Geer LY, Geer RC, He J, Gwadz M, Hurwitz DI, Lanczycki CJ, Lu F, Marchler GH, Song JS, Thanki N, Wang Z, Yamashita RA, Zhang D, Zheng C, Bryant SH.** 2015. CDD: NCBI's conserved domain database. *Nucleic Acids Res* **43**:D222-226.
4. **Marchler-Bauer A, Lu S, Anderson JB, Chitsaz F, Derbyshire MK, DeWeese-Scott C, Fong JH, Geer LY, Geer RC, Gonzales NR, Gwadz M, Hurwitz DI, Jackson JD, Ke Z, Lanczycki CJ, Lu F, Marchler GH, Mullokandov M, Omelchenko MV, Robertson CL, Song JS, Thanki N, Yamashita RA, Zhang D, Zhang N, Zheng C, Bryant SH.** 2011. CDD: a Conserved Domain Database for the functional annotation of proteins. *Nucleic Acids Res* **39**:D225-229.